



# Biologically Inspired Joints for Innovative Articulations Concepts

## Final Report

**Authors:** Rocco Vertechy, Vincenzo Parenti-Castelli

**Affiliation:** University of Bologna - DIEM

**ESA Research Fellow/Technical Officer:** Carlo Menon

### Contacts:

Prof. Vincenzo Parenti-Castelli

Tel: +39(0)512093459

Fax: +39(0)512093446

e-mail: [vincenzo.parenticastelli@mail.ing.unibo.it](mailto:vincenzo.parenticastelli@mail.ing.unibo.it)

Dr. Carlo Menon

Tel: +31(0)715658675

Fax: +31(0)715658018

e-mail: [act@esa.int](mailto:act@esa.int)



Available on the ACT website  
<http://www.esa.int/act>

**Ariadna ID:** 04/6401  
**Study Duration:** 6 months  
**Contract Number:** 18911/05/NL/MV

## **Abstract**

A great challenge for mechanical devices is environment interaction. Indeed, while machines excel in pick-and-place tasks, they are rather poor in operations such as running, flying and grasping. Current researches suggest “low impedance” as the key asset for environment interacting tasks.

Compliance and lightness are different aspects of impedance. Biological joints are inherently compliant and lightweight. Moreover, biological joints are organs and not only passive mechanism. Indeed, they are complex systems which behave actively in order to preserve their functional stability. Biological joints are able to adapt themselves to internal failures and to changes in the environment and/or in the operating conditions. Clearly, artificial equivalents of biological joints which embody the aforementioned features may be very useful for mechanical systems which interact with the environment.

With these premises, in this work we first present the state of the art and the needs of environment interacting devices. Then, we investigate, in depth, the active and passive features shown by biological joints, and examine how these features can be transferred into an artificial counterpart which has to be suited to environment interaction and to other applications as well. In this framework, we take the knee joint as a benchmark. In particular, we examine the active and passive roles ligaments play in the functional stability of the knee. Finally, synthesis, kinematic analysis, stiffness analysis and implementation issues of a novel biologically inspired joint which can be suited to environment interaction and to other applications are addressed. Since the new joint takes inspiration from the major features which are found in the knee joints of several animal species, it has been named “Almost TWO degree of freedoms Knee-Inspired” (ATWOKI) joint.

# Content

<b>Abstract</b>	<b>ii</b>
<b>Content</b>	<b>iii</b>
<b>1 Joint Technology: State of the Art, Limits and Needs</b>	<b>1</b>
1.1.1 The Actual Challenge for Mechanical Devices: Environment Interaction.....	1
1.1.2 Interacting Mechanical Devices: State of the Art and New Trends.....	1
1.1.3 Interacting Mechanical Devices: a Novel Paradigm in Machine Design.....	3
1.2 The Need of a Compliant Joint Technology.....	3
1.3.1 Traditional Joint Technology: State of the Art and Actual Limits.....	4
1.3.2 New Joint Technology: Requirements and Biomimetic Approach.....	4
<b>2 Analysis of Biological Joints</b>	<b>6</b>
2.1 Analysis of Biological Joints as Simple Passive Mechanisms.....	5
2.2 Analysis of Biological Joints as Real Organs: Active Mechanisms.....	9
2.3 Analysis of Biological Joints: Ligaments as Key Elements for Functional Stability.....	11
<b>3 Novel Types of Biologically Inspired Mechanisms</b>	<b>15</b>
3.1 Introduction.....	15
3.2 Diarthroses Inspired Articulation Concepts.....	15
3.2.1 Basic Idea.....	15
3.2.2 Practical Articulation Concepts.....	18
3.3 Idea and Tools for the Rational Synthesis of Biologically Inspired Joints.....	19
3.3.1 Fully Parallel Manipulators: Architecture, Singularities and Self-Motions.....	20
3.3.2 Self-Movable UPS Parallel Manipulators and Biologically Inspired UP Parallel Mechanisms.....	21
3.3.3 Tools for the Synthesis of Biologically Inspired Self-Movable US Parallel Mechanisms.....	24
3.4 Synthesis of Practical 2-dof Spherical US_PMs.....	26
3.4.1 Definition and Parameterization of the Desired Motion of the Mechanism.....	26
3.4.2 Generation of Self-Movable 2-dof Spherical US_PMs.....	27
3.5 Comparison between Biologically Inspired US_PMs and Traditional Mechanisms.....	33
3.6 Biologically Inspired US_PMs: Actuation and Control.....	39
<b>4 Kinematic Analysis</b>	<b>46</b>
4.1 Introduction.....	46
4.2 ATWOKI: System Description.....	46
4.3 ATWOKI: Direct Position Analysis (DPA).....	47
4.4 ATWOKI: Inverse Position Analysis (IPA).....	51
4.5 ATWOKI: Direct Velocity Analysis (DVA).....	53

4.6	ATWOKI: Inverse Velocity Analysis (IVA).....	54
4.7	ATWOKI: Direct Acceleration Analysis (DAA).....	55
4.8	ATWOKI: Inverse Acceleration Analysis (IAA).....	56
4.9	ATWOKI: Extended Direct Position Analysis (EDPA).....	57
<b>5</b>	<b>Stiffness Analysis</b>	<b>66</b>
5.1	Introduction.....	66
5.2	Premises: Parameterization of Manipulator Motion.....	67
5.3	Premises: Elastic Forces and Moments Associated to Manipulator Deflections.....	69
5.4	Manipulator Stiffness: General Expressions.....	70
5.5	Manipulator Stiffness: Practical Expressions.....	82
5.6	Selective Compliance and Principles of Mechanism Design.....	90
	<b>Conclusions</b>	<b>92</b>
	<b>References</b>	<b>93</b>

## Chapter 1

### Joint Technology: State of the Art, Limits and Needs

#### 1.1.1 The Actual Challenge for Mechanical Devices: Environment Interaction

Mechanical devices demonstrated very successful at performing tasks that require movements in free space or known environments under position or trajectory control of the device degrees of freedom. Indeed, machines can perform such tasks with great speed, endurance, precision and accuracy which are rather difficult and tedious for humans. On the other hand, to date, there are many tasks in which machine competence is inferior to that of the biological counterparts, i.e. live beings.

Despite extensive research, actions which require consistent interaction with the real world such as walking, running, swimming, catching, grasping and manipulation, and which are considered easy to most able-bodied live beings, have been proven difficult for mechanical devices. As a result, while machines such as pick-and-place robots that use position/trajectory control have found their way into effective applications (e.g. spray painting vehicle exteriors, pick and place of integrated circuit chips and arc/spot welding), for the most part, mechanical devices that contact the surrounding environment and work within kinematic constraints have been only limited to a laboratory research level.

Unfortunately, since our world is kinematically and inertially constrained, it is important for a mechanical device to be able to adapt to the environment. Frequently, the environment defines a flow interaction and leaves the machine with only the option to modulate its effort. In other words, while the machine can push on and give energy to the environment, it cannot specify how the environment will respond. If the machine tries to control the position at a constrained interface, there exists a basic incompatibility between the two physical systems. Therefore, whenever a mechanical device interacts with an environment or with a work piece and is not simply moving around in free space, while it is still important for the machine to understand its own sense of position, the machine also needs some capability of being compliant in order to allow the causality of the machine-environment interface to maintain a proper relationship.

In practice, all environments do have some compliance. While most constraints have high stiffness, there are other environments which are very compliant. Perhaps, the compliance is even variable, like in an inflated elastic balloon. In these cases it may be necessary for the mechanical device to control some combination of flow and effort, but once again, the machine must be capable of being compliant.

In technical language, such concepts are resumed by the following statement: mechanical devices must possess “low impedance”.

#### 1.1.2 Interacting Mechanical Devices: State of the Art and New Trends

In the recent past, different techniques, ideas and algorithms have been used by researchers in order to match the impedance requirements of mechanical devices with the impedance characteristics of the environment. Practically, it is possible to sort all the efforts in two classes: passive and active methods.

Passive methods are essentially based on the introduction of some concentrated compliance into the machine structure while leaving the control system to perform a traditional position control [1, 2].

A very clever example is the remote center compliance (RCC) which is a special compliant end-effector set up to automatically execute a peg-in-hole assembly [1].



Figure 1.1 Remote Center of Compliance (RCC)

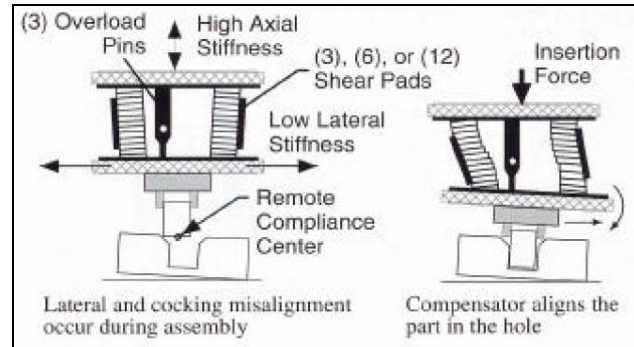


Figure 1.2 Behaviour of RCC in Peg-in-Hole Operations

A RCC is depicted in Fig. 1.1 (courtesy from ATI Industrial Automation). A representative schematic of the behavior of the RCC in peg-in-hole operations is shown in Fig. 1.2. The configuration of the RCC creates a compliance center at a certain point within its structure. Forces acting on the remote compliance center result in pure translations, while torques exerted about the remote compliance center cause pure rotations. By placing a peg tip right at the remote compliance center, it can be passively dropped into a hole without jamming.

Active methods [3, 4], conversely, do not introduce any form of passive compliance. Instead, compliance is actively generated by means of specific control algorithms. Among these approaches we can recall explicit force control, stiffness control [5], damping control [4], impedance control [6], hybrid position-force control [7], and virtual model control [8].

Despite the advances and the very interesting results achieved, unfortunately, both methods did not succeed by themselves in making mechanical devices perform as their biologic counterparts. Passive techniques are usually task specific oriented and, if not associated with a proper control system, render the machine *sloppy* during task execution so as to cause the system to miss the overall goals [2]. Active methods are limited by the performances of standard actuation systems which are poor at generating accurate forces in the machine joints. Accurate force generation is indeed essential to the active control techniques. In fact, force controlled, i.e. ideally zero-impedance, actuators are heavily affected by friction, stick-slip, breakaway forces on seals, backlash in transmissions, cogging in motors and reflected inertia through a transmission, which induce relevant force noise in the actuator output. Note that these effects are minimized, instead, when the mechanical device is controlled in position or trajectory. Indeed, in such circumstances, the mass of both the robot and the actuators low-pass filters the force noise on the positional output.

Owing to these limitations, a further trend is currently being undertaken. In essence, it is a hybrid approach which relies on the introduction of passive compliance in the machine structure [9] or in the machine actuators [10], and on the use of properly modified force-control schemes which take into account the flexibility of the structure to be controlled [11, 12]. These techniques are showing interesting results and seem very promising especially on the light of the emerging compliant actuator technologies such as the electroactive polymers [13].

Indeed, such materials, which seem to possess performances comparable to or even better than natural muscles, may provide a mean for building simple, slender and lightweight actuators which, by avoiding transmissions and sliding parts, may feature better actuator force output in addition to compliance.

### 1.1.3 Interacting Mechanical Devices: a Novel Paradigm in Machine Design

From the preceding sections, it can be seen that the need to make machines interact with the environment is leading the design community toward a controversial paradigm, i.e. the introduction of compliance into mechanisms and actuators.

Traditionally, mechanisms and actuators have been built to be as stiff as possible in order to increase the overall system bandwidth. Higher cut-off frequencies are indeed perfectly suited to pick-and-place robots where strict kinematic performances such as fast movements, high position accuracy and impending disturbance rejection are required. Besides, while these objectives are surely still welcomed, interacting machines call for different priorities. Stability when contacting environments of variable and unknown stiffness is the main target. Then, the ability to filter shock loads and, more generally, to insulate machine components from the environment, in addition to the possibility to store energy and control its flow for increasing the overall machine efficiency follow.

Elasticity complies with all these requirements. As a major example, note that the actuator benchmark for environment interacting operations, i.e. biological muscles, are intrinsically compliant. Further, it has to be understood that the frequency threshold of operation of interacting devices is much lower than the one sought for pick-and-place tasks and, therefore, the use of elasticity is not a limiting factor here.

## 1.2 The Need of a Compliant Joint Technology

As mentioned in Section 1.1.2, to date, research efforts in compliant mechanical devices have been mainly focused on actuator and control technologies. Few research groups concentrated on the features and properties of the mechanisms to be controlled. In such spare works, however, only topics related to link compliance have been addressed, while not much has been said about compliant joints. Note that, in the context of this research study, the definition of compliant joints goes beyond the concepts related to the well known flexible joints used in high accuracy micro-positioning devices and similar. Indeed, with compliant joint we intend a pair that provides lower stiffness and large relative motions in some directions, i.e. the practical degrees of freedom of the joint, and higher stiffness and very small motions in the remaining directions.

Compliant joints are a very potential topic which deserves to be addressed. Indeed, as attainable by the use of springs in series with actuators and/or flexibility of links, compliant joints may: a) compensate for poor positioning accuracy of gross motions, like the RCC device described in Section 1.2; b) allow for a more touch-gently action, which is essential in manipulation; and c) introduce shock reduction and energy storage capabilities, which are fundamental in locomotion [14] and in vibration damping. Moreover, compliant joints may also provide other positive features that could allow overcoming the manufacturing and the functional limitations shown by traditional joints in more common applications.

### 1.3.1 Traditional Joint Technology: State of the Art and Actual Limits

Traditional mechanical pairs are based on 1 degree-of-freedom (dof) joints made by rigid members with matching, i.e. congruent, conjugate surfaces. From a kinematical perspective traditional pairs are independent kinematic elements under bilateral geometric constraint. They are usually referred to as lower pairs and comprise rigid-pinned-hinges, sliders and lead screws. Among standardization, modularity and other aspects, the main advantage related to the success of lower pairs consists in the reduced contact pressure between the connected links that limits internal stresses and wear of the materials which make the pair.

However, this speculation is rather ideal and, in practice, the use of such joints involves several issues. Indeed, unless resorting to rather costly manufacturing processes, contacting surfaces of lower pairs are quite far from being congruent. Moreover, in order to assemble the mating links and the overall mechanisms they are placed in, lower pairs need to be provided with some clearance which, apart from decreasing contacting surface congruence, introduces backlash (that causes vibration and shock sensitivity) and leads to kinematic indeterminacy between the connected links (that causes accuracy and control issues). Of course, a possible alternative to clearance-affected pairs is the use of pre-loaded pairs; however, mechanisms presenting pre-loaded pairs require very precise tolerances and, consequently, very high manufacturing costs. Further, the bilateral constraint, which is inherent in lower pairs, does not allow for the take up of increased clearance which may arise as a consequence of reversible effects such as thermal deformations, or irreversible effects such as wear. The use of pre-loaded pairs may, once again, allow going around the problem, but, as said, the approach is not exempt from drawbacks. Still referring to the bilaterality of the geometrical constraints, lower pairs do not allow the connected links to compensate for misalignments which may occur during mounting and in operating conditions. As a result, excessive stresses, wear and even jamming may take place, especially if pre-loaded pairs are used.

To date, the use of 1-dof lower pairs dominates even when the links to be connected require more degrees of mobility. In such cases, suitable serial combinations of lower pairs, e.g. two revolute pairs with intersecting axes for the realization of a 2-dof spherical joint, are preferred to the use of monolithic higher-pairs. This results in bulky and heavy connections which feature all the drawbacks related to elements connected in series. Note that the choice of serially combining 1-dof pairs to devise multi-dof joints is partly a consequence of the technological limitations in sensor and actuator technologies. Indeed, even the 3-dof spherical pair, which exists as monolithic, is often replaced by three revolute pairs with co-intersecting axes because of problems related to the integration of sensors and actuators in the joint.

### 1.3.2 New Joint Technology: Requirements and Biomimetic Approach

As described in Section 1.3.1, it is clear that the joint technology needs to advance further. Of course, aspects such as long durability, inexpensiveness, lightness, compactness should be improved. But more than that, it comes up that one of the main drawbacks of the traditional joints technology is the lack of adaptability to varying operating conditions. Traditional joints cannot accommodate optimally for concurrent effects such as clearance, wear, stresses and other environment dependent phenomena. In practice, some sort of multi-functionality and “smart” behaviour for adapting to environment changes should be sought for a next generation of connecting elements.

With these objectives, many approaches may be undertaken. However, since the sought features can be found in biological joints and since these latter demonstrate to perform very well, the option of biologically inspired (biomimetic) approaches is very attractive. Indeed, live beings come as a result of a long natural selection in which deficiencies should be nullified while advantages should be maximized. Biologic creatures are the benchmark for environment-interaction tasks and thus it can be conjectured that their joints have been optimized by using as criterion the long lasting ability in performing such tasks. As a matter of fact, the design of joints across species has been quite consistent for about 300 millions of years [15]. Moreover, despite the huge differences between species, their joints are very similar and have the same morphological components [15].

However, by making this choice, one should be far from just copying nature's designs. In fact, while, from one side, biology may be inspiring and assisting, on the other side, artificial technologies and materials are very different from nature's technologies and materials. Indeed, the phenomenology of natural and artificial materials is rather different. In addition, the operational environments, the applications and the success criteria or the cost functions may be diverse. In particular, to date, artificial materials do not have to comply with metabolic needs. Furthermore, concerning the design, it is worth recalling that, although excellent, nature is not perfect since living creatures are the result of a selection among already built and very similar beings. Conversely, our systems may come from the comparison of unlimited potentially optimal designs which may be conceived by using a huge amount of tools and realized through an unrestricted number of materials. Thus, the correct use of biological inspired approaches for the design of new types of mechanical joints should respect the following steps: 1) start from the analysis and comprehension of the structure and the functionalities of biological joints; 2) identify the features which may be transferred to artificial types of joints; 3) taking into account the available materials and technologies, devise the most favourable articulation concept which may pursue the identified features; and 4) use the devised articulation concept and the available materials and technologies to design mechanisms which are optimized for the application at hand.

## Chapter 2

### Analysis of Biological Joints

#### 2.1 Analysis of Biological Joints as Simple Passive Mechanisms

With respect to traditional mechanical joints, the situation in biology is much more intricate.

Based on their anatomic structure and movement potentials, biological joints are classified in three groups: synarthroses (fibrous), amphiarthroses (cartilaginous) and diarthroses (synovial). In synarthroses, bones are connected by connective fibrous tissue. Synarthroses are designed for joint stability; they bind bones together and transmit forces from one bone to the next with minimal joint motion. Such joints allow forces to be dispersed across a relatively large area of contact, thereby reducing the possibility of injury. In amphiarthroses, bones are connected by ligaments and elastic cartilages such as fibrocartilage and hyaline cartilage. Amphiarthroses allow relatively restrained movements and are relatively stiff; they are mainly designated to provide stability and to absorb and disperse forces between adjacent bones. Note that, in order to facilitate a large range of motion, amphiarthroses are used in serial combination (e.g. connection of spinal vertebrae). In diarthroses, bones are in contact and connected by fibrous structures and cartilage, and are able to move with respect to each other. Within a defined and quite wide range of motion, diarthroses allow for rather free movements. They offer little friction and are designed to facilitate large motions and are able to transmit forces also.

Since artificial counterparts of synarthroses and amphiarthroses exist, in practice, in the mechanical world (e.g. link bonding, i.e. soldering or gluing, may be understood as the artificial counterpart of synarthroses; flexible joints, i.e. notch and leaf-spring joints, may be understood as the artificial counterparts of amphiarthroses), and since diarthroses are the only connections specialized for large movements, thus being crucial to the mechanics of motion (diarthroses are present in major number in both upper and lower extremities of biological bodies), we concentrate our attention on synovial joints.

From a mechanical point of view, diarthroses are multifunctional. Primarily, they allow motion, shock absorption, conservation of energy and transmission of forces.

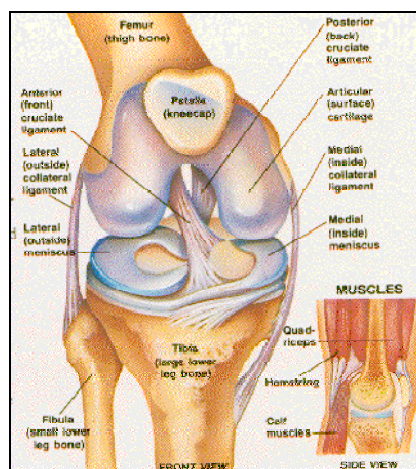


Figure 2.1 Knee Joint

Despite the differences among biological species and the functions they are suited for, from a movement functionality perspective, all diarthroses are made up of bone's conjugate surfaces, articular cartilage, articular capsule, ligaments and tendons muscles, and are filled with synovial fluid. Considering the knee as example, a picture of the elements which make a diarthrosis is given in Fig. 2.1 (picture from [www.ski-injury.com](http://www.ski-injury.com)).

Most joint surfaces are curved, with one surface being relatively convex and the other relatively concave. Contact surfaces are usually incongruent [16, 17] and the contact is mediated by the articular cartilage.

Cartilage provides a means of lubrication in order to distribute the contact forces over a wider contact surface as well as reducing friction during motion. Despite the various range of loading condition it is subjected to, cartilage surfaces sustain very little wear. The minimal wear is associated with a very complex lubrication system, i.e. a lubricating fluid-film forming between the articular cartilage surfaces and an adsorbed boundary lubricant on each surface during motion and loadings [18].

In highly stressed articulations, further fibrocartilage elements are present between the cartilage surfaces, e.g. the menisci in the knee joint. Such elements work as major force-bearers by making the contact surfaces of the joint far more congruent. Other than that, the functions of fibrocartilage elements include shock absorption, joint stabilization during motion, improved lubrication of the articular contact, additional friction reduction, and auxiliary guidance of the joint arthrokinematics. As said, referring to the knee joint, examples of fibrocartilage elements are the menisci [19]. They transform nearly flat articular surfaces of the tibia into shallow seats for the femoral condyles so as to increase the extension of the contact surfaces. Note that the menisci carry the entire force at lower loads; indeed, it takes about half a body weight to make the femoral cartilage actually contact the tibial cartilage [20]. Further, due to their disc-like crescent shape, when compressed, the menisci deform peripherally [19]. This mechanism allows part of the compression force at the knee to be absorbed as a circumferential tension throughout each meniscus. This confers very good shock absorption properties while walking, running and jumping. Note that, in such activities, compressive forces range from nearly 3 times the body weight, under normal conditions, to 9 times the body weight, under extreme conditions. In practice, menisci are able to nearly tripling the area of joint contact between femur and tibia [21]. Their effectiveness is proven by considering that a complete lateral meniscectomy increases the peak contact pressure by 230% [22], which likely increases the risk of developing stress related arthritis, i.e. contact surface wear.

Tendons, ligaments and joint capsules are the three principal structures that closely surround, connect, and stabilize diarthroses [23]. Even when considered as passive mechanical elements (the active properties are dealt in Section 2.2), these structures play a very essential role. Ligaments and joint capsules connect a bone to another and, acting as static restraints, augment the mechanical stability of the joints, contribute to guide joint motion and prevent excessive joint motion. Conversely, tendons attach muscles to bones and transmit tensile loads between them, thereby producing joint motion or maintaining joint posture. Tendons and muscles form the tendon-muscle units which act as active restraint. The tendon also allows the muscle belly to be at an optimal distance from the joint on which it acts without requiring the muscle itself to be extended between origin and insertion. Tendons and ligaments are viscoelastic structures with unique mechanical properties. Tendons are strong enough to sustain the high tensile forces that result from muscle contraction during joint motion, yet are sufficiently flexible to angulate around bone surfaces and to deflect beneath retinacula to change the final direction of the muscle pull. Tendon attachments on the bones are properly shaped so as to create a good level mechanism for the

efficient transmission of the muscle force between bones throughout the full range of motion of the joint. The ligaments are pliant and flexible so as to allow the natural movements of the bones they are attached to, but also strong and inextensible so as to drive the joint arthrokinematics accurately and to offer appropriate resistance to forces applied to the joint.

From a mobility perspective, a biological joint features multiple degrees of freedom in one compact and lightweight single system. As for their architecture, conversely to multi-dof traditional joints which are, usually, serial compositions of lower pairs, biological joints are, essentially, closed kinematic chains which make use of rigid (bones) as well as flexible (ligaments, cartilages, fibrocartilage) members. The constraint between rigid members is unilateral and the coupling surfaces are not congruent. The contact between these surfaces is mediated by some compliant means (cartilage and fibrocartilage) and, usually, is further lubricated by the synovial fluid. Separation of the contact surfaces is prevented by flexible and quite stiff elements, such as the ligaments. They act both as effective constraints which directly limit the joint arthrokinematics (ligaments reduce, by themselves, the degrees of freedom of the joint) and as preloading elements which force the contact between adjacent rigid members so as to indirectly limit the joint arthrokinematics (ligaments preload the unilateral coupling between adjacent bones so as to make this constraint effective). Note that due to their flexibility, the ligaments are allowed to bend and to twist around their axis during the joint motion.

From the kinematic point of view, the use of higher pairs, where the adjacent members can contemporarily roll, slide and spin, makes biological joints much more compact and lighter than if serial combinations of revolute, sliding or helical pairs were used.

Moreover, the association between the unilaterally-constrained architecture of the coupling between rigid members (bones) and the slight compliance of the flexible (ligaments and tendons) and the intervening (cartilage and fibrocartilage) elements allows for 6-dof compliance of the joint. This is fundamental for increasing the functionality of biological joints. Indeed, passive compliance allows the axis of relative motion of two adjacent bones to fluctuate within a small region so as to guarantee certain compulsory motions even in externally overconstrained situations. As an example, note that, when a knee is embedded in a brace, the leg can somehow flex and extend even if the brace is not placed properly across the joint. Indeed, due to the 6-dof compliance, the axis of flexion-extension of the knee shifts in order to match the axis of rotation of the brace.

Joint compliance is also a means to simply compensate for the poor control of the relative motion between the connected members, and allows the joint to adapt to events which may change, reversibly or permanently, the shape of the contacting surfaces. In this way, both backlash and the effects of wear may be nullified. Finally, compliance allows for shock and vibration reduction, limits the potential damages of uncontrolled movements and filters out noisy and impulsive forces which may be generated either by the muscles or by external disturbances coming from the environment. Thus, it simplifies the control of certain tasks and auto-protects the system itself.

The cam-shaped surfaces of the contacting members give the possibility of decreasing or increasing bone-surface congruence in certain positions of the joint motion. In this way, the joint could be made gain or lose some degree of freedom while moving. This feature is exploited by the knee joint which behaves as a 1-dof mechanism near full extension, i.e. the internal-external rotation is dependent on the flexion-extension movement, and behaves as a 2-dof joint when flexed, i.e. the internal-external rotation is fairly independent on the flexion-extension

movement [62, 63]. Note that this phenomenon depends mainly on the cam-shaped surface of the contacting members but also on the compliance of the elements which make the knee. Indeed, the gained degree of freedom is, more precisely, an “envelope” of motion because it is consistent only if the tibia is subjected to some torque (from the muscles or from the outside), while it is not consistent if the knee is in a completely unloaded state [62]. However, since in flexed configurations the compliance towards internal-external rotations of the tibia is much smaller than the compliance in the other directions (the knee is indeed much stiffer towards varus-valgus rotations and towards all the translations), i.e. internal-external rotations are much bigger than the motions in the other directions, and since the independent internal-external rotation of the tibia is fundamental for activities of daily living [63], then this “envelope” of motion must be considered as a practical degree of freedom. In this regard, note that the amount of torque required for the internal-external rotation of the tibia is about 3 Nm which is far lower than the 40 Nm an healthy knee joint can sustain [64]. In this context, while the passive (unloaded) motion of the knee is 1-dof, throughout this research work, the practical (or prevalent) motion of the knee is considered with 2-dof.

In cases where a single 1-dof motion in a plane is needed, the use of cam-shaped surfaces, which generate coupled motions outside that plane, may be a means for providing the joint with more stability than achieved through the use of a simple traditional planar pair. The passive motion of the knee joint works as example. In fact, the tibio-femoral joint is a special 1-dof mechanism which, in the ultimate degrees of extension, besides the rotation in the plane defined by the axes of the tibia and femur, provides also a coupled rotation of the tibia around its axis. This mechanism is known as the "screw home" mechanism. It is considered to be the key element of knee stability for standing upright and for performing activities which involve vigorous cuts (90 deg change in direction), jumps and rapid decelerations. Essentially, the slight twist of the tibia during extension allows the femoral condyles and the tibial plateau to share the maximal possible flat surface so as to distribute the contacting force over a greater area as well as to allow the knee to be held in full extension without undue fatigue of the surrounding musculature [24]. A similar phenomenon happens at the hip-joint and it is usually referred to as “true native bony” stability.

Usually, due to the eccentric nature of the conjugate surfaces, the rotation axes of links do not remain steady with respect to the links. This help adapting, probably optimizing, the internal moment arm of the extensor and flexor muscles during motion. This allows a more effective utilization and a more compact placement of the actuators (muscles).

During motion, the conjugate surfaces of the connected members always roll and slide. These offsetting arthrokinematics seem to help limiting the magnitude of relative translation of the limbs (with respect to a simpler rolling motion), thus allowing for a more compact joint architecture.

## 2.2 Analysis of Biological Joints as Real Organs: Active Mechanisms

In Section 2.1, biological joints have been considered as simple passive mechanisms. However, conversely to traditional joints, they are organs and, in order to comprehend their full advantage, they have to be considered as active systems. In this framework, the role of components such as ligaments, tendons, cartilage and capsules is augmented and each element gains a new level of importance.

The idea of joints as organs goes a step further from emphasizing the immediate mechanical relationships between the components, i.e. how the presence or the absence of one element affects the mechanics of the entire joint. Indeed, from a biologically perspective, a joint has the ability to adapt when boundary conditions change and even when one of its components fails. It is indeed observed that a disturbance in the joint mechanics causes adaptive responses of all the joint components which act in order to restore the loss of functional ability [25].

Organs operating inside the body can only function within narrow ranges of environmental conditions. An organism continuously receives perturbations from external forces and thus, in order not to be damaged, organs work actively so as to control and preserve their internal state. In physiology, this active process is often referred to as homeostasis. It is clear that preserving homeostasis becomes the major driving force underlying many, if not all, physiological functions of the body [25]. In a healthy individual, internal stability is maintained by the control systems that stimulate corrective responses after a homeostatic disruption has been detected. In the case of biological joints, homeostasis consists in joint stability. Inherently, joint stability is a complicated physiological process which goes beyond the purely mechanical aspects described in Section 2.1. The fact that many individuals, after a joint injury which impairs the joint mechanical stability, return to pre-injury levels through a proper neuromuscular training [26-28] suggests that some active compensatory mechanism must be developed in order to provide the joint with the supplemental stability shown.

In this context, the process of maintaining joint stability has to be understood as a complementary action between a passive and an active component. Thus, when talking about biological joints, two different definitions arise: passive stability, also called “clinical stability” and which may be not representative of the ability of the joint to perform a given task, and active stability, also called “functional stability”, which is instead fully representative of the ability to perform a given task.

Passive stability comes from the passive mechanical properties of ligaments, joint capsules, cartilage and bone’s conjugate surfaces [31]. This has been described in Section 2.1.

Functional stability comes from the mutual contribution between passive stability and neuromuscular control. That is, the reflexive response of the muscles, which cross the joint, is the active mechanism the body uses to preserve or restore joint homeostasis. Functional joint stability is provided by a complex system which is called sensorymotor system [29]. The sensorymotor system is a subcomponent of the motor control system of the body. Its role is to encompass all the sensory, central integration and processing activities involved in maintaining joint homeostasis while the body is moving (i.e. functional joint stability). In practice, the sensorymotor system operates through neuromuscular control. Neuromuscular control determines the muscle activation and, from a joint stability perspective, it governs the unconscious placement of the active restraints which are needed in preparation for and in response to joint constrained motion and loading in order to maintain and restore homeostasis of the overall system [30]. The active restraints are elicited in form of muscle reflexes. For example, when throwing a ball with the hand, a particular muscle activation sequence occurs in the rotator cuff muscles in order to ensure that the optimal gleno-humeral alignment and compression required for joint stability are provided. These muscle activations take place unconsciously and simultaneously with the voluntary muscle activation which, conversely, is only associated with a particular task (i.e. aiming, speed, distance).

For neuromuscular control to be effective, it is essential to have information concerning the status of the joint and its associated structures. Such information is referred to as proprioceptive. Proprioception correctly describes

all the afferent information that arise from internal peripheral areas (proprioceptors) of the body and that contribute to unconscious sensations (which are related to postural control and joint stability) as well as to several conscious sensations. Conscious sensations are also referred to as “muscle sense” [32] and comprise the sense of movement (kinesthesia), the sense of joint position, the sense of force and the sense of timing of muscular contraction [33]. In practice, these sensations arise from the integration, at different levels of the nervous control system, of the afferent proprioceptive information that arises from the discharge of the mechanoreceptors which are located in various areas of the body [34, 35].

Mechanoreceptors responsible for these proprioceptive information are primarily found in muscles, tendons, ligaments and capsules [30, 34, 36, 37, 38], with the mechanoreceptors located in deep skin and fascial layers being theorized as supplementary sources. The mechanoreceptors located in deep skin and fascial layers are indeed traditionally associated with tactile sensations [34, 37].

In addition to the essential role in maintaining functional joint stability, proprioception is also critical in executing conscious activities. Indeed, critical to effective motor control is the accurate sensory information which concerns both the external and internal conditions of the body [30, 39]. During goal directed tasks, such as picking up a box while walking, provisions must be made to adapt the motor program for walking changes which may occur in the external environment (e.g. an uneven ground) and in the internal environment (e.g. a change in the center of mass). In live beings, these provisions are stimulated by several sensory triggers. Although some of the afferent information may be redundant across all the sensory sources (proprioceptive, visual and vestibular), specific unique roles are associated with each source that may not be entirely compensated for by the other sensory sources.

The role of proprioceptive information in motor control can be separated in two categories. The first one involves the role of proprioception with respect to the external environment. Motor programs which govern the execution of given activities often have to be adjusted to accommodate for unexpected perturbations or changes in the external environment. Although the source of this information is usually associated with a visual input, there are many circumstances in which the proprioceptive input is the quickest or the most accurate or both [30]. In this context, proprioception has been described as essential during the execution of movements to update the primary commands which derive from the visual image [40, 41]. The second category of roles proprioceptive information plays in motor control is related to the complex mechanical interactions which exist between the components of the musculoskeletal system. Here, proprioception best provides the motor control system with the needed segmental force, movement and position information.

### **2.3 Analysis of Biological Joints: Ligaments as Key Elements for Functional Stability**

According to the literature [42], ligaments are the primary stabilizer of diarthroses. Ligaments connect articulating bones across a joint, guide the relative movement between bones and maintain joint congruence. Ligaments are made by collagen fibers and, usually, several structures (such as capsule, menisci and muscle tendons) blend with and reinforce them.

Study of the mechanical behaviour of ligaments through the analysis of the load-elongation curve of their fibers provides important information on how they work. The main tensile resisting substance in the ligament is collagen. Collagen is a tough material which permits very little deformation when stressed. However, under low

forces, collagen has a crimped shape. This provides the ligament fibers with some extensibility at the beginning of their tensioning. As a result, the first region of the force-deformation curve of a fiber is concave-shaped (the “toe zone”). As tension is added, the crimps gradually flatten out. Once no more crimps can be removed, an even-increasing amount of force is required for further stretching the tensioned fiber. Then, with increasing loads, more ligament fibers are recruited. When the recruitment of all the fibers is complete, the stiffness behavior of the ligament becomes more linear (the “linear zone”) and it remains as such until some fibers fail [45] (the “failure zone”). A typical displacement-force curve of a ligament is depicted in Fig. 2.2.

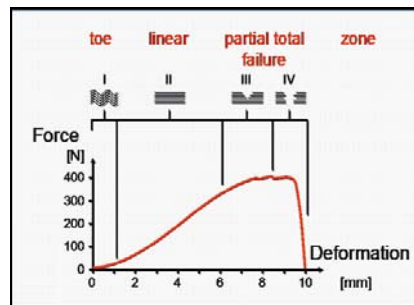


Figure 2.2 Typical Force-Deformation Curve of Ligaments

The effective amount of strain and stress that develop in the ligaments varies depending on joint position and joint stress. It is estimated that the strain in ligaments during normal activities such as walking or running ranges from 2% to 5% [46]. However, when at the end-point of joint motion, ligaments become highly stretched. Indeed, in the locked position of the knee, i.e. after the “screw home” motion has occurred, lateral ligaments are stretched roughly 20% beyond their length at full extension.

Although from a kinematic point of view ligaments may be considered as isometric thin cables [16, 43, 44], in reality, they have different and, eventually, quite complex shapes. They can be flat broad structures sub-divided in multiple parts (like the medial collateral and the cruciate ligaments of the knee joint), or, more simply, round shaped strong cords (like the lateral collateral ligament of the knee joint). As a matter of fact, the collagen fibers of a ligament can twist upon one another thereby forming spiraling fascicles, or bundles. Bundles can slide one with respect to the others. Ligaments have broad attachments on the connecting bones. As the joint undergoes motion, the length and orientation of the bundles generally change. The broad attachments, combined with the sliding of the fascicles, allow ligament bundles to be relatively taut or slack depending on the position of the joint. Indeed, in a ligament there exist fascicles that remain of the same length and taut throughout the full range of motion of the joint. Such fascicles are called “guiding bundles”, i.e. they guide the kinematics of the joint. The rest of the fascicles are referred to as “safety bundles”. Their main role is to convey certain solidity to the joint in addition to the permanent solidity which is granted by the guiding bundles. Further, if the movement which has tensioned a bundle is associated to a constant increase in the length of its fibers, then the bundle stops the movement and the joint is in an extreme position. Bundles of this type are referred to as “limiting bundles”.

The distinction in bundles holds for all ligament types. As first example, referring to Fig. 2.3, consider the anterior cruciate ligament (ACL) of the human knee joint. The ACL presents a cross-shaped architecture and comprises several fascicles which are taut or slack depending on the position of the joint. The anterior bundle of the ACL is a driving bundle which remains taut throughout the full motion of the knee. The rest of the fascicles

are safety bundles. In particular, the posterior bundle of the ACL acts also as limiting bundle. Indeed, the posterior bundle is rather relaxed in flexion and becomes tauter as the knee is extended. It blocks the motion as the knee reaches the fully extended position (0 deg. of flexion).

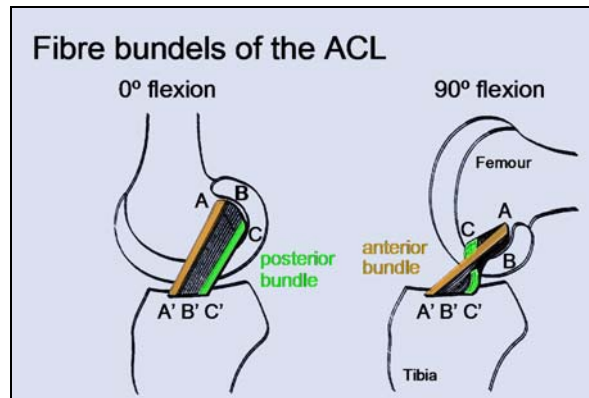


Figure 2.3 Knee Joint: Fiber Bundles of the Anterior Cruciate Ligament (ACL)

As second example, referring to Fig. 2.4, consider the medial collateral ligament (MCL) of the human knee joint. During extension, all the bundles of the MCL are in tension while, during flexion, the posterior bundle (safety bundle) relaxes and the anterior bundle (guiding bundle) retains its length.

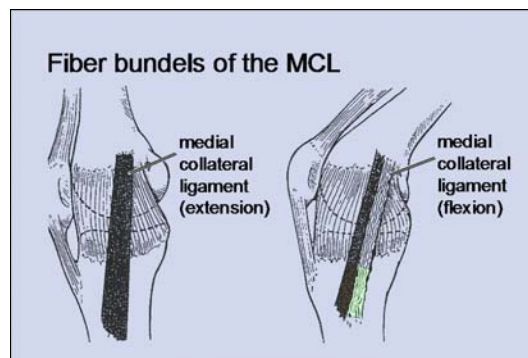


Figure 2.4 Knee Joint: Fiber Bundles of the Medial Collateral Ligament (MCL)

Summarizing, the bundles of the ligaments limit the available range of motion of the joint by gradually increasing the resistance to movement. This realizes a “soft stop” action, but also allows different portions of ligaments to take up stress at different angles of force so as to increase the force workspace that can be surely resisted by the joint in different configurations. Indeed, note that uniform stress is seldom achieved in a ligament.

To this point, we have focused only on the passive properties of ligaments. However, another fundamental role of ligaments is played in the context of proprioception and functional stability. In order to put this in evidence an example is provided. Consider the knee and let us focus on the ACL. The major mechanical (passive) function of the ACL is to prevent excessive anterior tibial translation. Indeed, according to [47], in certain degrees of flexion the ACL provides up to 85% of the restraining force to anterior tibial displacement. The complete failure of the human ACL occurs at stress levels of about 1725 N, while bone avulsions and ligament micro-failures occur at lower stress levels [48]. However, it has been demonstrated in vitro that during strenuous activities such as downhill skiing, the load on the knee joint and its ligaments may substantially exceed the aforementioned potential injury levels [49]. Thus, it is evident that the knee joint must rely on some mechanism other than the

passive mechanical resistance properties of its ligaments. Such mechanism is the active motroneuron control. Motorneuron control heavily relies on the ability of the mechanoreceptors inside and/or surrounding the joint to sense destabilizing effects. It is as far back as 1944 that researchers conjectured that ligaments supply fundamental input information that makes neuromuscular control of the knee joint possible [50]. As a matter of fact, it has been histologically demonstrated that ligaments contain mechanoreceptors that can detect changes in tension, speed, acceleration, direction of movement and position of the joint [51-53]. Moreover, with respect to injuries, it is observed that functional instability is often a consequence of torn ligaments. Of course this is associated to the diminished mechanical stability (one or more kinematic constraints are relaxed), but evidence shows that it is also related to the altered neuromuscular functions which follow from the reduced proprioceptive information [54, 55]. Other proofs of the importance of ligament mechanoreceptors on joint stability can be found in [38, 54, 55]. These papers show how, despite unaltered mechanical stability, functional stability can be impaired, in the early times, after ligament reconstruction by artificial means and after ligament anesthetization. Additionally, as for the knee, there is also the evidence [56] that the strain in the ACL is related not only to position but also to quadriceps muscle contraction. Less strain occurs with co-contractions of both the quadriceps and the hamstring muscle groups. This indicates that muscles contractions and co-contraction contribute to the stability of the knee joint by increasing the stiffness of the joint.

It is worth mentioning that due to the high redundancy of the mechanoreceptors which are spread around the joint, it is also shown that after ligament impairment, the overall proprioceptive information can be restored and the sensorymotor system can adapt so as the joint regains functional stability in later times [57-59].

Beside functional stability, altered “muscle sense” (in particular the inability to reproduce passive positioning and to detect passive motion) is another effect that has been observed after ligament injuries [60-61].

## Chapter 3

### Novel Types of Biologically Inspired Mechanisms

#### 3.1 Introduction

Chapter 1 presented the state of the art and the limits of the traditional joint technology referring, in particular, to the field of environment interaction robotics. Chapter 2 analyzed the main features and functionalities biological joints have which render them perfectly suited to environment interaction and other tasks. In practice, biological joints offer a wealth of interesting design and control solutions environment interaction and traditional robotics may take cue from.

Among the properties biological joints feature, in this research work, we are mainly interested in the high strength-to-weight and strength-to-encumbrance ratios, in the selective and controllable compliance, in the high dynamic capabilities, in the inherent multifunctionality (i.e. the ability of the joint structural elements not only to constrain joint kinematics but also to sense joint homeostasis) and in the inherent adaptability (i.e. the ability of the joint structural elements to react against disturbances so as to preserve joint homeostasis).

In this chapter, we first define a novel feasible biologically inspired (BI) articulation concept which features the aforementioned selected properties. Then, we investigate the availability of and devise mathematical tools for the synthesis of new mechanisms based on this articulation concept. Finally, we show how these tools can be used in order to synthesize a novel two-dof spherical mechanism which wants to replicate the practical (or prevalent) motion allowed by the knee joint (for controversies which may arise due to the number of degrees of freedom we attribute to the knee joint, the reader is demanded to Section 2.1). The novel mechanism is called “ATWOKI”, where the name stands for “Almost TWO degrees of freedom Knee-Inspired”. The word “Almost” is used for emphasizing the stiffness advantages related to the novel articulation concept. In practice, it means that despite the compliance of the elements which makes the mechanism, it only has two practical (or prevalent) degrees of freedom. Such degrees of freedoms are the ones the mechanism would retain if considered as perfectly rigid.

#### 3.2 Diarthroses Inspired Articulation Concepts

##### 3.2.1 Basic Idea

Two main types of mechanisms exist: serial mechanisms and parallel mechanisms. The serial mechanism is an open-ended structure consisting of several links connected in series; the end links are called base and platform, respectively. The parallel mechanism is a closed-loop kinematic chain made up of two bodies, i.e. the base and the platform, connected by at least two independent kinematic chains (usually called legs). Examples of serial and parallel mechanisms are depicted in Fig. 3.1 and Fig. 3.2, respectively.

In this perspective, diarthroses can be considered as parallel mechanisms. In particular, the joined bones are assumed as the mechanism base and the platform, while bone-to-bone couplings and ligament bundles (driving bundles, safety bundles and limiting bundles) are deemed as the mechanism legs. The parallel architecture of diarthroses can be understood by comparing Fig. 3.3, which depicts the anatomic structure of the human knee mechanism, and Fig. 3.1. (Fig. 3.3 is a courtesy from [www.skisocal.org](http://www.skisocal.org)).

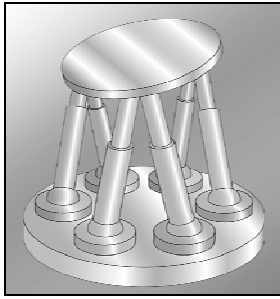


Figure 3.1 Parallel Mechanism

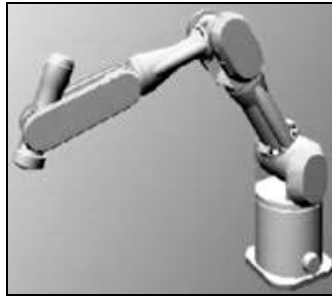


Figure 3.2 Serial Mechanism

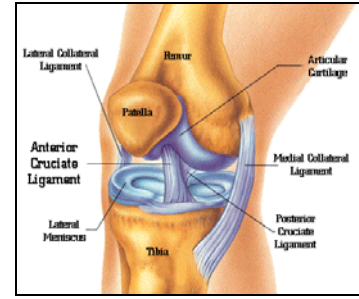


Figure 3.3 Human Knee Mechanism

Due to the large number of legs, i.e. bone-to-bone couplings and ligament bundles, diarthroses are extremely redundant mechanisms. The legs have different compliance which is tailored to the role they play in the joint. The stiffer legs constrain the diarthrosis arthrokinematics and bear the major quote of the forces which are produced by the joint motion and which are exerted from the outside of the joint. Conversely, the softer legs help stabilizing the joint, protect the joint from dangers and bear a minor quote of the aforementioned forces. Stiffer legs comprise ligament driving bundles and bone-to-bone couplings.

Driving bundles are flexible but almost inextensible. They can be thought as wireropes which are relatively-stiff under traction and fold under compression. A ligament bundle connects two articulating bones (one articulating bone per bundle end). As a matter of fact, a driving bundle provides a unilateral constraint which limits the motion of the bundle-to-bone attachment point of one articulating bone to stay within a sphere, which is centered at the bundle-to-bone attachment point of the other articulating bone and whose radius coincides with the length of the bundle.

Bone-to-bone couplings are high order pairs. They are unilaterally constrained pairs made of rigid conjugate surfaces whose contact is mediated by some relatively-stiff and low-friction means such as articular cartilage and fibrocartilage (e.g. menisci). Despite the variety and the complexity of the conjugate surfaces which can be found in nature, biomechanical studies show that the gross behavior of the contact between the bones of a given diarthrosis can be deemed equivalent to one or more sphere-to-sphere (SS) pairs. That is, from a motion perspective, diarthroses can be thought as parallel mechanisms made of SS pairs and wireropes.

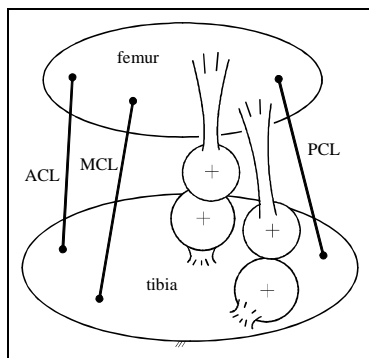


Figure 3.4 "SM" Model of the Knee Mechanism

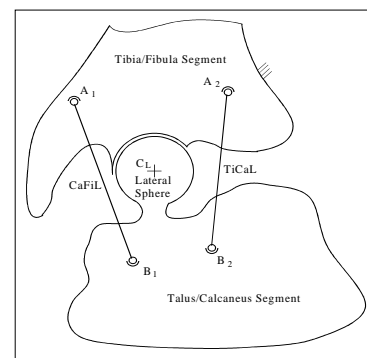
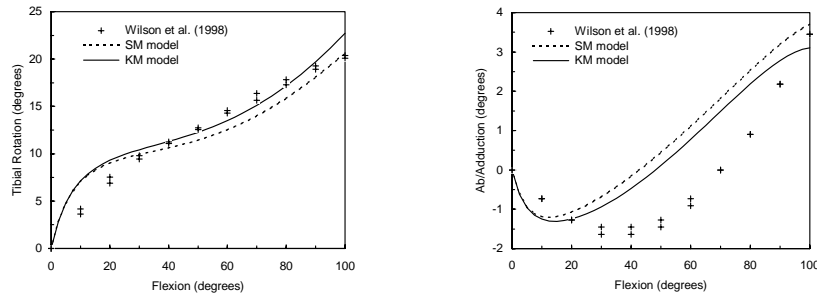


Figure 3.5 "KM2" Model of the Ankle Mechanism

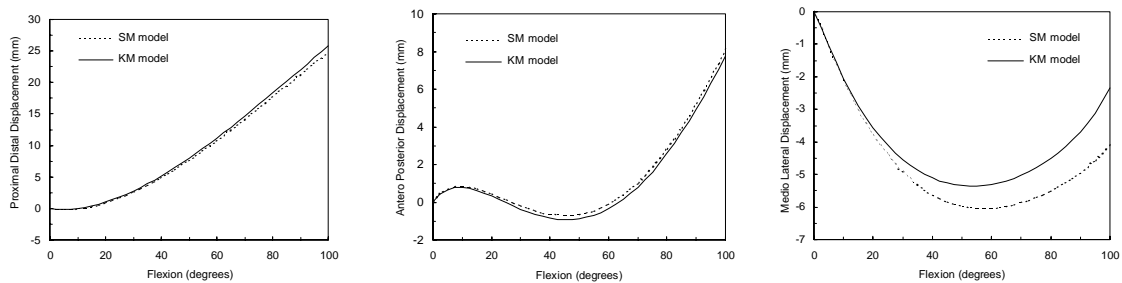
Examples of mechanisms used for the practical modeling of biological joints are given in Fig. 3.4 and Fig. 3.5. The figures depict, respectively, the “SM” model (mechanism) of the knee joint and the “KM2” model (mechanism) of the ankle joint which have been proposed in [44, 65] for the study of the passive motion of the respective biological joints.

The effectiveness of these mechanisms to adequately model the biological joint counterparts is demonstrated by the plots reported in Figs. 3.6-3.8.



Figures 3.6 Knee Joint Passive Motion: Experimental Data (Wilson et al.) vs. Simulated Data (“SM” and “KM” models)

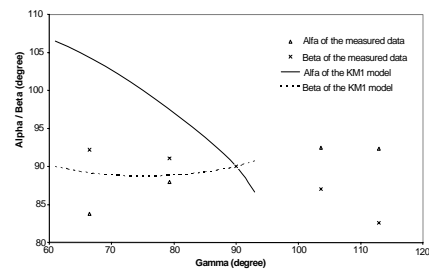
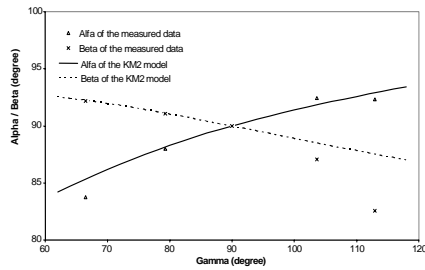
Figures 3.6 show the ability of the “SM” model to mimic the passive motion of the knee joint as measured through in-vitro experiments by Wilson et al. (1998). Figures 3.6 also show the simulation data obtained with the “KM” mechanism which, conversely to the “SM” mechanism, models the contact between femour and tibia by means of two sphere-to-ellipsoid pairs instead of two sphere-to-sphere pairs. A picture of the “KM” mechanism is given in Fig. 3.9.



Figures 3.7 Knee Joint Passive Motion: “SM” model simulated data vs. “KM” model simulated data

From figures 3.6 and 3.7 it can be seen that, despite the use of more complex shapes of the bone’s conjugate surfaces, the ability of the “KM” to model (Fig. 3.9) the passive behavior of the knee joint (Fig. 3.3) is rather similar to that of the simpler “SM” mechanism (Fig. 3.4).

Figures 3.8 confirm the ability of the “KM2” model to mimic the passive motion of the ankle joint given according to measured data obtained from an in-vitro experiment. The left plot shows the results obtained by the “KM2” mechanism (Fig. 3.5), while the right plot shows the ability of the “KM1” mechanism which, conversely to the “KM2” mechanism, models the contact between the tibia/fibula and talus/calcaneus segments by means of three plane-to-sphere pairs instead of one spherical pair (a particular type of SS pair). A picture of the “KM1” mechanism is given in Fig. 3.10.



Figures 3.8 Ankle Joint Passive Motion: Experimental Data vs. Simulated Data (“KM1” and “KM2” models)

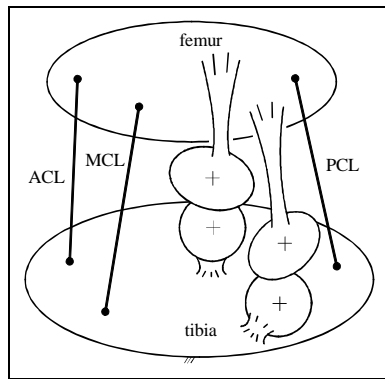


Figure 3.9 “KM” Model of the Knee Mechanism

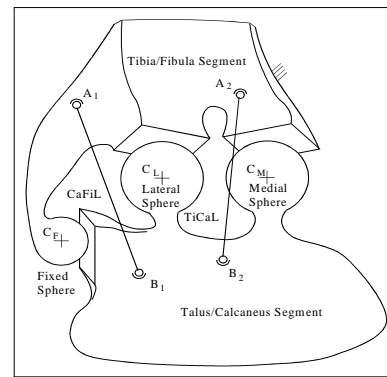


Figure 3.10 “KM1” Model of the Ankle Mechanism

### 3.2.2 Practical Articulation Concept

In the previous subsection, we have shown that diarthroses can be viewed as parallel mechanisms made of SS pairs and wireropes. As a consequence, the design of a novel BI joint can be reduced to the synthesis of a parallel mechanism which has base and platform connected by means of unilaterally constrained connections, i.e. SS pairs and wireropes. However, by means of biological and mechanistic considerations, a simpler and more practical design principle can be devised.

In a healthy diarthrosis, due to the inherent compliance of the elements it is featured by, a certain degree of preloading exists such that, during normal operating conditions, the ligament driving bundles always act under traction and the bone’s conjugate surfaces do not detach. This causes both the ligament driving bundles and the bone-to-bone connections to behave, in practice, as bilateral constraints. Thus, from the kinematic point of view, ligament driving bundles can be considered as stiff rods. In particular, due to the inherent flexibility of the ligament bundles, that is the inability to withstand torques in any direction, these stiff rods can be thought as being connected to the bones, i.e. to the base and to the platform, by means of a spherical S joint at one end and by means of a universal U joint at the other. Besides, also the SS pairs can be substituted by stiff rods connected to the base and to the platform by means of a spherical S joint at one end and by means of a universal U joint at the other. Indeed, a bilaterally constrained SS pair is equivalent to a connection which is made by a rod that has a spherical S joint placed at the center of one of the spheres of the SS pair and a universal U joint placed at the center of the other sphere of the SS pair.

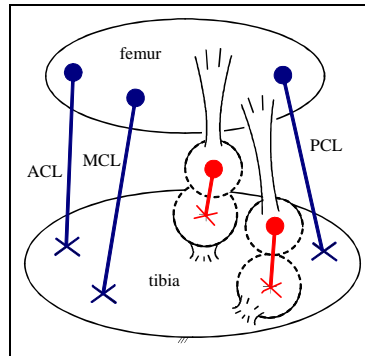


Figure 3.11 Practical Knee Inspired Articulation Concept

An example of practical mechanism inspired by the biomechanical analysis of the knee joint and obtained, through the aforementioned considerations, from the “SM” mechanism depicted in Fig. 3.4 is shown in Fig. 3.11. Blue lines represent the stiff rods which replace the ligament driving bundles. Besides, red lines represent the stiff rods which replace the SS pairs. The dot at the end of each rod indicates the spherical S joint which connects the rod to either the base or the platform. Conversely, the crossed lines at the end of each rod indicate the universal U joint which connects the rod to either the platform or the base. Note that, providing the leg with a U joint at one side and a S joint at the other, it is not important whether a joint type is attached either to the base or to the platform.

As a result, the design of a BI joint can be reduced to the synthesis of a parallel mechanism which has the base and the platform connected by means of a certain number of rods through spherical S joints at one end and by means of universal U joints at the other. Hereafter, the rods will be called structural legs also.

### 3.3 Idea and Tools for the Rational Synthesis of Biologically Inspired Joints

In Section 3.2 we showed a biologically inspired (BI) articulation concept, hereafter called US parallel mechanism (US\_PM). It is a parallel mechanism made by two bodies, i.e. the base and the platform, which are connected by means of a certain number of legs of fixed length through spherical S joints at one body and through universal U joints at the other body. A schematic of the US\_PM is depicted in Fig. 3.12.

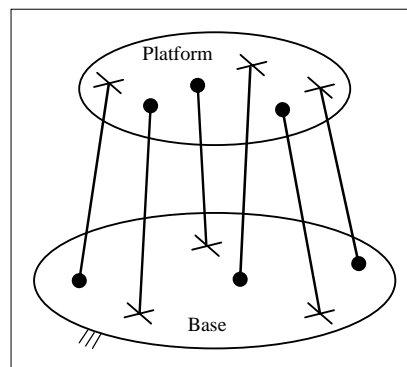


Figure 3.12 Biologically Inspired (BI) Articulation Concept: the US Parallel Mechanism (US\_PM)

The synthesis of a BI mechanism consists in finding the locations in the base and in the platform of the U joints and of the S joints so that the assembly of the rods fits within the desired relative motion of the base and the platform. In the context of kinematics this problem can be recasted into the synthesis of architecturally singular UPS parallel manipulators (UPS\_PMs) which have to satisfy desired self-motions.

### 3.3.1 Fully Parallel Manipulators: Architecture, Singularities and Self-Motions

A UPS\_PM is depicted in Fig. 3.13. In particular, the figure shows a 6-UPS\_PM. As a matter of facts, it is a fully parallel manipulator with 6 legs of UPS type. Fully parallel manipulator means a device made of a base and a platform which are connected by means of  $n$  equal kinematic chains (in figure  $n = 6$ ). Here, the kinematic chains consist in UPS-legs which are made of two links coupled together by a prismatic P joint and which are connected to the base and to the platform by means a spherical S joint at one end and by means of a universal U joint at the other. Note that in Fig. 3.13 the P joints are depicted as telescopic legs, the S joints as dots and the U joints as crossed lines.

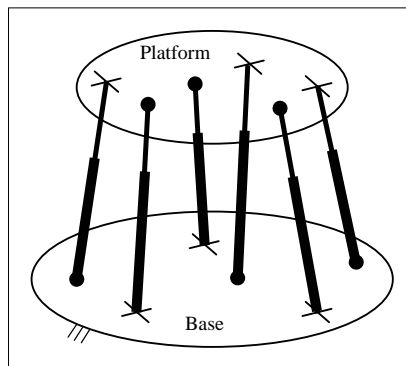


Figure 3.13 6-UPS Parallel Manipulator

The 6-UPS\_PM has 6 degree-of-freedom (dof) if all the P, U and S joints are unlocked, while it has, in general, none dof if all the P joints are locked. Indeed, if special configurations do not occur, from the Grubler's formula the mobility  $m$  of the  $n$ -UPS\_PM with all the P joints locked follows as

$$m = (6 - n). \quad (3.1)$$

If  $m > 0$ , the manipulator is movable with degree of mobility equals to  $m$ . Conversely, if  $m \leq 0$ , the manipulator becomes a structure and  $m$  stands for the degree of static indeterminacy. In particular,  $m = 0$  holds for an isostatic structure, while  $m < 0$  holds for a hyperstatic structure.

A singularity is a special configuration of the mechanism where Eq. (3.1) does not hold. In particular, despite all the P joints are locked, the manipulator has a mobility  $m$  such that

$$\{[m > (6 - n)] \wedge [m > 0]\}. \quad (3.2)$$

That is, a singularity is a configuration in which the manipulator gains some degree of mobility. In particular, if  $n \geq 6$ , a singularity is a configuration in which the structure corresponding to the  $n$ -UPS\_PM with all the P joints locked is shaky or movable. Usually, singularities occur in few configurations of the manipulator. That is,

the singularity loci are surfaces within the manipulator workspace. However, if the attachment points of the UPS legs are located according to certain geometries over the base and over the platform, respectively, singular configurations can span over the whole workspace or a significant part thereof. Manipulators of this type are called architecturally singular UPS\_PMs [66].

An architecturally singular UPS\_PM is a manipulator with a continuous realm of singularity positions, therefore being shaky in every configuration it can reach. However, a manipulator which is architecturally shaky for arbitrary six dimensional relative displacements between base and platform means more than mere shakiness. It means that, despite all the actuators are locked, the manipulator is already finitely mobile within its prospective workspace [67]. As a consequence, architecturally singular UPS\_PMs are also called architecturally mobile UPS\_PMs. The motions performed by such manipulators are usually referred to as self-motions and can be understood as any continuous motion of the UPS\_PM with all the leg lengths remaining constant [68], i.e. with all the P joints locked. In practice, such movements are possible because, due to the particular locations of the U joints and S joints on the base and on the platform, all the legs fulfill an assembly condition which fits into a motion such that every leg takes part in the motion prescribed by the others.

Architecturally singular UPS\_PMs and self-motions are not new paradigms. In particular, the latter have a precise historical dimension in which they are known as Borel-Bricard motions. Indeed, self-motions are related to the spherical motion problem, i.e. a class of continuous motions where some points on a rigid body are constrained to remain on the surface of as many given fixed spheres. As a matter of facts, such motions were addressed, in part, by Borel and Bricard [69, 70] in a mathematical competition (Le Prix Vaillant) organized by the French academy of Science in 1904.

In the robotics literature, self-motions of UPS\_PMs were not treated before Husty and Zsombor-Murray [71]. Systematic investigations of architecture singularity and self-motions started with Karger and Husty [72]. To date, the study on architecturally singular UPS\_PMs and self motions has been carried on extensively. The tools for addressing such problems together with the most important architectures are summarized in [68, 73-75].

### **3.3.2 Self-Movable UPS Parallel Manipulators and Biologically Inspired UP Parallel Mechanisms**

Despite the very successful results of the aforementioned studies, the potentials of architecturally singular manipulators and self-motions have not been fully exploited yet. Indeed, to date, the tools for their synthesis have been applied only to the construction of traditional UPS\_PMs in order to avoid architecturally singular configurations beforehand in the design process. Instead, the concept of self-movable parallel manipulators has not been employed, at least consciously or explicitly, in order to build innovative robotic devices. This is so because, within the context of traditional robotics, architecturally singular UPS\_PMs are considered the worst devices and are deemed useless since they cannot be controlled directly. In fact, because of their geometry, such manipulators fail to transfer a full wrench from the actuated P joints of the UPS-legs to the base and to the platform, therefore being unable to completely balance external and inertial loads which act on them.

Conversely, on the light of the articulation concept inspired by the biomechanical analysis of diarthroses, the theoretical conjectures regarding architecturally singular manipulators and self-motions can be used for the rational development of novel mechanisms. Indeed, as we mentioned, architecturally singular UPS\_PMs are movable for almost every fixed length of the UPS-legs they are built by. Besides, for a given set of fixed leg

lengths, a UPS\_PM corresponds to a US\_PM (compare Fig. 3.12 and Fig. 3.13). Therefore, by merging together the theoretical conjectures regarding self-movable UPS\_PMs and the conceptual idea of biologically inspired US\_PMs, self-movable US\_PMs can be conceived to be used as unconventional joints for innovative robotic devices.

The parallel and eventually redundant architecture of these mechanisms should allow the realization of very compact multi-dof joints characterized by: 1) high strength-to-weight and strength-to-encumbrance ratios; 2) selective and controllable compliance; 3) high dynamic capabilities; 3) inherent multifunctionality, i.e. the ability of the joint not only to guide the motion but also to sense motion parameters, solicitations and disturbances; 4) inherent adaptability, i.e. the ability to react to solicitation and disturbances; 5) easy deployability. Note that the features (3-5) can be rather easily implemented if multifunctional elements (e.g. rods and wires made by piezoelectric ceramics, magnetostrictive and superelastic/shape-memory alloys, and electroactive polymers) are used as structural components.

Observe that, different than UPS parallel manipulator, the self-movable US\_PM is a mechanism which does not comprise actuators. Of course, in order for the joint degrees of freedom to be controlled, say  $m$  the number of dof,  $m$  actuators in parallel to the  $n$  US legs of the US\_PM must be placed between the mechanism base and the platform. For instance, this can be done by using  $m$  UPS-legs (the  $\underline{P}$  joint being actuated) which are placed so that each one of them does not fit into the motion prescribed by the other  $(m+n-1)$  legs once all the actuated  $\underline{P}$  joints are locked.

In order to point up the idea and to ease the understanding, in the following we provide with an example which shows how self-movable US\_PMs can be used to devise simple but useful unconventional mechanisms. Consider the “Wren’s Platform” depicted in Fig. 3.14.

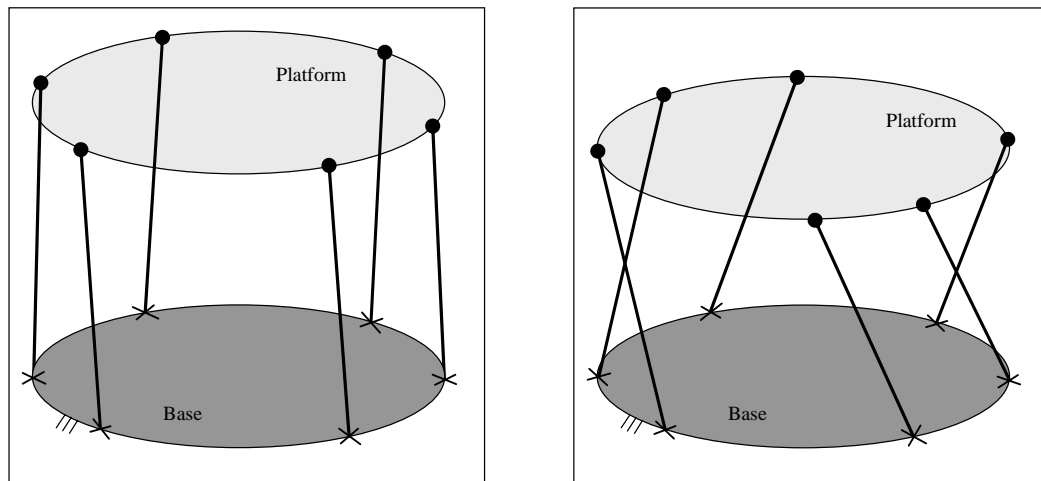


Figure 3.14 The “Wren’s Platform” and the corresponding 1-dof Self-Motion

The mechanism consists of a base and a platform connected by equal US-legs (figure depicts only 6 of these legs) whose universal and spherical joint centers are located on equal circles over the base and over the platform, respectively. Independently on the number of legs, for all the configurations in which the legs are not parallel to each other, the “Wren’s Platform” is a self-movable US\_PM with finite mobility  $m = 1$ . Indeed, according to the

speculations by Sir Christopher Wren (which used the homonymous mechanism to show that the one-sheeted hyperboloid of revolution contains straight lines), the axes of the US-legs lie on a linear line complex for any relative displacement of the platform with respect to the base. That is, the “Wren’s Platform” has 1-dof self-motion which consists in a screw motion about a fixed axis which coincides with the central axis of the linear line complex. As for the possible applications, due to the allowed screw motion, the “Wren’s Platform” can be used as a transmission from linear motion to rotary motion and vice-versa, thus offering an alternative to the more traditional gears or ball screws systems. Control of the motion of the system can be accomplished by the addition of a UPS-leg (the P joint being actuated) which is placed so that its axis does not belong to the linear line complex defined by the other US-legs. As shown in Fig. 3.15, a possibility consists in placing the actuated UPS-leg along the central axis of the linear line complex (In figure, the actuated UPS leg is depicted in blue).

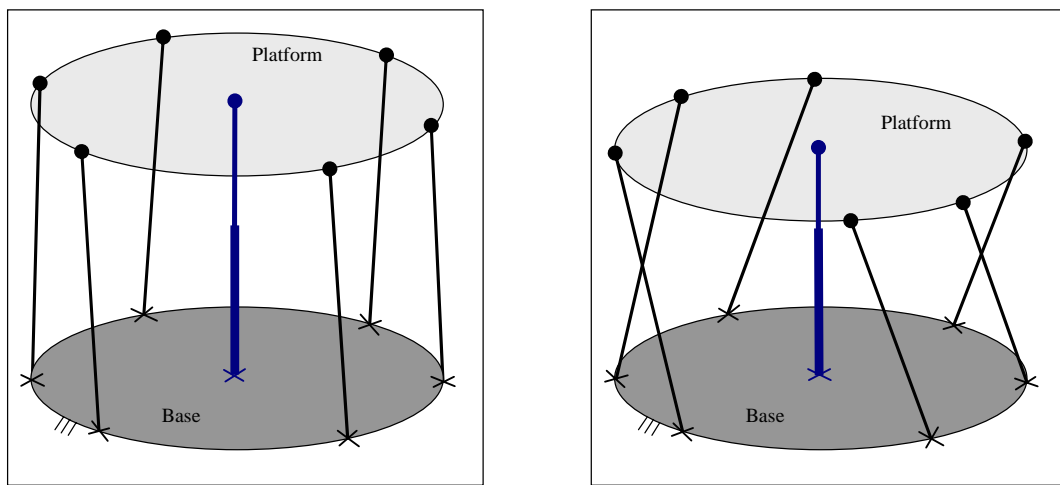


Figure 3.15 Actuated “Wren’s Platform” mechanism

Though derived through far less general speculations than BI self-movable US\_PMs, a practical and successful application of this transmission principle can be found in the Jacobsen’s “Linear to Angular Displacement Device” (LADD) and “Concentric LADD” (CLADD) [76]. The LADD and CLADD transmissions are depicted in Fig. 3.16 (figure from [77]). They are transmission for converting rotational to translational motion.

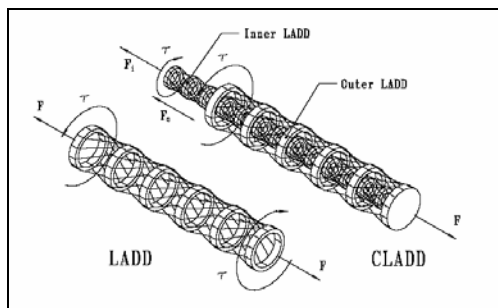


Figure 3.16 LADD and CLADD transmissions

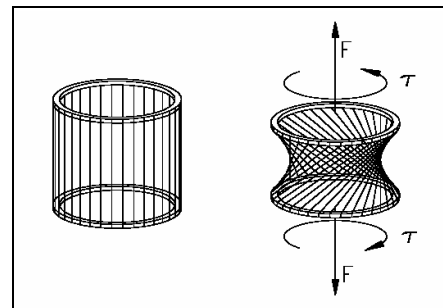


Figure 3.17 LADD cell element

The basic element of LADD and CLADD is the single cell depicted in Fig. 3.17 (figure from [77]) which consists of two rings joined by high strength fibers. The behavior of this single cell describes the LADD's basic operating characteristics. As the cell is twisted, the distance between the rings decreases, thus rotary motion is translated to linear motion. Conversely, if a twisted cell is subjected to a linear displacement it will unwind, producing rotation. Concentric LADD (CLADD) transmissions are composed of two sizes of multi-stage LADDs placed coaxially inside one another as shown in Fig. 3.16. In a CLADD actuator system, a stationary motor rotates one end of the inner LADD. The remaining end of the inner LADD is rigidly connected to one end of the outer LADD. At this connection point the inner and outer LADDs rotate and translate together; this connection is also where the external load is applied. The remaining end of the outer LADD is fixed (no rotation or translation) at a position close to the motor. The major advantage of a CLADD over the single LADD chain is the elimination of the linear slider mechanism at the load end which is necessary to maintain the torque differential across the cells. Instead, the reaction torque of the CLADD cells occurs near the motor where the torque was initially generated. Now the load end of the CLADD must be permitted to rotate freely. The key advantages of LADDs and CLADDs compared to more traditional transmissions, like gears or ball screws, are their high strength, low weight, high efficiency, absence of lubricants and low cost. Indeed, LADDs and CLADDs could be manufactured quite inexpensively. Furthermore LADD and CLADD based systems integrate very well and thus result in tight packaging. These properties make LADD and CLADD systems highly attractive in both robotics and prosthetic applications [77].

### 3.3.3 Tools for the Synthesis of Biologically Inspired Self-Movable US Parallel Mechanisms

As described in the previous subsection and as exemplified in Fig. 3.15, self-movable US<sub>PM</sub>s can be used conveniently as mechanical transmissions for converting the linear motions of actuated UPS legs (the P joint is actuated) into complex relative motions of the US<sub>PM</sub> base and platform. Note that the actuated UPS legs are placed in parallel to the structural (rods of fixed length) US-legs of the US<sub>PM</sub>. In this context, the key-point consists in synthesizing self-movable US<sub>PM</sub>s which allow for desired motions of the platform with respect to the base. This subsection is aimed at devising the tools for the rational synthesis of self-movable US<sub>PM</sub>s.

As said, the study of architecturally singular and self-movable UPS<sub>PM</sub>s is a very well addressed topic in the literature. As for the design issues, the following approaches exist for the generation of architecturally singular UPS<sub>PM</sub>s:

- a) The first is the method based on the determinant of the Jacobian matrix [78]. A self-movable UPS<sub>PM</sub> is obtained when the parameters, which describe the locations of the U joints and of the S joints on the base and on the platform, make the determinant of the Jacobian matrix vanish independently on the relative location of the base and of the platform.
- b) The second is the method based on linear manifolds of correlations and on quadratic transformations [73]. A self-movable UPS<sub>PM</sub> is obtained when the centers of their U joints and the S joints are conjugate points with respect to three-dimensional linear manifolds of correlations.
- c) The third is the method based on the forward displacement analysis [79]. A self-movable UPS<sub>PM</sub> is obtained when the parameters, which describe the locations of the U joints and of the S joints on the base

and on the platform, and which describe the length of the legs, provide the mechanism with continuous solutions of the forward displacement problem.

- d) The fourth is the component approach [74]. The generation of self-movable UPS\_PMs is reduced to the generation of over-constrained components or architecturally singular components.

As a matter of fact, all these approaches only allow finding the conditions that the coordinates of the US-legs attachment points over the base and over the platform must satisfy for a UPS\_PM to be architecturally singular. Instead, these approaches do not allow synthesizing architecturally singular US\_PMs which have to perform desired/prescribed self-motions. This is a rather different problem which has been only partially addressed in the literature.

The problem of designing a mechanism that must perform a prescribed motion (the so called “body-guidance” problem) is indeed very difficult, particularly when special mechanisms, which have higher mobility than predicted by the Grubler’s formula, are concerned. The only existing results concern the problem of finding the values of the geometrical parameters of a mechanism which make it pass through a few prescribed precision points.

If the problem is planar, one has the classical Burmester problem: given five placement of a moving body in the plane, find the points of the moving body that lie on a common circle fixed in the plane. These points are called “circlepoints”, and the centers of the fixed circles are called “centerpoints”. The solution states that there are, in general, six centerpoint/circlepoints pairs. If only four placements are specified instead of five, one can get a centerpoint curve and a circlepoint curve, each of which are cubic [80].

If the problem is spatial, one has the Schönflies problem (a spatial generalization of the planar Burmester problem) which asks for the points of the body that lie on a common fixed sphere for several given placements of the body in space. The solution states that seven general positions determine twenty centerpoints/spherepoints pairs [81-83].

That is, to our knowledge, results concerning the issue of designing a self-movable US\_PM to follow a continuous trajectory rather than to pass through a few points only are not available. In the following, we suggest two methods that may be used to address the problem.

- Method 1 (adaptation of the procedure by Karger and Husty, 1998): It is based on the closure equations of the mechanism. Upon expression of the closure equations as a function of the parameters used to describe the desired motion, the synthesis problem amounts to finding the locations of the U and S joint centers, on the base and on the platform, of a set of US-legs, with unknown and constant lengths, whose axes (defined by the centers of the U and S joints) belong to a  $n$ -system of lines and which satisfy the closure equations for every set of given values of the motion parameters.
- Method 2 (adaptation of the procedure by Wohlhart, 2003): It is based on the virtual work principle. By considering the expressions of the velocity vectors of the attachment points of the US-legs on the moving platform as functions of the motion parameters and their first time derivatives, the synthesis problem amounts to finding the locations of the U and S joint centers, on the base and on the platform, of a set of US-legs, with unknown and constant lengths, whose axes belong to a  $n$ -system of lines which are

orthogonal to the aforementioned velocity vectors for every set of given values of the motion parameters and their derivatives.

The effectiveness of these methods is shown in the following subsection where they are applied in order to devise the 2-dof BI mechanism which is the main objective of this research work.

### 3.4 Synthesis of Practical 2-dof Spherical US\_PMs

The major aim of this research work is to conceive a novel spherical 2-dof US\_PM, hereafter called also ATWOKI (Almost Two degrees of freedom Knee Inspired) joint, which allows for two independent rotations, the first about an axis fixed to the base and the second about an axis fixed to the platform of the US\_PM. As said, such a motion resembles the prevalent motion performed by the biological knee joint.

In the frame of the work done by Jacobsen, ATWOKI might be thought as the first 2-dof linear-to-spherical mechanical transmission based on architecturally singular US\_PM. This is, indeed, what the biological knee does. It converts the linear motion of the muscles into a prevalent 2-dof spherical motion of the tibia with respect to the femur.

Like the human knee joint, the parallel architecture provides ATWOKI joint with selective compliances in directions other than the ones granted by the 2-dof, so that the mechanism may gain further (usually infinitesimal) degrees of freedom when forces or torques are applied. For this reason we say that the mechanism is an “almost two degrees of freedom” device.

In addition, because of the parallel architecture, building the mechanism with multifunctional structural elements allows the ATWOKI joint to be provided with the abilities to sense and to adapt so as to resemble its biological counterpart not only in the structure, but also in the functionality.

As for the potential applications, the novel mechanism may be optimized to be used in several different devices spanning from environment-interacting robots to pointing systems.

#### 3.4.1 Definition and Parameterization of the Desired Motion of the Mechanism

Consider the fixed and moving bodies depicted in Fig. 3.18 and attach the reference coordinate systems  $S_0 = \{O, \mathbf{i}_0, \mathbf{j}_0, \mathbf{k}_0\}$  and  $S_1 = \{C, \mathbf{i}_1, \mathbf{j}_1, \mathbf{k}_1\}$  to the fixed and moving body, respectively.

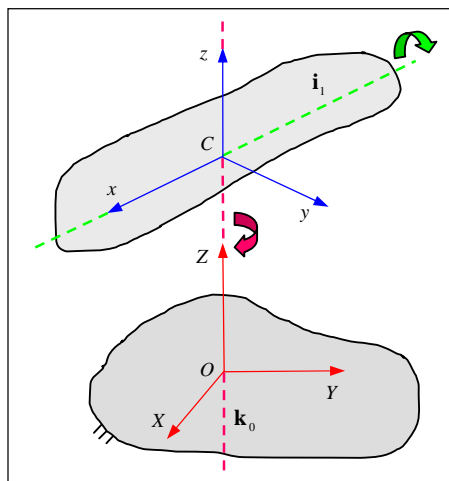


Figure 3.18 Bodies and Axes of Rotation

Consider the motion which is obtained by rotating the moving body about the fixed axis along the unit vector  $\mathbf{k}_0$  of the reference system  $S_0$  and about the moving axis along the unit vector  $\mathbf{i}_1$  of the reference system  $S_1$ , and which maintains the centers  $O$  of  $S_0$  and  $C$  of  $S_1$  coincident. This motion is defined as “spherical” with two degrees of freedom.

Such a motion can be parameterized by means of two rotations, the first by  $\vartheta$  about the vector  $\mathbf{k}_0$  and the second by  $\beta$  about the vector  $\mathbf{i}_1$ . Indeed, upon the introduction of the rotation matrices  $\mathbf{R}_\vartheta$  and  $\mathbf{R}_\beta$ , i.e.

$$\mathbf{R}_\vartheta = \begin{bmatrix} c_\vartheta & -s_\vartheta & 0 \\ s_\vartheta & c_\vartheta & 0 \\ 0 & 0 & 1 \end{bmatrix}, \quad \mathbf{R}_\beta = \begin{bmatrix} 1 & 0 & 0 \\ 0 & c_\beta & -s_\beta \\ 0 & s_\beta & c_\beta \end{bmatrix} \quad (3.3)$$

where  $c_\vartheta = \cos \vartheta$ ,  $s_\vartheta = \sin \vartheta$ ,  $c_\beta = \cos \beta$  and  $s_\beta = \sin \beta$ , the relative pose of the platform with respect to the base is completely described by the relationship

$$\mathbf{X} = \mathbf{R}\mathbf{x}, \quad (3.4)$$

being  $\mathbf{R}$  the rotational matrix

$$\mathbf{R} = \mathbf{R}_\vartheta \mathbf{R}_\beta = \begin{bmatrix} c_\vartheta & -s_\vartheta c_\beta & s_\vartheta s_\beta \\ s_\vartheta & c_\vartheta c_\beta & -c_\vartheta s_\beta \\ 0 & s_\beta & c_\beta \end{bmatrix} \quad (3.5)$$

which, for any point of the platform, maps the vector  $\mathbf{x} = [x \ y \ z]^T$  of point coordinates in  $S_1$  into the vector  $\mathbf{X} = [X \ Y \ Z]^T$  of point coordinates in  $S_0'$ , which is a fixed reference frame parallel to  $S_0$  but centered in  $C$ .

### 3.4.2 Generation of Self-Movable 2-dof Spherical US\_PMs

In Section 3.3.3 the general conditions for the generation of self-movable US\_PMs have been presented. Here those concepts are applied to the synthesis of two-dof self-movable spherical US\_PMs. As said, US\_PMs comprise a fixed body, called base, a moving body, called platform, and a certain number (say  $n$ ) of rods, called legs, which are connected by means of a spherical S joint to the base and by means of a universal U joints to the platform, or vice versa.

The synthesis of a US\_PM consists in finding the location of the joints on the base and on the platform, respectively, and the lengths of the connecting legs. That is, if for each leg  $h$ , one introduces the coordinate vector  $\mathbf{p}_h = [p_h \ q_h \ r_h]^T$  with respect to  $S_1$  of the point  $P_h$  which is the center of either the U joint or the S joint on the platform, the coordinate vector  $\mathbf{B}_h = [A_h \ B_h \ C_h]^T$  with respect to  $S_0'$  of the point  $B_h$  which is the center of either the S joint or the U joint on the base, and the length  $l_h = |\mathbf{P}_h - \mathbf{B}_h|$  of the connecting leg between  $P_h$  and  $B_h$ , we have to search for  $n$  unknown vectors of geometric parameters, i.e.  $\mathbf{g}_h = [A_h \ B_h \ C_h \ p_h \ q_h \ r_h \ l_h]^T$  for  $h = 1, \dots, n$ .

**Method 1**

Assuming the description and the parameterization of the orientation introduced in Section 3.4.1, the inverse kinematics analysis of a US\_PM states that the length of the  $h$ -th US-leg is given by

$$l_h = |\mathbf{I}_h| = |\mathbf{P}_h - \mathbf{B}_h| = |\mathbf{R}\mathbf{p}_h - \mathbf{B}_h|, \quad (3.6)$$

which is function, in general, of the motion parameters  $\mathcal{G}$  and  $\beta$ . Indeed,  $\mathbf{R}$  depends on these angles.

However, for the  $h$ -th US-leg to comply within the desired 2-dof spherical self-motion of the mechanism, the length  $l_h$  must not depend on  $\mathcal{G}$  and  $\beta$ . This means that if one considers the expression

$$l_h = \sqrt{l_h^2} = \sqrt{\begin{bmatrix} p_h c_\beta - q_h s_\beta + r_h c_\beta - A_h \\ p_h s_\beta + q_h c_\beta - r_h s_\beta - B_h \\ q_h s_\beta + r_h c_\beta - C_h \end{bmatrix}^2} = \sqrt{2f(\mathcal{G}, \beta)}, \quad (3.7.a)$$

where

$$f(\mathcal{G}, \beta) = \begin{pmatrix} -A_h p_h c_\beta + A_h q_h s_\beta - A_h r_h s_\beta - B_h p_h s_\beta - B_h q_h c_\beta + B_h r_h c_\beta + \\ -C_h q_h s_\beta - C_h r_h c_\beta + p_h^2 + q_h^2 + r_h^2 + A_h^2 + B_h^2 + C_h^2 \end{pmatrix}, \quad (3.7.b)$$

all the coefficients in  $c_\beta$ ,  $s_\beta$ ,  $c_\beta$  and  $s_\beta$  of the polynomial  $f(\mathcal{G}, \beta)$  must vanish, and the length of the  $h$ -th leg must become

$$l_h = \sqrt{p_h^2 + q_h^2 + r_h^2 + A_h^2 + B_h^2 + C_h^2}. \quad (3.8)$$

That is, the equations

$$A_h p_h = 0, \quad (3.9.a)$$

$$A_h q_h = 0, \quad (3.9.b)$$

$$A_h r_h = 0, \quad (3.9.c)$$

$$B_h p_h = 0, \quad (3.9.d)$$

$$B_h q_h = 0, \quad (3.9.e)$$

$$B_h r_h = 0, \quad (3.9.f)$$

$$C_h q_h = 0, \quad (3.9.g)$$

$$C_h r_h = 0, \quad (3.9.h)$$

must be satisfied simultaneously.

It turns out that the only non trivial solutions, i.e.  $l_h \neq 0$ , are obtained for the following two sets of leg geometric parameters

$${}^1\mathbf{g}_i = \left[ A_i = \forall \quad B_i = \forall \quad C_i = \forall \quad p_i = 0 \quad q_i = 0 \quad r_i = 0 \quad l_i = \sqrt{A_i^2 + B_i^2 + C_i^2} \right], \quad (3.10.a)$$

$${}^2\mathbf{g}_j = \left[ A_j = 0 \quad B_j = 0 \quad C_j = \forall \quad p_j = \forall \quad q_j = 0 \quad r_j = 0 \quad l_j = \sqrt{p_j^2 + C_j^2} \right]. \quad (3.10.b)$$

## Method 2

Since for a general motion of the US\_PM the parameters  $\mathcal{G}$  and  $\beta$  are function of time, based on the time derivative of the equation

$$\mathbf{l}_h = \mathbf{R}\mathbf{p}_h - \mathbf{B}_h = \begin{bmatrix} p_h c_\mathcal{G} - q_h s_\mathcal{G} c_\beta + r_h s_\mathcal{G} s_\beta - A_h \\ p_h s_\mathcal{G} + q_h c_\mathcal{G} c_\beta - r_h c_\mathcal{G} s_\beta - B_h \\ q_h s_\beta + r_h c_\beta - C_h \end{bmatrix}, \quad (3.11)$$

for the relative velocity vector  $\mathbf{v}_h$ , of point  $P_h$  with respect to point  $B_h$ , one obtains

$$\mathbf{v}_h = \begin{bmatrix} -p_h s_\mathcal{G} - q_h c_\mathcal{G} c_\beta + r_h c_\mathcal{G} s_\beta \\ p_h c_\mathcal{G} - q_h s_\mathcal{G} c_\beta + r_h s_\mathcal{G} s_\beta \\ 0 \end{bmatrix} \dot{\mathcal{G}} + \begin{bmatrix} q_h s_\mathcal{G} s_\beta + r_h s_\mathcal{G} c_\beta \\ -q_h c_\mathcal{G} s_\beta - r_h c_\mathcal{G} c_\beta \\ q_h c_\beta - r_h s_\beta \end{bmatrix} \dot{\beta}, \quad (3.12)$$

where  $\dot{\mathcal{G}}$  and  $\dot{\beta}$  are the first time derivatives of the motion parameters  $\mathcal{G}$  and  $\beta$ , respectively.

Since legs with constant length  $l_h$  are inserted between points  $P_h$  and  $B_h$ , it must hold that, during the allowed motion, the components of the velocity  $\mathbf{v}_h$  in the direction of the leg axis must be zero, i.e.

$$\mathbf{v}_h \cdot \mathbf{l}_h = g(\mathcal{G}, \beta) \dot{\mathcal{G}} + h(\mathcal{G}, \beta) \dot{\beta} = 0, \quad (3.13)$$

where

$$g(\mathcal{G}, \beta) = p_h A_h s_\mathcal{G} + q_h A_h c_\mathcal{G} c_\beta - r_h A_h c_\mathcal{G} s_\beta - p_h B_h c_\mathcal{G} + q_h B_h s_\mathcal{G} c_\beta - r_h B_h s_\mathcal{G} s_\beta, \quad (3.14.a)$$

$$h(\mathcal{G}, \beta) = -q_h A_h s_\mathcal{G} s_\beta - r_h A_h s_\mathcal{G} c_\beta + q_h B_h c_\mathcal{G} s_\beta + r_h B_h c_\mathcal{G} c_\beta - q_h C_h c_\beta + r_h C_h s_\beta. \quad (3.14.b)$$

Since this condition must hold for every location and motion of the manipulator (that is it should not depend on  $\mathcal{G}$ ,  $\beta$ ,  $\dot{\mathcal{G}}$  and  $\dot{\beta}$ ), all the coefficients in  $c_\beta$ ,  $s_\beta$ ,  $c_\mathcal{G}$  and  $s_\mathcal{G}$  of the two polynomials  $g(\mathcal{G}, \beta)$  and  $h(\mathcal{G}, \beta)$  must vanish. That is, the equations

$$A_h p_h = 0, \quad (3.15.a)$$

$$A_h q_h = 0, \quad (3.15.b)$$

$$A_h r_h = 0, \quad (3.15.c)$$

$$B_h p_h = 0, \quad (3.15.d)$$

$$B_h q_h = 0, \quad (3.15.e)$$

$$B_h r_h = 0, \quad (3.15.f)$$

$$C_h q_h = 0, \quad (3.15.g)$$

$$C_h r_h = 0 \quad (3.15.h)$$

must be satisfied simultaneously.

It turns out that the only non trivial solutions, i.e.  $l_h \neq 0$ , are obtained for the following two sets of leg geometric parameters

$${}^1\mathbf{g}_i = \left[ A_i = \forall \quad B_i = \forall \quad C_i = \forall \quad p_i = 0 \quad q_i = 0 \quad r_i = 0 \quad l_i = \sqrt{A_i^2 + B_i^2 + C_i^2} \right], \quad (3.16.a)$$

$${}^2\mathbf{g}_j = \left[ A_j = 0 \quad B_j = 0 \quad C_j = \forall \quad p_j = \forall \quad q_j = 0 \quad r_j = 0 \quad l_j = \sqrt{p_j^2 + C_j^2} \right], \quad (3.16.b)$$

which, as they should be, coincide exactly to the vectors obtained previously through method (1).

As a matter of fact, legs characterized by the set of parameters  ${}^1\mathbf{g}_i$  and  ${}^2\mathbf{g}_j$  are the only ones which comply within the desired 2-dof spherical motion.

The choice of the number  $I$  of the legs of type 1 and of the number ( $J = n - I$ ) of the legs of type 2, and the definition of the geometric parameter vectors  ${}^1\mathbf{g}_i$ , for  $i = 1, \dots, I$ , and  ${}^2\mathbf{g}_j$ , for  $j = (I + 1), \dots, n$ , closes the synthesis of the US\_PM to be designed. The choice of the numbers  $I$  and  $J$  clearly affects the mechanism feasibility and architecture. In particular, certain conditions on  $I$  and  $J$  must be satisfied.

First, in order for the mechanism to have 2-dof, the axes of the legs in the set  $\{ {}^1\mathbf{g}_1 \dots {}^1\mathbf{g}_I \quad {}^2\mathbf{g}_{I+1} \dots {}^2\mathbf{g}_n \}$  must belong to a linear variety of lines of dimension 4, usually referred to as linear line congruence. Therefore, at least four legs with linear independent axes are needed, i.e.  $n \geq 4$ .

Second, since the legs (of type 1) in the set  $\{ {}^1\mathbf{g}_1 \dots {}^1\mathbf{g}_I \}$  pass through the common point  $C$ , i.e. the center of the reference frame  $S_1$ , while the legs (of type 2) in the set  $\{ {}^2\mathbf{g}_{I+1} \dots {}^2\mathbf{g}_n \}$  lie in the plane defined by the vectors  $\mathbf{k}_0$  and  $\mathbf{i}_1$ , the axis lines of the legs within each type form, at most, a linear variety of lines of dimension 3. Indeed, the axes of the legs within the family of type (1) generate at most a bundle of lines, while the axes of the legs within the family of type (2) generate at most a plane of lines. For convenience, a bundle of lines is depicted in Fig. 3.19, while a plane of line is depicted in Fig. 3.20. Therefore, in order for the set of geometric parameters  $\{ {}^1\mathbf{g}_1 \dots {}^1\mathbf{g}_I \quad {}^2\mathbf{g}_{I+1} \dots {}^2\mathbf{g}_n \}$  to define a linear variety of dimension 4, at least one leg for each type is needed, i.e.  $(I \geq 1) \wedge (J \geq 1)$ .

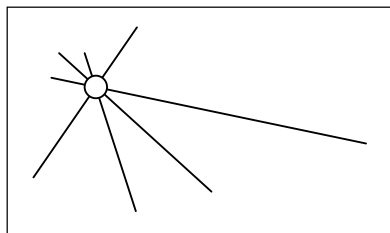


Figure 3.19 Bundle of Lines (all lines through a point)

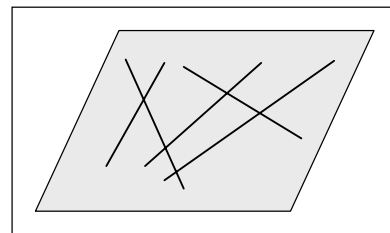


Figure 3.20 Plane of Lines (all lines in a plane)

As for the mechanism architecture, we said that all the axes of the legs  ${}^1g_i$ ,  $i=1,\dots,I$ , and  ${}^2g_j$ ,  $j=(I+1),\dots,n$ , must belong to a linear line congruence. More precisely the congruence should be degenerate, i.e. the variety of lines which lie in the plane defined by the vectors  $\mathbf{k}_0$  and  $\mathbf{i}_1$  or which pass through the point C of that plane. For convenience, a degenerate congruence of lines is depicted in Fig. 3.21.

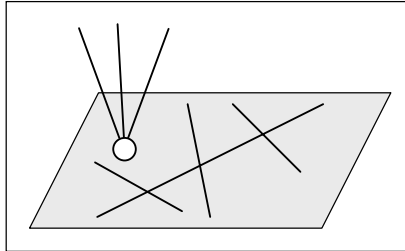


Figure 3.21 Degenerate Line Congruence (all lines in a plane or passing through one point of that plane)

In practice, depending on the varieties of lines spanned by the axes of the legs within a type, three families of mechanism architectures can be identified:

- 1) The axes of the legs in the set  $\{{}^1g_1 \dots {}^1g_I\}$  define a linear variety of dimension 1, i.e. a single line passing through C but with direction different than  $\mathbf{k}_0$ , and the axes of the legs in the set  $\{{}^2g_{I+1} \dots {}^2g_n\}$  define a linear variety of lines of dimension 3, i.e. a plane of lines defined by the vectors  $\mathbf{k}_0$  and  $\mathbf{i}_1$ .
- 2) The axes of the legs in the set  $\{{}^1g_1 \dots {}^1g_I\}$  define a linear variety of dimension 2, i.e. a planar pencil of lines with center in C but which does not contain the line through  $\mathbf{k}_0$ , and the axes of the legs in the set  $\{{}^2g_{I+1} \dots {}^2g_n\}$  define a linear variety of lines of dimension 2, i.e. a planar pencil of lines in the plane defined by  $\mathbf{k}_0$  and  $\mathbf{i}_1$ . For convenience, a planar pencil of lines is depicted in Fig. 3.22.
- 3) The axes of the legs in the set  $\{{}^1g_1 \dots {}^1g_I\}$  defines a linear variety of dimension 3, i.e. a bundle of lines centered in C, and the axes of the legs in the set  $\{{}^2g_{I+1} \dots {}^2g_n\}$  define a linear variety of lines of dimension 1, i.e. a single line in the plane defined by the vectors  $\mathbf{k}_0$  and  $\mathbf{i}_1$  but which does not pass through C.

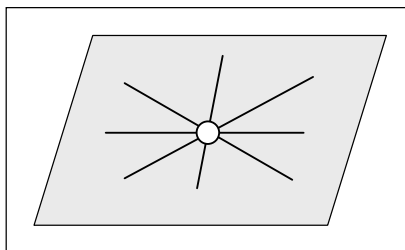


Figure 3.22 Planar Pencil of Lines (all lines in a plane and passing through one point in that plane)

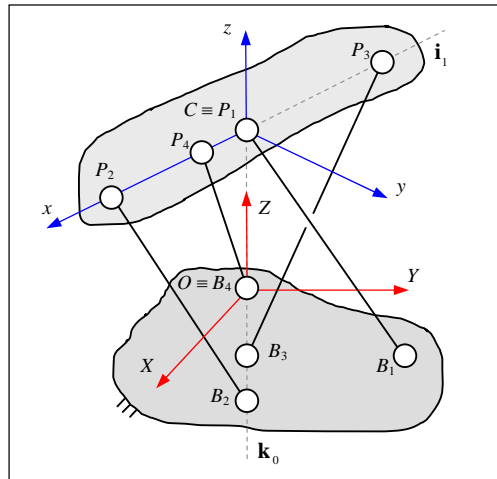


Figure 3.23 Family 1 Two-dof Spherical US\_PM

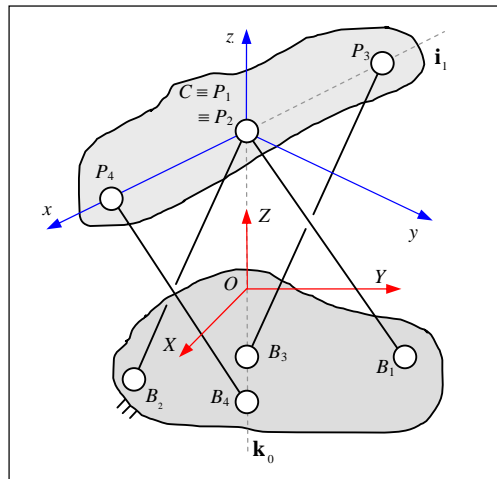


Figure 3.24 Family 2 Two-dof Spherical US\_PM

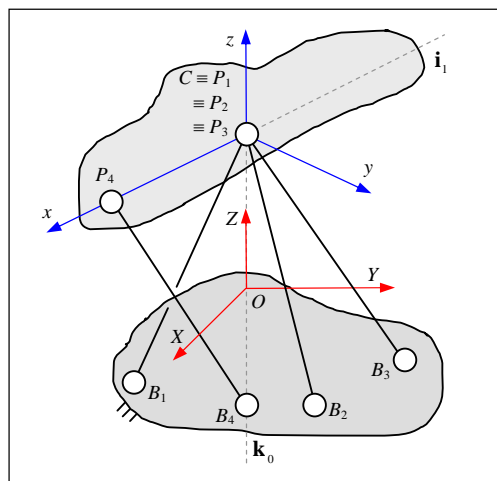


Figure 3.25 Family 3 Two-dof Spherical US\_PM

For the three families of US\_PM architectures, the basic mechanisms which contain only the four US-legs, whose axis lines are the generators of the linear line degenerate congruence, are depicted in Fig. 3.23, Fig. 3.24 and Fig. 3.25, respectively. For convenience, in the figures, both U joints and S joints are represented by circles.

Such mechanisms are not redundant, i.e. one can always statically determine the reaction forces exerted by the legs in order to react against the workless forces and moments the mechanism is subjected to during its motion.

Addition of type (1) and/or type (2) legs to the basic US\_PMs depicted in figures 3.23-3.25 does not alter the mechanism kinematics but renders the systems redundant and self-movable. That is, the aforementioned reaction forces cannot be statically determined anymore. An Example of redundant self-movable US\_PM with six US-legs is shown in Fig. 3.26. The mechanism is obtained from the system depicted in Fig. 3.25 by the addition of the redundant legs  $P_5B_5$  and  $P_6B_6$  (in figure, the redundant legs are depicted in magenta).

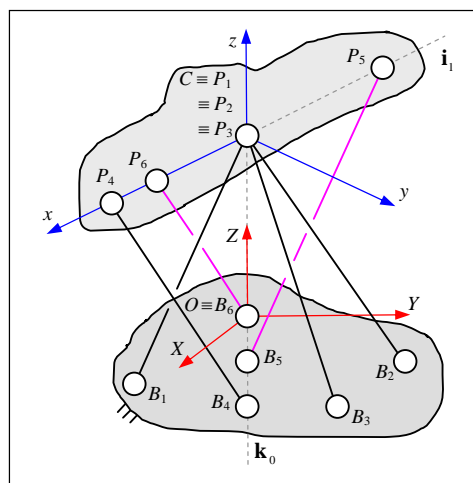


Figure 3.26 Two-dof Spherical Self-Movable US\_PM

Redundant architectures have several advantages with respect to the basic US\_PM configurations. Indeed, the former allow augmenting the mechanism stiffness-to-weight or to-encumbrance ratios, the mechanism strength-to-weight or to-encumbrance ratios, the mechanism resilience and reliability, allow the mechanism to be preloaded, and allow diminishing the mechanism sensitivity to disturbances and the mechanism backlash (in this way the mechanism can be built using rougher manufacturing tolerances). Besides, redundant architectures impose more strict limits in the range of motion of the mechanism and render more complex the mechanism analysis, synthesis, design and assembly.

### 3.5 Comparison between Biologically Inspired US\_PMs and Traditional Mechanisms

The parallel mechanisms presented in Section 3.4 are very interesting. Indeed, though they look quite complicate with respect to traditional systems, they can offer unparalleled advantages in many robotic applications. In order to understand such advantages, this section compares the features and the performances of biologically inspired (BI) mechanisms to those of more traditional systems.

A traditional (T) mechanism which can be used for realizing the desired 2-dof spherical motion is depicted in Fig. 3.27.

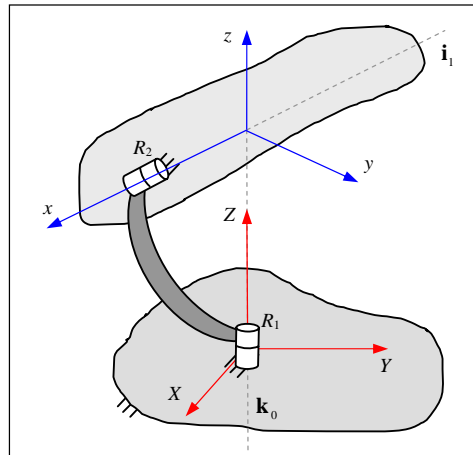


Figure 3.27 Traditional (T) 2-dof Spherical Mechanism

The mechanism is very simple and features a single RR-leg which connects the base and the platform by means of two traditional rotary pairs  $R_1$  and  $R_2$ . The pair  $R_1$  is fixed to the base and lies on the axis  $k_0$ , while the pair  $R_2$  is fixed to the platform and lies on the axis  $i_1$ .

From the kinematic perspective, the BI mechanisms and the T mechanism perform the same 2-dof spherical motion. The major difference consists in the range of movement. Indeed, while the T mechanism allows for almost unlimited turns about the  $k_0$  and  $i_1$  axes, the BI mechanisms limit the stroke to less than a turn. However, in the context of this research work, the limited range of motion is not crucial since it is an intrinsic characteristic of the animal joints we want to mimic. Moreover, many important applications exist which only require rotations by few degrees about given axes. In these cases, use of traditional rotary pairs with unlimited motion would be way too excessive and unneeded. As examples, devices which only require limited ranges of motion are pointing systems such as mirrors and antennas, steering systems of vehicles and limbs of biomimetic robots.

As for the strength, the parallel architecture of the BI mechanisms is more suited than the serial architecture of the T mechanism for realizing systems with high strength-to-weight and strength-to-encumbrance ratios.

First, the US-legs of the BI mechanisms only act in tension and compression. Thus, the resistance of the material which makes the legs is exploited uniformly both along the leg length and across the leg section. Conversely, in addition to tensile and compressive stresses, the RR-leg of the T mechanism must bear shear, flexional and torsional loads also. This does not allow to fully exploit the resistance of the material neither along the leg length nor across the leg section. That is, in order to withstand the same forces, the leg of the T mechanism needs more material than the amount required by all the legs of the BI counterpart. This makes the T mechanism result bulkier and heavier than the BI mechanisms.

Second, the R joints of the T mechanism are solicited by more complex states of loading and, in particular, must bear higher flexional loads which, in line with resistance criteria, oblige to overdimension such pairs with respect to the ones of BI mechanisms. This leads the joints of the traditional mechanism to be way too bulky and heavy so as to reduce the advantage of using just two R joints instead of the four S joints and the four U joints which the BI mechanisms need (compare Figs. 3.23-3.25 with Fig. 3.27). In fact, every R joint of the traditional

mechanism must stand, at the same time, both radial and axial loads, and consistent flexional loads. Note that these flexional loads correspond to the moments, with respect to the midpoints of the R joint, which act on the platform or on the base, and which are directed along the vector  $\mathbf{j}_s$  (which is normal to  $\mathbf{k}_0$  and  $\mathbf{i}_1$ ). Conversely, the revolute pairs which make the universal U joints and, eventually, the spherical S joints bear either axial or radial loads only and, perhaps, very little flexional loads. Indeed, thanks to the system architecture, the force resultant, which acts on a U (or a S) joints of the BI mechanisms, passes through the U (or the S) joint center. Thus, flexional loads may arise for construction issues only when the midpoint of the revolute pairs which make the U or the S joint needs to be placed slightly offset with respect to the center of the U or of the S joint. In addition, because of the parallel architecture of the biologically inspired US\_PMs, the total torque and force that act on the base and on the platform of the BI mechanisms are resisted cooperatively by the US-legs, i.e. the total torque and force are never resisted by a single US-leg, thus allowing the U joints and the S joints to be dimensioned to withstand loads of smaller magnitude than the ones that act on the R joints of the T mechanism. Therefore, in analogy to the partitioning concept exploited in many bearing system such as bushings and ball bearings, this makes it possible to reduce the strength-to-weight and strength-to-encumbrance ratios of the overall mechanism in spite of the increased system complexity. Besides, it has to be realized that many of the joints of the BI mechanisms do not move, in practice, if not for compensating the small deflections which may be caused by the loads due to the inherent compliance of the mechanism. Of course, the narrow motion required by these pairs could allow the designer to devise alternative/simpler solutions (e.g. compliant joints) which may limit the system complexity and reduce backlash or friction.

Third, other than yielding a mechanism with higher stiffness-to-weight and stiffness-to-encumbrance ratios, the parallel architecture of the BI mechanisms eases the design of systems with desired spatial compliance. In particular, the addition of many US-legs with a given stiffness and whose axes belong to the linear line congruence defined by the axes of the other legs (e.g. the self-movable US\_PM depicted in Fig. 3.26) is an easy means for synthesizing the desired stiffness while containing the mass and the encumbrance of the mechanisms themselves. This may be very important especially if the system to be designed must be very accurate, adaptable, tolerant to shocks and insensitive to disturbances.

The use of redundant US-legs could also be adopted in order to pretension the mechanism. System pretensioning may reduce system backlash, failures or damages caused by shocks and vibrations.

As an example, like depicted in Fig. 3.28, the use of only five US-legs of proper length would allow the design of a system whose elements only act either in tension such as wireropes (legs depicted in green) or in compression such as compression-rods (legs depicted in magenta). This may allow the realization of lighter and foldable mechanisms, and may ease the manufacturing process (with the use of wireropes the realization of the U and S joints may be easier).

Thus, as compared with the T mechanism, for the same payload, the biologically inspired US\_PMs should result in lighter, stiffer, more accurate and more robust systems. Their slenderness should allow, in general, for faster movements and better dynamic performances.

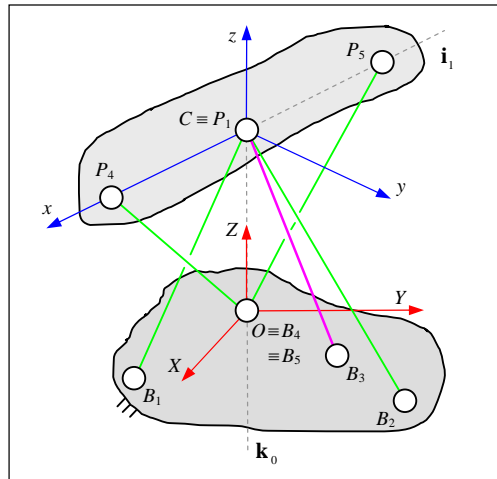


Figure 3.28 Two-dof Self-Movable US\_PM made by one Compression-rod (magenta line) and four Wirerope (blue lines)

Note that all the aforementioned properties are based simply on the passive behavior of the US-legs. In addition, if the US-legs are instrumented in order to acquire proprioceptive information (like the animal ligaments) and/or are actuated in order to modify the system homeostasis (as done in animals by the tendon-muscle units), then other advantages can be gained.

As an example, force sensor may be added to the US-legs in order to measure the forces which act on the base and on the platform plates.

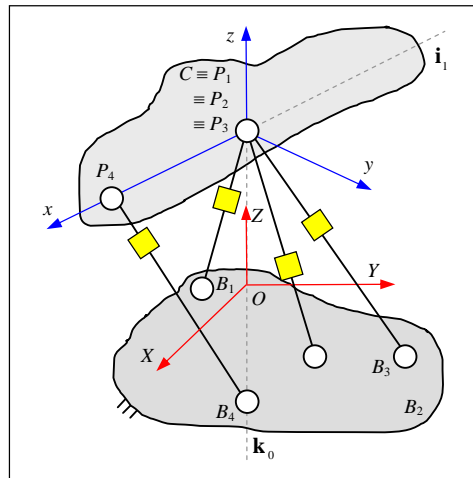


Figure 3.29 Two-dof Spherical US\_PM with Active (Sensorized) Structural US-Legs

In particular, with reference to Fig. 3.29 which depicts a US\_PM with four force sensors (represented as yellow boxes), the four sensors on the legs  $P_1B_1$ ,  $P_2B_2$ ,  $P_3B_3$  and  $P_4B_4$  allow measuring the resultant force which acts on the center C, while only the sensor on  $P_4B_4$  allows measuring the moment which acts about the axis lying along the vector  $\mathbf{j}_*$ , i.e. the axis which is normal to  $\mathbf{k}_0$  and  $\mathbf{i}_1$ .

Moreover, displacement sensors can also be added in order to determine the effective posture of the US\_PM which may be altered as a consequence of the deflections the mechanism may undergo, under thermal and/or

mechanical loads, because of the inherent compliance of the system. In particular, with reference to Fig. 3.29 which depicts a US\_PM with four displacement sensors (represented as yellow boxes), the three sensors on the legs  $P_1B_1$ ,  $P_2B_2$ ,  $P_3B_3$  allow measuring the displacement undergone by the center  $C$  because of the deflections of the legs  $P_1B_1$ ,  $P_2B_2$ ,  $P_3B_3$ , while the four sensors on the legs  $P_1B_1$ ,  $P_2B_2$ ,  $P_3B_3$  and  $P_4B_4$  allow measuring the relative rotation (with respect to  $\mathbf{k}_0$ ) undergone by the axis  $\mathbf{i}_1$  because of the deflections of the legs  $P_1B_1$ ,  $P_2B_2$ ,  $P_3B_3$  and  $P_4B_4$ .

Note that if the US\_PM is made by more than the four US-legs depicted in Fig. 3.29, instrumentation of all the US-legs would provide with a redundant measurement system which could be more robust to failures and less sensitive to measurement errors. Indeed, least square approaches may be used for obtaining very accurate and robust estimates of the forces and torques which act on the system, or very accurate and robust estimates of the relative displacements and rotations undergone by the mechanism.

Details on the implementation of in-parallel force-torque and translation-rotation sensors based on US\_PMs can be found in [84-89].

In addition, if actuators are provided in combination with the sensors, proper control of the active structural US-legs may allow the system to “smartly” adapt and compensate against disturbances such as thermal or mechanical loads, and to absorb and damp vibrations or shocks. A possible architecture of a US\_PM with sensorized and actuated structural US-legs is depicted in Fig. 3.30. The yellow boxes represent the sensors, while the green boxes represent the actuators. This US\_PM is called “smart” (or intelligent) since the mechanism is able to sense and to adapt to the environmental conditions.

Details on methods and strategies, which may be used to control the smart US\_PM such that it can satisfy given application requirements, can be found in [90, 91].

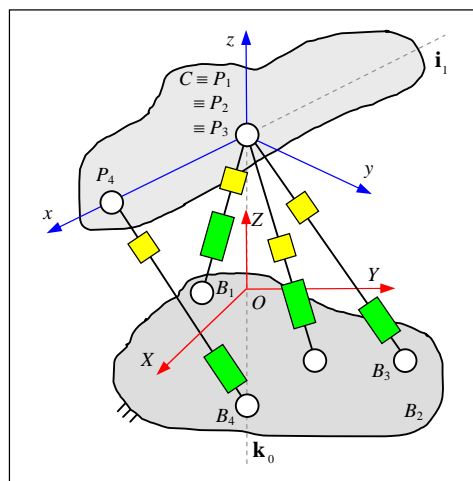


Figure 3.30 Two-dof Spherical “Smart” US\_PM with Multiactive (Sensorized and Actuated) Structural US-Legs

As for the actuator types, if the purpose of the active US-legs is only to preserve the system homeostasis, then high-bandwidth limited-stroke (with respect to the leg lengths) motors such as piezoelectric, magnetostrictive and voice-coils actuators are necessary and sufficient. Conversely, limited-bandwidth large-stroke actuators such

as electromagnetic, hydraulic, pneumatic motors and electro/magneto-sensitive elastomer based actuators should be used if reconfigurable and self-deployable mechanisms are desired.

As an example, a binarily actuated self-deployable mechanism is shown in Fig. 3.31.

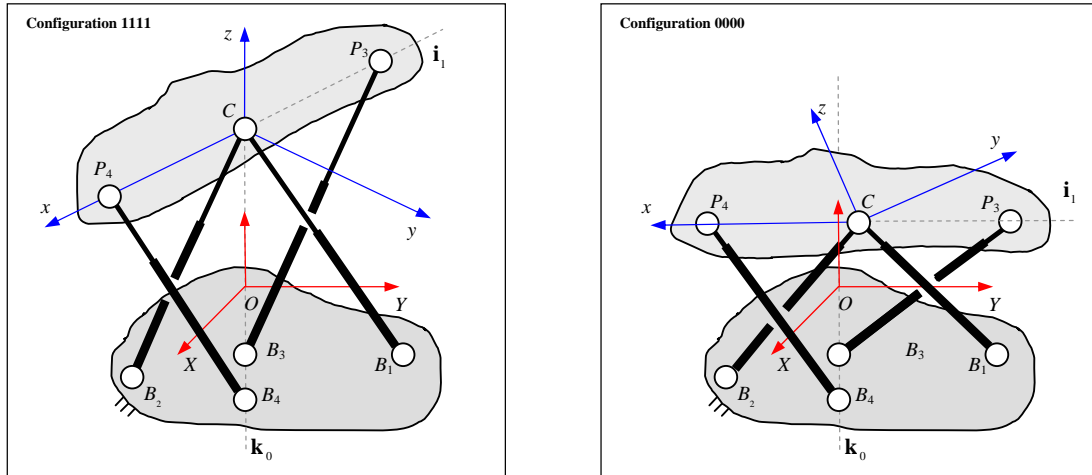


Figure 3.31 Binarily Activated US\_PM

The mechanism comprises four US-legs, each one of them being made by a bi-stable telescopic actuator, i.e. an actuator that can be either fully extended (state 1) or fully contracted (state 0). Among all the possible  $2^4$  configurations the binarily activated mechanism can attain, the left figure corresponds to the configuration (1111) where all the US-legs are fully extended, while the right figure corresponds to the configuration (0000) where all the US-legs are fully contracted. Note that by properly locating the U joints and S joints on the base and on the platform, it may be possible to make self-deployable mechanisms which use only one binarily activated telescopic US-leg and three US-legs of constant length.

Details on the analysis and on the implementation of binary reconfigurable robotic systems can be found in [92, 93].

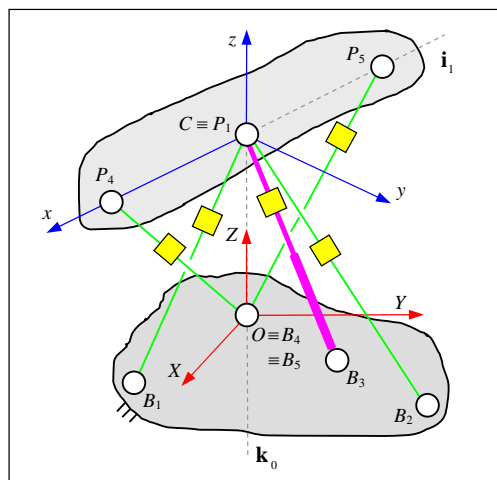


Figure 3.32 Two-dof Self-Movable "Smart" US\_PM



In practice, the addition of two UPS-legs (P stands for actuated prismatic P joint), each attached to the base and to the platform by means of a U and a S joint, provides a very simple means to fully control the mechanism throughout the desired range of motion. Note that, for the actuators to work properly, the system of lines which comprises the axes of the structural US-legs and those of the two actuated UPS-legs must define a linear variety of dimension 6. That is, the axes of the actuated UPS-legs must not belong to the linear line congruence generated by the axes of the structural US-legs. An example of manipulator which can be obtained starting from a US\_PM similar to the one we showed in Fig. 3.25 is depicted in the Fig. 3.33. The manipulator is indeed obtained by adding two actuated UPS legs, i.e.  $P_5B_5$  and  $P_6B_6$ , to a US\_PM of type (3). For ease of understanding, in the figure, the actuated UPS-legs have been depicted as telescopic legs and are colored in magenta, while the structural US-legs have been shaded in grey.

As a matter of fact, the addition of two UPS legs to the 2-dof biologically inspired US\_PM we devised in Section 3.4 leads to a system which is equivalent to a fully parallel manipulator of Gough-Stewart type (throughout this work also called 6-UPS\_PM and depicted in Fig. 3.13) [94] with four P joints locked. In particular, starting from the biologically inspired US\_PM of type (3), the resulting manipulator coincides with the General Fully Parallel Spherical Wrist (GFPSW) [95] with one P joint locked. For convenience, the corresponding GFPSW is represented in Fig. 3.34. In the picture, the locked P joint is depicted in green.

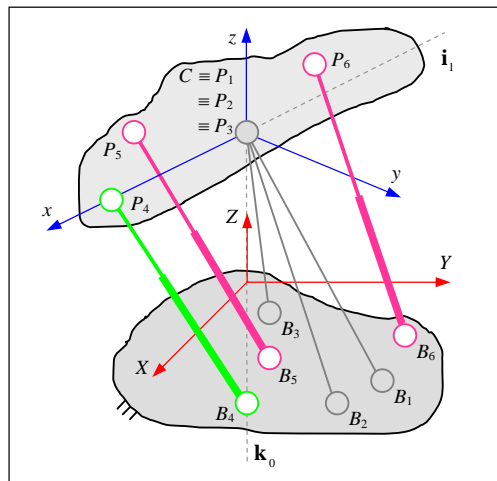


Figure 3.34 General Fully Parallel Spherical Wrist

A very important feature of the biologically inspired US\_PMs presented in this research work is the possibility to decouple the motion about the two axes  $\mathbf{k}_0$  and  $\mathbf{i}_1$ . That is, by properly placing the U- and S joints of the actuated UPS-legs over the base and over platform, each axis of motion can be controlled independently by a single prismatic actuator. Indeed, since a force is not able to generate moments about the lines it crosses, it is clear that every UPS leg whose connecting joint on the base is centered in a point  $B_h$ , which lies on  $\mathbf{k}_0$ , allows to control rotations about  $\mathbf{i}_1$  only, while every UPS leg whose connecting joint on the platform is centered in a point  $P_h$ , which lies on  $\mathbf{i}_1$ , allows to control rotations about  $\mathbf{k}_0$  only.

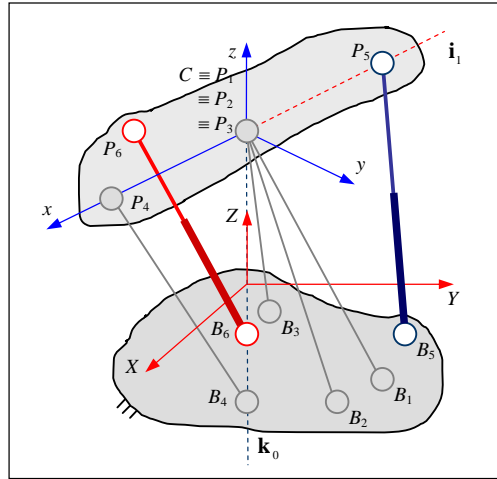


Figure 3.35 Decoupled Actuated 2-dof US\_PM

A decoupled actuated manipulator obtained from a US\_PM of type (3) is represented in Fig. 3.35. The actuated UPS-leg  $P_5B_5$  (depicted in blue) controls the rotation about axis  $\mathbf{k}_0$  only, while the actuated UPS-leg  $P_6B_6$  (depicted in red) controls the rotation about axis  $\mathbf{i}_1$  only.

As for the optimal placement of the actuators, the location of the pair of points  $\{P_5, B_5\}$  should be chosen in order maximize the ratio between the available moment about  $\mathbf{k}_0$  and the actuator force applied along  $P_5B_5$ , while the location of the pair of points  $\{P_6, B_6\}$  should be chosen in order maximize the ratio between the available moment about  $\mathbf{i}_1$  and the actuator force applied along  $P_6B_6$ . Moreover, the pairs of points  $\{P_5, B_5\}$  and  $\{P_6, B_6\}$  should be chosen such that the manipulator does not show singular configurations within its workspace.

With reference to the actuator placed on the leg  $P_5B_5$ , the moment  $\mathbf{m}^{(5)}$  the actuator exerts to the platform is given by

$$\mathbf{m}^{(5)} = f_5 (\mathbf{P}_5 - \mathbf{C}) \times \frac{(\mathbf{P}_5 - \mathbf{B}_5)}{\|\mathbf{P}_5 - \mathbf{B}_5\|}, \quad (3.17)$$

where  $f_5$  is the force generated by the actuator along the leg  $P_5B_5$ . Little manipulation of Eq. (3.17) yields

$$\mathbf{m}_5 = \frac{f_5}{l_5} (\mathbf{P}_5 - \mathbf{C}) \times (\mathbf{C} - \mathbf{B}_5), \quad (3.18)$$

which, since the center  $C$  has the coordinates  $[0 \ 0 \ h]^T$  with respect to  $S_0$ , the point  $B_5$  has the coordinates  $[A_5 \ B_5 \ C_5]^T$  with respect to  $S_0$  and the point  $P_5$  has the coordinate vector  $[p_5 \ 0 \ 0]^T$  with respect to  $S_1$ , can be rewritten as

$$\mathbf{m}_5 = -\frac{f_5}{l_5} p_5 \left[ (h - C_5) \mathbf{k}_0 \times \mathbf{i}_1 - A_5 \mathbf{i}_0 \times \mathbf{i}_1 - B_5 \mathbf{j}_0 \times \mathbf{i}_1 \right]. \quad (3.19)$$

By considering the relations

$$\mathbf{j}_s = \mathbf{k}_0 \times \mathbf{i}_1, \quad (3.20.a)$$

$$\mathbf{k}_0 s_g = \mathbf{i}_0 \times \mathbf{i}_1, \quad (3.20.b)$$

$$\mathbf{k}_0 c_g = -\mathbf{j}_0 \times \mathbf{i}_1, \quad (3.20.c)$$

where  $c_g$  and  $s_g$  are as defined in Section 3.4.1, the moment  $\mathbf{m}^{(5)}$  expressed by Eq. (3.19) can be decomposed in the component  $m_{\mathbf{k}_0}^{(5)}$  about  $\mathbf{k}_0$  and in the component  $m_{\mathbf{j}_s}^{(5)}$  about  $\mathbf{j}_s$ , i.e.

$$m_{\mathbf{k}_0}^{(5)} = -\frac{f_5 p_5 [B_5 c_g - A_5 s_g]}{\sqrt{(h - C_5)^2 + A_5^2 + B_5^2 + p_5^2 - 2p_5(A_5 c_g + B_5 s_g)}}, \quad (3.21)$$

$$m_{\mathbf{j}_s}^{(5)} = -\frac{f_5 p_5 (h - C_5)}{\sqrt{(h - C_5)^2 + A_5^2 + B_5^2 + p_5^2 - 2p_5(A_5 c_g + B_5 s_g)}}. \quad (3.22)$$

Optimization of the placement of the actuator  $P_5 B_5$  can be carried on considering equations (3.21) and (3.22). In particular, Eq. (3.21) shows that, for the absolute value of the ratio  $m_{\mathbf{k}_0}^{(5)}/f_5$  to be maximized for every location  $g$ , the value of  $h$  must be as close as possible to the value of  $C_5$ . This also minimizes the absolute value of the disturbing moment  $m_{\mathbf{j}_s}^{(5)}$  which only solicits the structure of the manipulator without producing any useful effect. Moreover, Eq. (3.21) shows that, despite the force  $f_5$  is different than zero, the moment  $m_{\mathbf{k}_0}^{(5)}$  vanishes for

$${}^1g_s = \arctan\left(\frac{B_5}{A_5}\right), \quad (3.23.a)$$

$${}^2g_s = {}^1g_s + \pi. \quad (3.23.b)$$

These correspond to the singular configurations of the actuated leg  $P_5 B_5$ . Since in such configurations the manipulator becomes uncontrollable, they must be excluded from the manipulator usable workspace. Therefore, the manipulator should be made work either within the range  $g \in ]{}^1g_s, {}^1g_s + \pi[$  or within the range  $g \in ]{}^1g_s - \pi, {}^1g_s[$ .

With reference to the actuator placed on the leg  $P_6 B_6$ , the moment  $\mathbf{m}^{(6)}$  the actuator exerts to the platform is given by

$$\mathbf{m}^{(6)} = f_6 (P_6 - C) \times \frac{(P_6 - B_6)}{\|P_6 - B_6\|}, \quad (3.24)$$

where  $f_6$  is the force generated by the actuator along the leg  $P_6 B_6$ . Little manipulation of Eq. (3.24) yields

$$\mathbf{m}^{(6)} = \frac{f_6}{l_6} (\mathbf{P}_6 - \mathbf{C}) \times (\mathbf{C} - \mathbf{B}_6), \quad (3.25)$$

which, since the center  $\mathbf{C}$  has the coordinates  $[0 \ 0 \ h]^T$  with respect to  $S_0$ , the point  $\mathbf{B}_6$  has the coordinates  $[0 \ 0 \ C_6]^T$  with respect to  $S_0$  and the point  $\mathbf{P}_6$  has the coordinate vector  $[p_6 \ q_6 \ 0]^T$  with respect to  $S_1$ , can be rewritten as

$$\mathbf{m}^{(6)} = -\frac{f_6}{l_6} [p_6 (h - C_6) \mathbf{k}_0 \times \mathbf{i}_1 + q_6 (h - C_6) \mathbf{k}_0 \times \mathbf{j}_1]. \quad (3.26)$$

By considering the relations

$$\mathbf{j}_* = \mathbf{k}_0 \times \mathbf{i}_1, \quad (3.27.a)$$

$$\mathbf{i}_1 \mathbf{c}_\beta = -\mathbf{k}_0 \times \mathbf{j}_1, \quad (3.27.b)$$

where  $\mathbf{c}_\beta$  is as defined in Section 3.4.1, the moment  $\mathbf{m}^{(6)}$  expressed by Eq. (3.26) can be decomposed in the components  $m_{\mathbf{i}_1}^{(6)}$  about  $\mathbf{i}_1$  and in the components  $m_{\mathbf{j}_*}^{(6)}$  about  $\mathbf{j}_*$ , i.e.

$$m_{\mathbf{i}_1}^{(6)} = \frac{f_6 q_6 (h - C_6) \mathbf{c}_\beta}{\sqrt{p_6^2 + q_6^2 + (h - C_6)^2 + 2q_6 (h - C_6) s_\beta}}, \quad (3.28)$$

$$m_{\mathbf{j}_*}^{(6)} = -\frac{f_6 p_6 (h - C_6)}{\sqrt{p_6^2 + q_6^2 + (h - C_6)^2 + 2q_6 (h - C_6) s_\beta}}. \quad (3.29)$$

Optimization of the placement of the actuator  $\mathbf{P}_6 \mathbf{B}_6$  can be carried on considering equations (3.28) and (3.29). In particular, Eq. (3.28) shows that for the absolute value of the ratio  $m_{\mathbf{i}_1}^{(6)} / f_6$  to be maximized for every location  $\beta$ , the value of  $p_6$  must be as close as possible to zero. This also minimizes the absolute value of the disturbing moment  $m_{\mathbf{j}_*}^{(6)}$  which only solicits the structure of the manipulator without producing any useful effect. Moreover, Eq. (3.28) shows that, despite the force  $f_6$  is different than zero, the moment  $m_{\mathbf{i}_1}^{(6)}$  vanishes for

$${}^1\beta_s = \pi/2, \quad (3.30.a)$$

$${}^2\beta_s = -\pi/2. \quad (3.30.b)$$

These correspond to the singular configurations of the actuated leg  $\mathbf{P}_6 \mathbf{B}_6$ . Since in such configurations the manipulator becomes uncontrollable, they must be excluded from the manipulator usable workspace. Therefore, the manipulator should be made work either within the range  $\beta \in ]-\pi/2, \pi/2[$  or within the range  $\beta \in ]\pi/2, 3\pi/2[$ .

In order to fully understand the advantages and in order to identify the applications the decoupled actuated US\_PMs may be suited for, in the following we compare their potential performances to those of a traditional spherical manipulator. With reference to the traditional mechanism we depicted in Fig. 3.27, a controllable traditional 2-dof spherical manipulator can be conceived by the placement of a rotary actuator on each of the R joints. Such a system is represented in Fig. 3.36, where the rotary motors  $\underline{R}_1$  and  $\underline{R}_2$  are depicted in red.

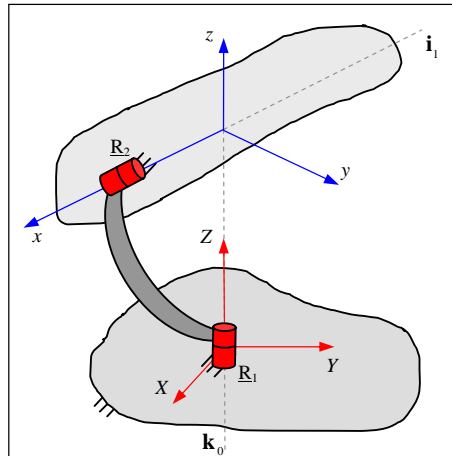


Figure 3.36 Traditional 2-dof Spherical Manipulator

The manipulator is of serial type. The direct placement of two rotary motors on the R joints allows the control of the motion to be decoupled about the axes  $\mathbf{k}_0$  and  $\mathbf{i}_1$ . Though the solution seems rather simple, when compared to the parallel architecture of the actuated US\_PMs, it shows several disadvantages.

First, when the traditional mechanism is actuated, the middle link, i.e. the RR-leg, and the R joints have to withstand the torques exerted by the motors also. Such torques generate additional flexional/torsional moments and sum up to the loads we mentioned in Section 3.5. This complicates further the state of sollicitation of the RR-leg and of the R joints. As a result, the middle link, the R joints and the motors become heavier and bulkier. This makes the traditional manipulator have lower payload-to-weight, lower payload-to-encumbrance ratios and lower dynamic performances than the actuated US\_PMs.

Second, due to the serial architecture, the guaranteed accuracy of the traditional serial manipulator is lower than that of the actuated US\_PMs. Indeed, the open chain architecture does not allow measuring by the internal sensor the mechanism passive compliance (i.e. link deflections and backlash in the drives) and, therefore, forbids the accurate control of the manipulator motion.

Third, as depicted in Fig. 3.36, the actuator  $\underline{R}_1$  is the only one placed over the base and has to carry and move the whole manipulator (which comprises the links and the other actuator). Besides, the actuator  $\underline{R}_2$  is placed far from the base of the manipulator and is required to carry and move only a small part thereof. Hence, the actuator  $\underline{R}_1$  needs to be overdimensioned and requires some sort of reduction stage, which is deleterious for the overall system performance. Conversely, in the actuated US\_PMs, all the actuators can be placed collectively near the base. This allows achieving a very light motion mechanism and adopting high power direct drive motors.

Summarizing, the novel BI manipulators based on biologically inspired US\_PM mechanisms enjoy the advantages of high speed, high accuracy, high loading capacity, high stiffness and high strength over the traditional systems. They however suffer from the limited amplitude of motions.

## Chapter 4

### Kinematic Analysis

#### 4.1 Introduction

Chapter 3 presented three novel families of 2-dof biologically inspired (BI) parallel mechanisms and discussed the features and the advantages they offer with respect to traditional (T) serial mechanisms. In addition, actuation issues were addressed which showed that the motion of the BI mechanisms can be decoupled about two axes which are fixed, respectively, one to the mechanism base and the other to the mechanism platform.

In the following chapters the analysis of a BI mechanism of type (2) is addressed. Hereafter, such mechanism will be called “ATWOKI” joint, where the name “ATWOKI” stands for “Almost TWO-dof Knee-Inspired”. Note that the word “Almost” is used for emphasizing the stiffness advantages which are related to the novel articulation concept. Indeed, despite the compliance of the elements which makes the mechanism, ATWOKI only has two practical (or prevalent) degrees of freedom (i.e. the degrees of freedom which would be retained by the mechanism if its members were considered perfectly rigid).

This chapter concerns the kinematic analysis of ATWOKI.

#### 4.2 ATWOKI: System Description

Among the manipulators which may be conceived starting from the novel mechanisms devised in Chapter 3, the system chosen for the following analyses has the architecture depicted in Fig. 4.1.

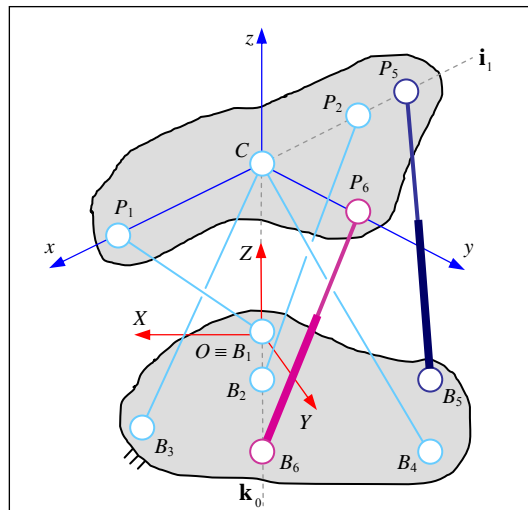


Figure 4.1 ATWOKI (Almost TWO-dof Knee Inspired) Joint

The manipulator has two degrees of freedom which are controlled by the telescopic actuators (legs of variable length) depicted in magenta and in blue respectively. Legs depicted in cyan are structural (legs of fixed length) and are placed so as to maintain fixed, during the manipulator motion, the location of point C with respect to the base and the reciprocal position of the axes  $i_1$  and  $k_0$ .

In particular, the center  $C$  lies on the axis  $\mathbf{k}_0$  and the axis  $\mathbf{i}_1$  is orthogonal to  $\mathbf{k}_0$ , i.e.  $\mathbf{i}_1 \cdot \mathbf{k}_0 = 0$ . Thus, the motion is spherical with center  $C$  and can be understood as made of two sequential rotations, the first about the vector  $\mathbf{k}_0$  and the second about the vector  $\mathbf{i}_1$ .

Because of the special arrangement of the actuators, i.e. point  $B_6$  of the actuator  $P_6B_6$  lies on  $\mathbf{k}_0$  and point  $P_5$  of the actuator  $P_5B_5$  lies on  $\mathbf{i}_1$ , the aforementioned rotations are controlled by the actuators independently. That is, the motion of the manipulator is fully decoupled.

### 4.3 ATWOKI: Direct Position Analysis (DPA)

By definition, the Direct Position Analysis (DPA) consists in the problem of finding the location of the platform with respect to the base once the geometrical parameters of the manipulator and the lengths of the actuated legs are known. For a given manipulator, the geometrical parameters are fixed and specified at the outset. They consist in the locations (the coordinates) of points  $B_i$ , for  $i = 1, \dots, 6$ , on the base, in the location of points  $P_i$ , for  $i = 1, \dots, 6$ , on the platform and the lengths  $l_j$ ,  $j = 1, \dots, 4$ , of the structural legs  $B_jP_j$ . Conversely, the lengths  $l_5$  and  $l_6$  of the actuated legs vary with the manipulator motion and are measured in real-time by sensors which are placed on the actuated legs.

Recall that the DPA is fundamental for control purposes since it is the cheapest and most practical way to determine the pose of the manipulator.

Here, because of the decoupled motion, the solution of the DPA is very simple and fast. In practice, the DPA reduces to solve for the angle  $\mathcal{G}$  of rotation of the vector  $\mathbf{i}_1$  about the axis  $\mathbf{k}_0$  and to solve for the angle of rotation  $\beta$  of the vector  $\mathbf{k}_1$  about the axis  $\mathbf{i}_1$ , once the lengths  $l_5$  and  $l_6$  are known.

Beginning with equation

$$(\mathbf{P}_5 - \mathbf{B}_5) = (\mathbf{P}_5 - \mathbf{C}) + (\mathbf{C} - \mathbf{O}) + (\mathbf{O} - \mathbf{B}_5), \quad (4.1)$$

rewrite it as

$$(\mathbf{P}_5 - \mathbf{B}_5) = p_5 \mathbf{i}_1 + h \mathbf{k}_0 - A_5 \mathbf{i}_0 - B_5 \mathbf{j}_0 - C_5 \mathbf{k}_0, \quad (4.2)$$

where, according to the definitions introduced in previous sections,  $p_5$  is the norm of the vector  $\mathbf{P}_5\mathbf{C}$ ,  $h$  is the norm of the vector  $\mathbf{CO}$ , and  $A_5$ ,  $B_5$  and  $C_5$  are the coordinates of point  $B_5$  with respect to  $S_0$ . Moreover, since the following scalar products hold

$$\mathbf{i}_1 \cdot \mathbf{i}_0 = \cos \mathcal{G}, \quad (4.3.a)$$

$$\mathbf{i}_1 \cdot \mathbf{j}_0 = \sin \mathcal{G}, \quad (4.3.b)$$

modify Eq. (4.2) as

$$(\mathbf{P}_5 - \mathbf{B}_5) = (p_5 \cos \mathcal{G} - A_5) \mathbf{i}_0 + (p_5 \sin \mathcal{G} - B_5) \mathbf{j}_0 + (h - C_5) \mathbf{k}_0. \quad (4.4)$$

Then, by squaring Eq. (4.4), obtain

$$\frac{l_5^2}{D} = E - (A_5 \cos \vartheta + B_5 \sin \vartheta), \quad (4.5.a)$$

where

$$D = 2p_5, \quad (4.5.b)$$

$$E = \frac{p_5^2 + A_5^2 + B_5^2 + (h - C_5)^2}{D}. \quad (4.5.c)$$

Moreover, resorting to the well-known relationships

$$\cos \vartheta = \frac{1 - t^2}{1 + t^2}, \quad (4.6.a)$$

$$\sin \vartheta = \frac{2t}{1 + t^2}, \quad (4.6.b)$$

rewrite Eqs. (4.5) as

$$\left( \frac{l_5^2 - F}{D} \right) t^2 + 2B_5 t + \left( \frac{l_5^2 - G}{D} \right) = 0, \quad (4.7.a)$$

where

$$F = p_5^2 + A_5^2 + B_5^2 + (h - C_5)^2 + 2p_5 A_5, \quad (4.7.b)$$

$$G = p_5^2 + A_5^2 + B_5^2 + (h - C_5)^2 - 2p_5 A_5. \quad (4.7.c)$$

Then, the angle  $\vartheta$  can be found by means of the relation

$$\vartheta = 2 \arctan \left( - \left( \frac{H}{l_5^2 - F} \right) \pm \sqrt{\left( \frac{H}{l_5^2 - F} \right)^2 - \left( \frac{l_5^2 - G}{l_5^2 - F} \right)} \right), \quad (4.8.a)$$

where

$$H = B_5 D = 2B_5 p_5. \quad (4.8.b)$$

That is, the solution is not unique. However, by means of the following consideration, one of the solutions can be disregarded in a straightforward manner. In facts, the solutions  ${}^1\vartheta$  and  ${}^2\vartheta$  correspond to two different assembly modes of the manipulator. Such assemblies are separated by the singular configurations characterized by

$${}^1\vartheta_s = 2 \arctan \left( \frac{B_5}{A_5 + \sqrt{A_5^2 + B_5^2}} \right). \quad (4.9.a)$$

$${}^2\vartheta_s = 2 \arctan \left( \frac{B_5}{A_5 - \sqrt{A_5^2 + B_5^2}} \right). \quad (4.9.b)$$

which happen when the length  $l_5$  of the leg  $B_5P_5$  coincides with one of the following values

$${}^1l_5 = \sqrt{p_5^2 + A_5^2 + B_5^2 + (h - C_5)^2 - 2p_5\sqrt{A_5^2 + B_5^2}}, \quad (4.9.c)$$

$${}^2l_5 = \sqrt{p_5^2 + A_5^2 + B_5^2 + (h - C_5)^2 + 2p_5\sqrt{A_5^2 + B_5^2}}, \quad (4.9.d)$$

Since, for matters of controllability, the manipulator must be designed in order to have a singularity-free workspace, then, for every location the manipulator is allowed to reach, the angle of rotation  $\mathcal{G}$  must always satisfy either the condition

$$\mathcal{G} \in ]\min({}^1\mathcal{G}_s, {}^2\mathcal{G}_s), \max({}^1\mathcal{G}_s, {}^2\mathcal{G}_s)[, \quad (4.9.e)$$

or the condition

$$\mathcal{G} \in ]\max({}^1\mathcal{G}_s, {}^2\mathcal{G}_s), \min({}^1\mathcal{G}_s, {}^2\mathcal{G}_s)[. \quad (4.9.f)$$

Therefore, if the manipulator is configured such that its workspace is characterized by Eq. (4.9.e), then, due to the monotonicity of the  $\arctan(\cdot)$  function, the solution  $\mathcal{G}$  is found as

$$\mathcal{G} = 2\arctan\left(-\left(\frac{H}{l_5^2 - F}\right) + \sqrt{\left(\frac{H}{l_5^2 - F}\right)^2 - \left(\frac{l_5^2 - G}{l_5^2 - F}\right)}\right), \quad (4.10.a)$$

if

$$t'_s < -\left(\frac{H}{l_5^2 - F}\right) + \sqrt{\left(\frac{H}{l_5^2 - F}\right)^2 - \left(\frac{l_5^2 - G}{l_5^2 - F}\right)} < t''_s, \quad (4.10.b)$$

or

$$\mathcal{G} = 2\arctan\left(-\left(\frac{H}{l_5^2 - F}\right) - \sqrt{\left(\frac{H}{l_5^2 - F}\right)^2 - \left(\frac{l_5^2 - G}{l_5^2 - F}\right)}\right), \quad (4.10.c)$$

if

$$t'_s < -\left(\frac{H}{l_5^2 - F}\right) - \sqrt{\left(\frac{H}{l_5^2 - F}\right)^2 - \left(\frac{l_5^2 - G}{l_5^2 - F}\right)} < t''_s, \quad (4.10.d)$$

where

$$t'_s = \min\left(\frac{B_5}{A_5 - \sqrt{A_5^2 + B_5^2}}, \frac{B_5}{A_5 + \sqrt{A_5^2 + B_5^2}}\right), \quad (4.10.e)$$

$$t_s'' = \max \left( \frac{B_5}{A_5 - \sqrt{A_5^2 + B_5^2} + A_5}, \frac{B_5}{A_5 + \sqrt{A_5^2 + B_5^2}} \right). \quad (4.10.f)$$

Conversely, if the manipulator is configured such that its workspace is characterized by Eq. (4.9.f), then, due to the monotony of the  $\arctan(\cdot)$  function, the solution  $\mathcal{G}$  is found as

$$\mathcal{G} = 2 \arctan \left( - \left( \frac{H}{l_5^2 - F} \right) + \sqrt{\left( \frac{H}{l_5^2 - F} \right)^2 - \left( \frac{l_5^2 - G}{l_5^2 - F} \right)} \right), \quad (4.11.a)$$

if

$$\left[ - \left( \frac{H}{l_5^2 - F} \right) + \sqrt{\left( \frac{H}{l_5^2 - F} \right)^2 - \left( \frac{l_5^2 - G}{l_5^2 - F} \right)} > t_s'' \right] \vee \left[ - \left( \frac{H}{l_5^2 - F} \right) + \sqrt{\left( \frac{H}{l_5^2 - F} \right)^2 - \left( \frac{l_5^2 - G}{l_5^2 - F} \right)} < t_s' \right], \quad (4.11.b)$$

or

$$\mathcal{G} = 2 \arctan \left( - \left( \frac{H}{l_5^2 - F} \right) - \sqrt{\left( \frac{H}{l_5^2 - F} \right)^2 - \left( \frac{l_5^2 - G}{l_5^2 - F} \right)} \right), \quad (4.11.c)$$

if

$$\left[ - \left( \frac{H}{l_5^2 - F} \right) - \sqrt{\left( \frac{H}{l_5^2 - F} \right)^2 - \left( \frac{l_5^2 - G}{l_5^2 - F} \right)} > t_s'' \right] \vee \left[ - \left( \frac{H}{l_5^2 - F} \right) - \sqrt{\left( \frac{H}{l_5^2 - F} \right)^2 - \left( \frac{l_5^2 - G}{l_5^2 - F} \right)} < t_s' \right]. \quad (4.11.d)$$

The determination of the angle  $\beta$  is simpler than that of  $\mathcal{G}$ . Recalling that the angle  $\beta$  is the angle of rotation of the axis  $\mathbf{k}_1$  about the axis  $\mathbf{i}_1$ , use of trigonometry yields

$$\sin(\beta) = \left( \frac{l_6^2 - I}{L} \right), \quad (4.12.a)$$

where

$$I = (h - C_6)^2 + q_6^2, \quad (4.12.b)$$

$$L = 2q_6(h - C_6). \quad (4.12.c)$$

Note that, according to the definitions introduced in previous sections,  $q_6$  is the norm of the vector  $P_6C$  and  $C_6$  is the non-zero coordinate of point  $B_6$  with respect to  $S_0$ . Equations (4.12) allow for two solutions, i.e.  ${}^1\beta$  and  ${}^2\beta$ . However, as for the unknown angle  $\mathcal{G}$ , one of the two solutions can be disregarded a priori. Indeed, the solutions  ${}^1\beta$  and  ${}^2\beta$  correspond to different manipulator assemblies which are separated by the singularities at  ${}^1\beta_s = \pi/2$  and  ${}^2\beta_s = -\pi/2$ . Then, for controllability issues, the manipulator must be configured such that its

workspace is defined by either  $\beta \in ]-\pi/2, \pi/2[$  or  $\beta \in ]\pi/2, -\pi/2[$ . Therefore, by taking into account the useful manipulator workspace one obtains the single solution

$$\beta = \arcsin\left(\frac{l_6^2 - I}{L}\right), \quad (4.13)$$

where the  $\arcsin(\cdot)$  function must be evaluated in the first-fourth quadrant if the manipulator workspace is defined for  $\beta \in ]-\pi/2, \pi/2[$ , or must be evaluated in the second-third quadrant if the manipulator workspace is defined for  $\beta \in ]\pi/2, -\pi/2[$ .

### **Implementation of the DPA Algorithm**

As for the implementation standpoint, the DPA algorithm comprises two parts, namely, the initialization and the main parts. The initialization has to be performed off-line one time for each manipulator, while the main part is the on-line procedure which leads to the solution of the DPA as soon as sensor data are acquired. The pseudocode for the implementation is:

0. INITIALIZATION (off-line calculations):

- i. Given the manipulator base and platform, with reference to Fig. (4.1), define the two frames  $S_0$  (i.e.  $O, \mathbf{i}_0, \mathbf{j}_0$  and  $\mathbf{k}_0$ ) and  $S_1$  (i.e.  $C, \mathbf{i}_1, \mathbf{j}_1$  and  $\mathbf{k}_1$ );
- ii. Given the manipulator geometry and the definitions in (0.i.), evaluate  $A_5, B_5, C_5, p_5, C_6, q_6$  and  $h$ ;
- iii. Given the definitions (0.ii), according to Eq. (4.7.b), Eq. (4.7.c), Eq. (4.8.b), Eq. (4.12.b), Eq. (4.12.c), Eq. (4.10.e) and Eq. (4.10.f), evaluate  $F, G, H, I, L, t'_5$  and  $t''_5$ .

1. MAIN (on-line calculations):

- i. Acquire sensor data, i.e.  $l_5$  and  $l_6$ ;
- ii. Find  $\mathcal{G}$  and  $\beta$  by means of Eqs. (4.10), Eqs. (4.11) and Eq. (4.13), respectively.

### **Computational Cost of the DPA Algorithm**

As for the computational cost, the algorithm is very fast. Since only the main calculations need to be performed on line, the solution of the DPA requires 7 multiplications/divisions, 5 sums/subtractions and 2 trigonometric operations.

Moreover, note that Eqs. (4.10), Eqs. (4.11) and Eq. (4.13) involve independent calculations which can be performed in parallel to further speed-up the solution of the DPA.

## **4.4 ATWOKI: Inverse Position Analysis (IPA)**

By definition, the Inverse Position Analysis (IPA) consists in the problem of finding the lengths of the actuated legs  $l_5$  and  $l_6$  once the geometrical parameters of the manipulators and the reciprocal location between base and platform are known. Since, for a given manipulator, the geometrical parameters are fixed and specified at the

outset, in practice the IPA reduces to solving for  $l_5$  and  $l_6$  once the angle  $\vartheta$  of rotation of the vector  $\mathbf{i}_1$  about the axis  $\mathbf{k}_0$ , and the angle of rotation  $\beta$  of the vector  $\mathbf{j}_1$  about the axis  $\mathbf{i}_1$  are defined.

Recall that the IPA is fundamental for control purposes since it sets the reference lengths of the legs which must be attained by the servo system in order to place the manipulator in the desired configuration.

Reviewing the procedure outlined for the DPA, the solution of the IPA is very straightforward. In fact, from Eq. (4.5) one gets the relation

$$l_5 = \sqrt{M - N \cos \vartheta - O \sin \vartheta}, \quad (4.14.a)$$

where

$$N = DA_5, \quad (4.14.b)$$

$$O = DB_5, \quad (4.14.c)$$

$$M = p_5^2 + A_5^2 + B_5^2 + (h - C_5)^2. \quad (4.14.d)$$

Moreover, from Eq. (4.12) one gets the relation

$$l_6 = \sqrt{L \sin(\beta) + I}, \quad (4.15.a)$$

where

$$I = (h - C_6)^2 + q_6^2, \quad (4.15.b)$$

$$L = 2q_6(h - C_6). \quad (4.15.c)$$

### **Implementation of the IPA Algorithm**

As for the implementation point of view, the IPA algorithm comprises two parts, namely, the initialization and the main parts. The initialization has to be performed off-line one time for each manipulator, while the main part is the on-line procedure which leads to the solution of the IPA as soon as the desired configuration of the manipulator is defined. The pseudocode for the implementation is:

0. INITIALIZATION (off-line calculations):

- i. Given the manipulator base and platform, with reference to Fig. (1) define the two frames  $S_0$  (i.e.  $O$ ,  $\mathbf{i}_0$ ,  $\mathbf{j}_0$  and  $\mathbf{k}_0$ ) and  $S_1$  (i.e.  $C$ ,  $\mathbf{i}_1$ ,  $\mathbf{j}_1$  and  $\mathbf{k}_1$ );
- ii. Given the manipulator geometry and the definitions in (0.i.), evaluate  $A_5$ ,  $B_5$ ,  $C_5$ ,  $p_5$ ,  $C_6$ ,  $q_6$  and  $h$ ;
- iii. Given the definitions (0.ii), according to Eq. (4.14.b), Eq. (4.14.c), Eq. (4.15.b) and Eq. (4.15.c), evaluate  $D$ ,  $M$ ,  $I$  and  $L$ , respectively.

1. MAIN (on-line calculations):

- i. Define the desired configuration of the manipulator, i.e. define  $\vartheta$  and  $\beta$ ;
- ii. Find  $l_5$  and  $l_6$  by means of Eq. (4.14.a) and Eq. (4.15.a), respectively.

### Computational Cost of the IPA Algorithm

As for the computational cost, the algorithm is very fast. Since only the main calculations need to be performed on line, the solution of the IPA requires 4 multiplications/divisions, 3 sums/subtractions, 3 trigonometric operations and 2 transcendental operations.

Moreover, note that Eq. (4.14.a) and Eq. (4.15.a) involve independent calculations which can be performed in parallel to further speed-up the solution of the IPA.

### 4.5 ATWOKI: Direct Velocity Analysis (DVA)

By definition, the Direct Velocity Analysis (DVA) consists in the problem of finding the velocity of the platform with respect to the base once the geometry and the location of the manipulator, and the velocities of the actuated legs are given. Recall that the DVA is fundamental for control purposes since it is the cheapest and most practical way to determine the manipulator velocity.

Since for a particular manipulator the geometrical parameters are fixed and known from the outset and the manipulator location is known from the position analyses, in practice the DVA reduces to solving for the angular velocity  $\dot{\mathcal{G}}$  (about the axis  $\mathbf{k}_0$ ) and the angular velocity  $\dot{\beta}$  (about the axis  $\mathbf{i}_1$ ) once the velocities  $\dot{l}_5$  and  $\dot{l}_6$  of the actuated legs are given. Indeed, the manipulator velocity is

$$\boldsymbol{\omega} = \dot{\mathcal{G}}\mathbf{k}_0 + \dot{\beta}\mathbf{i}_1. \quad (4.16)$$

Note that the lengths  $l_5$  and  $l_6$ , and the velocities  $\dot{l}_5$  and  $\dot{l}_6$  are measured by sensors which are placed on the legs of the manipulator.

Considering the procedure outlined for the DPA, the solution of the DVA is very straightforward. In fact, upon time-differentiation of Eq. (4.5), one gets

$$\dot{\mathcal{G}} = \left( \frac{l_5}{P \sin \mathcal{G} - Q \cos \mathcal{G}} \right) \dot{l}_5, \quad (4.17.a)$$

where

$$P = N/2, \quad (4.17.b)$$

$$Q = O/2. \quad (4.17.c)$$

Moreover, upon time differentiation of Eq. (4.12), one gets

$$\dot{\beta} = \left( \frac{l_6}{R \cos(\beta)} \right) \dot{l}_6, \quad (4.18.a)$$

$$R = L/2. \quad (4.18.b)$$

### Implementation of the DVA Algorithm

As for the implementation point of view, the DVA algorithm comprises two parts, namely, the initialization and the main parts. The initialization has to be performed off-line one time for each manipulator, while the main

part is the on-line procedure which leads to the solution of the DVA, as sensor data are acquired. The pseudocode for the implementation is:

0. INITIALIZATION (off-line calculations):

- iv. Given the definitions introduced for the position analysis algorithms, according to Eq. (4.17.b), Eq. (4.17.c) and Eq. (4.18.b), evaluate  $P$ ,  $Q$  and  $R$  respectively.

1. MAIN (on-line calculations):

- i. Consider the solution of the position analysis algorithms.
- ii. Acquire sensor data, i.e.  $\dot{l}_5$  and  $\dot{l}_6$ ;
- iii. Find  $\dot{\vartheta}$  and  $\dot{\beta}$  by means of Eq. (4.17.a) and Eq. (4.18.a), respectively.

#### **Computational Cost of the DVA Algorithm**

As for the computational cost, the algorithm is very fast. Since only the main calculations need to be performed on line, the solution of the DVA requires 4 multiplications/divisions, 1 sums/subtractions and 3 trigonometric operations (in addition to the calculations required for the solution of the position analyses).

Moreover, note that Eq. (4.17.a) and Eq. (4.18.a) involve independent calculations which can be performed in parallel to further speed-up the solution of the DVA.

### **4.6 ATWOKI: Inverse Velocity Analysis (IVA)**

By definition, the Inverse Velocity Analysis (IVA) consists in the problem of finding the velocities  $\dot{l}_5$  and  $\dot{l}_6$  of the actuated legs once the geometry and location of the manipulator, and the velocity of the platform with respect to the base are given. Recall that the IVA is fundamental for control purposes since it sets the reference velocity of the legs which must be attained by the servo system in order to move the manipulator with a certain speed, i.e. with a certain angular velocity  $\boldsymbol{\omega} = \dot{\vartheta}\mathbf{k}_0 + \dot{\beta}\mathbf{i}_1$ .

Since, for a particular manipulator, the geometrical parameters are fixed and known from the outset, while the manipulator location is known from the position analyses, in practice, the IVA reduces to solve for the velocities  $\dot{l}_5$  and  $\dot{l}_6$  of the actuated legs once the angular velocity  $\dot{\vartheta}$  (about the axis  $\mathbf{k}_0$ ) and the angular velocity  $\dot{\beta}$  (about the axis  $\mathbf{i}_1$ ) are defined.

Considering the procedure outlined for the DVA, the solution of the IVA is very straightforward. In fact, upon inversion of Eq. (4.17.a), one gets

$$\dot{l}_5 = \left( \frac{P \sin \vartheta - Q \cos \vartheta}{l_5} \right) \dot{\vartheta}. \quad (4.19)$$

Moreover, upon inversion of Eq. (4.18.a), one gets

$$\dot{l}_6 = \left( \frac{R \cos(\beta)}{l_6} \right) \dot{\beta}. \quad (4.20)$$

### Implementation of the IVA Algorithm

As for the implementation point of view, the resulting algorithm comprises two parts, namely, the initialization and the main parts. The initialization has to be performed off-line one time for each manipulator, while the main part is the on-line procedure which leads to the solution of the IVA as soon as the desired velocity of the manipulator is defined. The pseudocode for the implementation is:

0. INITIALIZATION (off-line calculations):

- iv. Given the definitions introduced for the position analysis algorithms, according to Eq. (4.17.b), Eq. (4.17.c) and Eq. (4.18.c), evaluate  $P$ ,  $Q$  and  $R$ , respectively.

1. MAIN (on-line calculations):

- iii. Consider the solution of the position analysis algorithms.
- iv. Define the desired velocity of the manipulator, i.e. define  $\dot{\mathcal{G}}$  and  $\dot{\beta}$ ;
- v. Find  $\dot{l}_5$  and  $\dot{l}_6$  by means of Eq. (4.19) and Eq. (4.20), respectively.

### Computational Cost of the IVA Algorithm

As for the computational cost, the algorithm is very fast. Since only the main calculations need to be performed on line, the solution of the IVA requires 4 multiplications/divisions, 1 sums/subtractions and 3 trigonometric operations (in addition to the calculations required for the solution of the position analyses).

Moreover, note that Eq. (4.19) and Eq. (4.20) involve independent calculations which can be performed in parallel to further speed-up the solution of the IVA.

## 4.7 ATWOKI: Direct Acceleration Analysis (DAA)

By definition, the Direct Acceleration Analysis (DAA) consists in the problem of finding the acceleration of the platform with respect to the base once the geometry, the velocity and the location of the manipulator and the accelerations of the actuated legs are given. Recall that the direct acceleration analysis is fundamental for control purposes since it is the cheapest and most practical way to determine the manipulator acceleration.

Since, for a particular manipulator, the geometrical parameters are fixed and known from the outset, while the manipulator velocity and location are known from the position and velocity analyses, in practice, the DAA reduces to solving for the angular acceleration  $\ddot{\mathcal{G}}$  (about the axis  $\mathbf{k}_0$ ) and the angular acceleration  $\ddot{\beta}$  (about the axis  $\mathbf{i}_1$ ) once the accelerations  $\ddot{l}_5$  and  $\ddot{l}_6$  of the actuated legs are given. Indeed, the manipulator acceleration is

$$\dot{\omega} = \ddot{\mathcal{G}}\mathbf{k}_0 + \ddot{\beta}\mathbf{i}_1 + \dot{\mathcal{G}}\dot{\beta}\mathbf{k}_0 \times \mathbf{i}_1. \quad (4.21)$$

Note that like the lengths  $l_5$  and  $l_6$ , and the velocities  $\dot{l}_5$  and  $\dot{l}_6$ , also the accelerations  $\ddot{l}_5$  and  $\ddot{l}_6$  are measured by sensors which are placed on the legs of the manipulator.

Considering the procedure outlined for the DVA, the solution of the DAA is very straightforward. In fact, upon time-differentiation of Eq. (4.17.a), one gets

$$\ddot{\vartheta} = \left[ \frac{\dot{\vartheta}}{l_5} \dot{l}_5 - \frac{(P \cos \vartheta + Q \sin \vartheta)}{(P \sin \vartheta - Q \cos \vartheta)} \dot{\vartheta}^2 \right] + \frac{\dot{\vartheta}}{l_5} \ddot{l}_5. \quad (4.22)$$

Moreover, upon time-differentiation of Eq. (4.18.a), one gets

$$\ddot{\beta} = \left[ \frac{\dot{\beta}}{l_6} \dot{l}_6 - \frac{\sin(\beta)}{\cos(\beta)} \dot{\beta}^2 \right] + \frac{\dot{\beta}}{l_6} \ddot{l}_6. \quad (4.23)$$

### Implementation of the DAA Algorithm

As for the implementation point of view, the DAA algorithm comprises two parts, namely, the initialization and the main parts. The initialization has to be performed off-line one time for each manipulator, while the main part is the on-line procedure which leads to the solution of the DAA as soon as sensor data are acquired. The pseudocode for the implementation is:

0. INITIALIZATION (off-line calculations):

- v. Consider the definitions introduced for the position and velocity analysis algorithms.

1. MAIN (on-line calculations):

- vi. Consider the solution of the position and velocity analysis algorithms.
- vii. Acquire sensor data, i.e.  $\ddot{l}_5$  and  $\ddot{l}_6$ ;
- viii. Find  $\ddot{\vartheta}$  and  $\ddot{\beta}$  by means of Eq. (4.22) and Eq. (4.23), respectively.

### Computational Cost of the DAA Algorithm

As for the computational cost, the algorithm is very fast. Since only the main calculations need to be performed on line, the solution of the DAA requires 14 multiplications/divisions, 5 sums/subtractions and 2 trigonometric operations (in addition to the calculations required for the solution of the position and velocity analyses).

Moreover, note that Eq. (4.22) and Eq. (4.23) involve independent calculations which can be performed in parallel to further speed-up the solution of the DAA.

## 4.8 ATWOKI: Inverse Acceleration Analysis (IAA)

By definition, the Inverse Acceleration Analysis (IAA) consists in the problem of finding the accelerations  $\ddot{l}_5$  and  $\ddot{l}_6$  of the actuated legs once the geometry, the location and the velocity of the manipulator, and the acceleration of the platform with respect to the base are given. Recall that the IAA is fundamental for control purposes since it sets the reference acceleration of the legs which must be attained by the servo system in order to move the manipulator with a certain acceleration, i.e. with a certain angular acceleration  $\dot{\omega}$ .

Since, for a particular manipulator, the geometrical parameters are fixed and known from the outset, while the manipulator velocity and location are known from the velocity and position analyses, in practice the IAA reduces

to solving for the accelerations  $\ddot{l}_5$  and  $\ddot{l}_6$  of the actuated legs once the angular acceleration  $\ddot{\vartheta}$  (about axis  $\mathbf{k}_0$ ) and the angular acceleration  $\ddot{\beta}$  (about the axis  $\mathbf{i}_1$ ) are defined.

Considering the procedure outlined for the IVA, the solution of the IAA is very straightforward. In fact, upon time-differentiation of Eq. (4.19), one gets

$$\ddot{l}_5 = \frac{1}{l_5} \left[ (P \cos \vartheta + Q \sin \vartheta) \dot{\vartheta}^2 - \dot{l}_5^2 + (P \sin \vartheta - Q \cos \vartheta) \ddot{\vartheta} \right]. \quad (4.24)$$

Moreover, upon time-differentiation of Eq. (4.20), one gets

$$\ddot{l}_6 = \frac{1}{l_6} \left[ -(R \sin(\beta)) \dot{\beta}^2 - \dot{l}_6^2 + (R \cos(\beta)) \ddot{\beta} \right]. \quad (4.25)$$

### **Implementation of the IAA Algorithm**

As for the implementation point of view, the resulting algorithm comprises two parts, namely, the initialization and the main parts. The initialization has to be performed off-line one time for each manipulator, while the main part is the on-line procedure which leads to the solution of the IAA as soon as the desired acceleration of the manipulator is defined. The pseudocode for the implementation is:

0. INITIALIZATION (off-line calculations):

- vi. Consider the definitions introduced for the position and velocity analysis algorithms.

1. MAIN (on-line calculations):

- vi. Consider the solution of the position and velocity analysis algorithms.
- vii. Define the desired acceleration of the manipulator, i.e. define  $\ddot{\vartheta}$  and  $\ddot{\beta}$ ;
- viii. Find  $\ddot{l}_5$  and  $\ddot{l}_6$  by means of Eq. (4.24) and Eq. (4.25), respectively.

### **Computational Cost of the IAA Algorithm**

As for the computational cost, the algorithm is very fast. Since only the main calculations need to be performed on line, the solution of the IAA requires 11 multiplications/divisions, 5 sums/subtractions and 2 trigonometric operations (in addition to the calculations required for the solution of the position and velocity analyses).

Moreover, note that Eq. (4.24) and Eq. (4.25) involve independent calculations which can be performed in parallel to further speed-up the solution of the IAA.

## **4.9 ATWOKI: Extended Direct Position Analysis (EDPA)**

When accurate positioning is of concern, the direct position analysis presented in Section 4.3 may not be sufficient for the correct estimation and control of the manipulator pose.

As an example, due to the inherent compliance of the legs, a load that acts on the manipulator platform could induce deflections in the legs which may cause the manipulator to move away from its ideal location (i.e. the location the manipulator would attain if the legs were infinitely rigid). Of course, the discrepancy between the

ideal and the effective location of the manipulator depends on the magnitude of the force which acts on the platform and on the compliance of the legs.

One of the major advantages BI mechanisms feature with respect to the serial T mechanisms, is that the parallel architecture of the former allows for the easy estimation of the effective manipulator location through the use of simple and highly integrated internal sensors which are placed in order to measure the leg deflections. This feature is important since it may allow the control system of the BI manipulator to take actions in order to compensate for the positioning errors. Conversely, in serial architectures, member deflections cannot be measured so easily and this may yield the T mechanisms to be submitted to higher positioning errors than the BI mechanisms.

A method for the estimation of the effective location of a BI manipulator of type (2), in which both structural and actuated legs are considered of variable length, is presented in the sequel. Here, for manipulator location we mean the position and orientation of the platform with respect to the base. That is, this analysis involves the solution of a problem in six unknowns. Note that the DPA, which we discussed in Section 4.3, concerned only the orientation of the platform with respect to the base and, in practice, it was a problem in two unknowns. Hereafter, the problem in six unknowns will be called “Extended Direct Position Analysis” (EDPA).

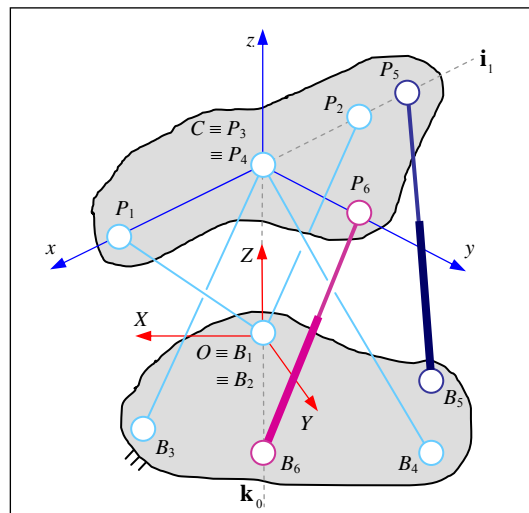


Figure 4.2 Special Version of the ATWOKI Joint

Consider the manipulator depicted in Fig. 4.2, which has points  $B_1$  and  $B_2$  co-located and coincident with the center  $O$  of the reference frame  $S_0$ . All of the six legs  $B_iP_i$ , for  $i=1,\dots,6$ , are considered of variable length. The structural legs  $B_jP_j$ , for  $j=1,\dots,4$ , are equipped with linear displacement sensors (e.g. strain-gages) which, together with the sensors of the servos which are placed on the actuated legs, i.e.  $B_5P_5$  and  $B_6P_6$ , allow measuring the six leg lengths  $l_i = \|P_i - B_i\|$ , for  $i=1,\dots,6$ .

Upon identification of the location of the leg attachment points by means of the following sets of coordinates:

$$B_1 = B_2 = [0 \ 0 \ 0]^T, \tag{4.26.a}$$

$$\mathbf{B}_3 = [A_3 \quad B_3 \quad C_3]^T, \quad (4.26.b)$$

$$\mathbf{B}_4 = [A_4 \quad B_4 \quad C_4]^T, \quad (4.26.c)$$

$$\mathbf{B}_5 = [A_5 \quad B_5 \quad C_5]^T, \quad (4.26.d)$$

$$\mathbf{B}_6 = [0 \quad 0 \quad C_6]^T, \quad (4.26.e)$$

i.e. the coordinates of the position vectors  $(\mathbf{B}_i - \mathbf{O})$  with respect to  $S_0$ , and

$$\mathbf{P}_1 = [p_1 \quad 0 \quad 0]^T, \quad (4.27.a)$$

$$\mathbf{P}_2 = [p_2 \quad 0 \quad 0]^T, \quad (4.27.b)$$

$$\mathbf{P}_3 = \mathbf{P}_4 = [0 \quad 0 \quad 0]^T, \quad (4.27.c)$$

$$\mathbf{P}_5 = [p_5 \quad 0 \quad 0]^T, \quad (4.27.d)$$

$$\mathbf{P}_6 = [0 \quad q_6 \quad 0]^T, \quad (4.27.e)$$

i.e. the coordinates of the position vectors  $(\mathbf{P}_i - \mathbf{C})$  with respect to  $S_1$ , then the EDPA can be accomplished according to the following steps.

**Step 1:** solve for the location of the center  $\mathbf{C}$ , i.e. for the set of coordinates  $\mathbf{C} = [X \quad Y \quad Z]^T$  of the position vector  $(\mathbf{C} - \mathbf{O})$  with respect to  $S_0$ .

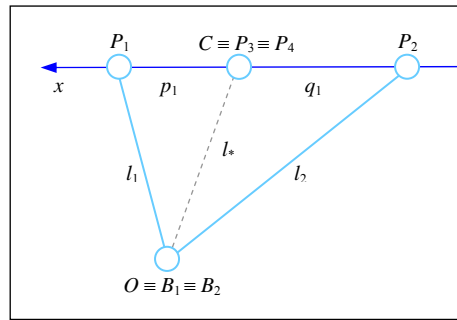


Figure 4.3 Subsystem of ATWOKI: Triangle  $P_1\hat{O}P_2$

Referring to the manipulator shown in Fig. 4.2, consider the triangle  $P_1\hat{O}P_2$  which is depicted in Fig. 4.3. Given the leg lengths  $l_1$  and  $l_2$ , the distance  $l_* = \|\mathbf{C} - \mathbf{O}\|$  follows as

$$l_*^2 = l_1^2 + p_1^2 + \frac{l_2^2 - l_1^2 - (p_1 + p_2)^2}{(p_1 + p_2)} p_1 = \frac{l_1^2 p_2 + p_1 l_2^2 - p'}{p''}, \quad (4.28.a)$$

where

$$p' = p_1 p_2^2 + p_1^2 p_2, \quad (4.28.b)$$

$$p'' = p_1 + p_2. \quad (4.28.c)$$

Then, consider the tetrahedron  $OB_3B_4C$ , which is depicted in Fig. 4.4. Given the edge lengths  $l_3$ ,  $l_4$ ,  $b_3 = \|B_3\| = \sqrt{A_3^2 + B_3^2 + C_3^2}$  and  $l_*$ , which are completely known from the manipulator geometry and from the measurements, it is possible to solve for the location of the center  $C$ .

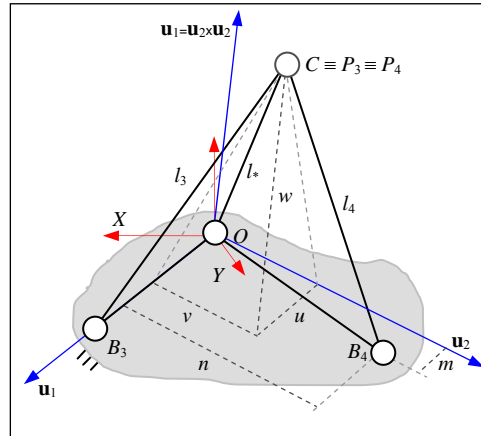


Figure 4.4 Subsystem of ATWOKI: Tetrahedron  $OB_3B_4C$

Indeed, upon definition of the unit vectors

$$\mathbf{u}_1 = (B_3 - O) / b_3, \quad (4.29.a)$$

$$\mathbf{u}_2 = \frac{(B_4 - O) - \mathbf{u}_1 m}{n}, \quad (4.29.b)$$

$$\mathbf{u}_3 = \mathbf{u}_1 \times \mathbf{u}_2, \quad (4.29.c)$$

where

$$m = (B_4 - O) \cdot \mathbf{u}_1, \quad (4.29.d)$$

$$n = \|(B_4 - O) - \mathbf{u}_1 m\|, \quad (4.29.e)$$

the location of the center  $C$  can be identified by the position vector  $(C - O)$

$$(C - O) = u\mathbf{u}_1 + v\mathbf{u}_2 + w\mathbf{u}_3, \quad (4.30.a)$$

being

$$u = \frac{b_3' + l_*^2 - l_3^2}{b_3''}, \quad (4.30.b)$$

$$v = \frac{m' + l_*^2 - l_4^2 - m''u}{n'}, \quad (4.30.c)$$

$$w = \pm \sqrt{l_*^2 - u^2 - v^2}, \quad (4.30.d)$$

and

$$m' = n^2 + m^2, \quad (4.30.e)$$

$$m'' = 2m, \quad (4.30.f)$$

$$n' = 2n, \quad (4.30.g)$$

$$b_3' = b_3^2, \quad (4.30.h)$$

$$b_3'' = 2b_3. \quad (4.30.i)$$

Note that Eq. (4.30.d) gives two solutions for  $w$ , i.e.  ${}^1w = \sqrt{l_*^2 - u^2 - v^2}$  and  ${}^2w = -\sqrt{l_*^2 - u^2 - v^2}$ . However, in practical applications, only one solution is feasible and the other can be disregarded. Indeed, since the base (and therefore the triangle  $B_3\hat{O}B_4$ ) cannot be penetrated by the point  $C$ , the feasible solution is  ${}^1w$  (or  ${}^2w$ ) if, in the initial configuration of the manipulator, the value of  $w$  is positive (or negative).

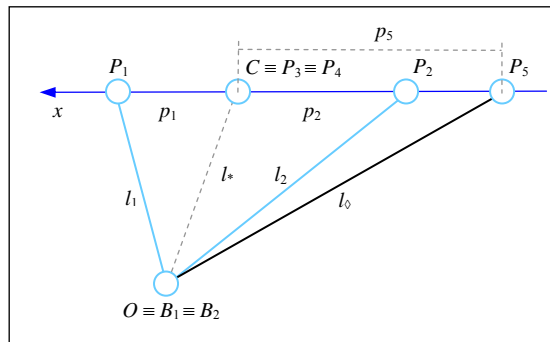


Figure 4.5 Subsystem of ATWOKI: Triangle  $P_2\hat{O}P_5$

**Step 2:** solve for the vector  $\mathbf{i}_1$ . Consider the triangle  $P_2\hat{O}P_5$ , which is depicted in Fig. 4.5. The length  $l_0 = \|P_5 - O\|$  follows as

$$l_0^2 = l_2^2 + p''', \quad (4.31.a)$$

where

$$p''' = -p_2^2 + p_5^2. \quad (4.31.b)$$

Then, refer to the tetrahedron  $OP_5B_5C$ , which is depicted in Fig. 4.6. Given the edges  $p_5$ ,  $l_0$ ,  $l_5$ ,  $l_*$  and  $b_5 = \|B_5\| = \sqrt{A_5^2 + B_5^2 + C_5^2}$ , which are completely known from the manipulator geometry and from the measurements, it is possible to solve for the location of point  $P_5$ .



$$b_5'' = 2b_5, \quad (4.33.f)$$

$$p_5' = p_5^2. \quad (4.33.g)$$

Note that Eq. (4.33.d) gives two solutions for  $f$ , i.e.  $^1f = \sqrt{l_0^2 - d^2 - e^2}$  and  $^2f = -\sqrt{l_0^2 - d^2 - e^2}$ . However, in practical applications, only one solution is feasible and the other can be disregarded. Indeed, the two solutions are separated by a singular configuration which happens for  $f = 0$ . Since, for control issues, the manipulator is not allowed to go across the singularity, the feasible solution is  $^1f$  (or  $^2f$ ) if, in the initial configuration of the manipulator, the value of  $f$  is positive (or negative).

As a consequence, the direction  $\mathbf{i}_1$  follows as

$$\mathbf{i}_1 = (C - P_5) / p_5. \quad (4.34)$$

**Step 3:** solve for the vector  $\mathbf{j}_1$ .

Refer to the tetrahedron  $P_5CB_6P_6$ , which is depicted in Fig. 4.7. Given the edges  $q_6$ ,  $p_5$ ,  $p_{56}$  and  $l_6$ , which are completely known from the manipulator geometry and from the measurements, it is possible to solve for the location of  $P_6$ .

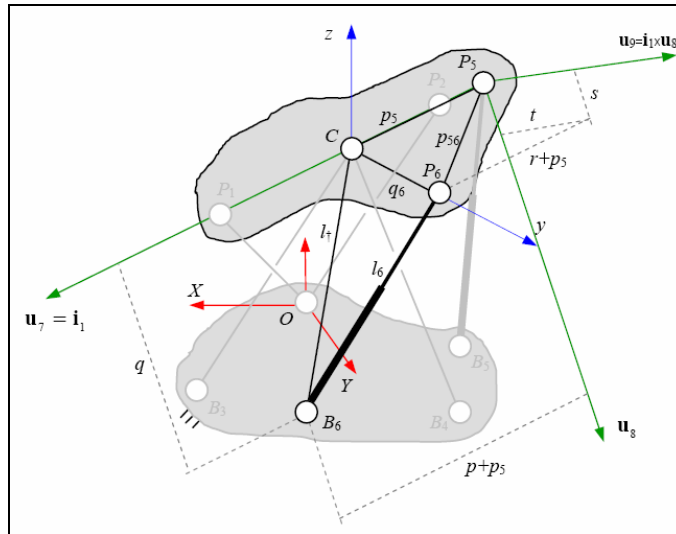


Figure 4.7 Subsystem of ATWOKI: Tetrahedron  $P_5CB_6P_6$

Indeed, upon definition of the unit vectors

$$\mathbf{u}_7 = \mathbf{i}_1, \quad (4.35.a)$$

$$\mathbf{u}_8 = \frac{(B_6 - C) - \mathbf{u}_7 p}{q}, \quad (4.35.b)$$

$$\mathbf{u}_9 = \mathbf{u}_7 \times \mathbf{u}_8, \quad (4.35.c)$$

where

$$p = (\mathbf{B}_6 - \mathbf{C}) \cdot \mathbf{u}_7, \quad (4.35.d)$$

$$q = \|(\mathbf{B}_6 - \mathbf{C}) - \mathbf{u}_7 p\|, \quad (4.35.e)$$

the vector of  $(\mathbf{P}_6 - \mathbf{C})$  can be found as

$$(\mathbf{P}_6 - \mathbf{C}) = r\mathbf{u}_7 + s\mathbf{u}_8 + t\mathbf{u}_9, \quad (4.36.a)$$

being

$$r = \frac{p_5^2 + q_6^2 - p_{56}^2}{2p_5}, \quad (4.36.b)$$

$$s = \frac{q^2 + p^2 + q_6' - l_2^2 - r^2 p}{2q}, \quad (4.36.c)$$

$$t = \pm \sqrt{k - s^2}, \quad (4.36.e)$$

and

$$q_6' = q_6^2, \quad (4.36.f)$$

$$r' = 2r, \quad (4.36.g)$$

$$k = q_6' - r^2. \quad (4.36.h)$$

Note that Eq. (4.36.e) gives two solutions for  $t$ , i.e.  ${}^1t = \sqrt{k - s^2}$  and  ${}^2t = -\sqrt{k - s^2}$ . However, in practical applications, only one solution is feasible and the other can be disregarded. Indeed, the two solutions are separated by a singular configuration which happens for  $t = 0$ . Since, for control issues, the manipulator is not allowed to go across the singularity, the feasible solution is  ${}^1t$  (or  ${}^2t$ ) if, in the initial configuration of the manipulator, the value of  $t$  is positive (or negative).

As a consequence, the direction  $\mathbf{j}_1$  follows as

$$\mathbf{j}_1 = (\mathbf{P}_6 - \mathbf{C}) / q_6. \quad (4.37)$$

**Step 4:** the unit vector  $\mathbf{k}_1$  is calculated as

$$\mathbf{k}_1 = \mathbf{i}_1 \times \mathbf{j}_1. \quad (4.38)$$

Note that the three tetrahedrons  $\text{OB}_3\text{B}_4\text{C}$ ,  $\text{OP}_5\text{B}_5\text{C}$  and  $\text{P}_5\text{CB}_6\text{P}_6$  have been solved by means of the procedure described in [96]. Equivalently, the tetrahedrons can be solved by means of the procedure described in [97].

### Implementation of the EDPA Algorithm

As for the implementation point of view, the EDPA algorithm comprises two parts, namely, the initialization and the main parts. The initialization has to be performed off-line one time for each manipulator, while the main

part is the on-line procedure which leads to the solution of the EDPA as soon as sensor data are acquired. The pseudocode for the implementation is:

0. INITIALIZATION (off-line calculations):

- i. Given the manipulator base and platform, with reference to Fig. (4.2), define the two frames  $S_0$  (i.e.  $O$ ,  $\mathbf{i}_0$ ,  $\mathbf{j}_0$  and  $\mathbf{k}_0$ ) and  $S_1$  (i.e.  $C$ ,  $\mathbf{i}_1$ ,  $\mathbf{j}_1$  and  $\mathbf{k}_1$ );
- ii. Given the manipulator geometry and the definitions in (0.i.), evaluate the point coordinates  $A_3$ ,  $B_3$ ,  $C_3$ ,  $A_4$ ,  $B_4$ ,  $C_4$ ,  $A_5$ ,  $B_5$ ,  $C_5$ ,  $C_6$ ,  $p_1$ ,  $p_2$ ,  $p_5$  and  $q_6$ , as defined by Eqs. (4.26) and Eqs. (4.27);
- iii. Given the definitions (0.ii), according to equations (4.28)-(4.36), evaluate  $p'$ ,  $p''$ ,  $b_3$ ,  $b'_3$ ,  $b''_3$ ,  $\mathbf{u}_1$ ,  $\mathbf{u}_2$ ,  $\mathbf{u}_3$ ,  $m$ ,  $n$ ,  $m'$ ,  $m''$ ,  $n'$ ,  $p'''$ ,  $b_5$ ,  $b'_5$ ,  $b''_5$ ,  $p'_5$ ,  $\mathbf{u}_5$ ,  $r$ ,  $q'_6$  and  $k$ .

1. MAIN (on-line calculations):

- i. Acquire sensor data, i.e.  $l_1$ ,  $l_2$ ,  $l_3$ ,  $l_4$ ,  $l_5$  and  $l_6$ ;
- ii. Evaluate  $l_4^2$ , according to Eq. (4.28), and then find the location of  $C$  according to Eq. (4.30);
- iii. Evaluate  $l_6^2$ , according to Eq. (4.31), and the vectors  $\mathbf{u}_4$  and  $\mathbf{u}_6$ , according to Eq. (4.32);
- iv. Evaluate the location of  $P_5$  according to (4.33);
- v. Evaluate the vector  $\mathbf{i}_1$  according to Eq. (4.34).
- vi. Evaluate the vectors  $\mathbf{u}_7$ ,  $\mathbf{u}_8$  and  $\mathbf{u}_8$  according to Eq. (4.35);
- vii. Evaluate the vector  $(P_6 - C)$  according to Eq. (4.36);
- viii. Evaluate  $\mathbf{j}_1$  according to Eq. (4.37);
- ix. Evaluate  $\mathbf{k}_1$  according to Eq. (4.38).

### **Computational Cost of the EDPA Algorithm**

As for the computational cost, the algorithm is very fast. Since only the main calculations need to be performed on line, the solution of the EDPA requires 81 multiplications/divisions, 64 sums/subtractions and 5 transcendental operations. Namely, the EDPA requires about 145 *flops* and, therefore, is very cheap as compared to the direct position analysis of other fully parallel manipulators which have six degrees of freedom [98-101].

Note that the fast and unique solution is achieved without the addition of extra-sensors. These may be added for speeding up further the computation of the extended DPA as well as decreasing the sensitivity of the pose estimation to measurements errors.

## Chapter 5

### Stiffness Analysis

#### 5.1 Introduction

Section 4.1 and Section 4.2 presented the ATWOKI joint. For convenience, the system architecture is shown again in Fig. 5.1.

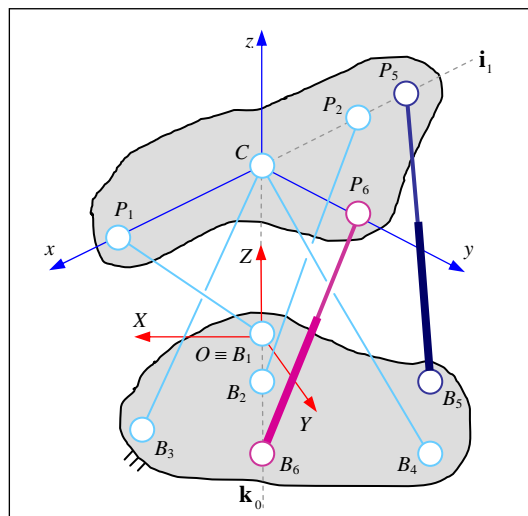


Figure 5.1 ATWOKI Joint (figure 4.1 repeated)

Legs depicted in cyan are the structural rods (of fixed length) which constrain the manipulator to the desired motion, i.e. a 2-dof spherical motion with center in  $C$  and independent axes of rotation  $\mathbf{i}_1$  and  $\mathbf{k}_0$ . Legs depicted in magenta and blue represent the actuators (of controllable length).

The manipulator motion is decoupled. That is, each actuator controls the rotation about only one of the independent axes. In particular, the actuator depicted in magenta controls the rotation about the axis  $\mathbf{i}_1$  only, while the actuator depicted in blue controls the rotation about the axis  $\mathbf{k}_0$  only.

According to the classification we presented in Section 3.4, the ATWOKI joint belongs to the family of US\_PMs of type (2). In particular, it corresponds to the minimal architecture since it has the minimum number of structural legs.

Structurally redundant architectures can be obtained by adding structural US-legs (rods of fixed length) of type  $B_jP_j$ , where the center  $B_j$  of the leg joint which belongs to the base lies along the vector  $\mathbf{k}_0$ , while the center  $P_j$  of the leg joint which belongs to the platform lies along the vector  $\mathbf{i}_1$ , and/or by adding structural legs of type  $CB_i$ , where the point  $C$  belongs to the movable platform (it is the center of the spherical motion of the manipulator) and the point  $B_i$  is located anywhere on the base. An example of redundant architecture is depicted in Fig. 5.2. Recall that a structurally redundant architecture has the advantages of improving the mechanism strength and stiffness and allows the mechanism to be pre-tensioned so as to reduce backlash and so on.



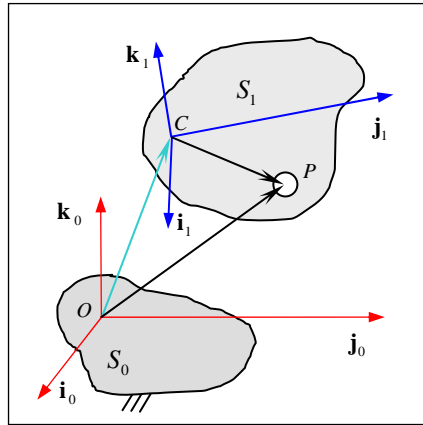


Figure 5.3 Relative Placement between two Bodies

As for the relative displacement of the bodies, considering the position vector  $(C-O)$ , which is depicted in cyan in Fig. 5.3, the translation of the platform with respect to the base can be described by the array of components  $[X \ Y \ Z]^T$  of the position vector  $(C-O)$  expressed in the frame of reference  $S_0$ . Such array of components is indicated, in the following, by

$$C = [X \ Y \ Z]^T. \quad (5.1)$$

As for the relative orientation of the bodies, considering that the placement of the frame of reference  $S_1$  with respect to the frame of reference  $S_0$  can be obtained through three sequential rotations about moving frames, the orientation of the moving body with respect to the fixed body can be described by means of the rotation matrix  $\mathbf{R}$

$$\mathbf{R} = \mathbf{R}_g \mathbf{R}_\delta \mathbf{R}_\beta = \begin{bmatrix} c_\delta c_g & s_\delta c_g s_\beta - s_g c_\beta & s_\delta c_g c_\beta + s_g s_\beta \\ c_\delta s_g & s_\delta s_g s_\beta + c_g c_\beta & s_\delta s_g c_\beta - c_g s_\beta \\ -s_\delta & c_\delta s_\beta & c_\delta c_\beta \end{bmatrix}, \quad (5.2)$$

where  $g$  is the angle of rotation about the axis  $\mathbf{k}_0$  of the initial frame of reference  $S_0$ ,  $\delta$  is the angle of rotation about the axis  $\mathbf{j}_*$  of an intermediate frame of reference  $S_* = \{C, \mathbf{i}_*, \mathbf{j}_*, \mathbf{k}_0\}$  which is obtained upon the first rotation of the moving system by  $g$  about  $\mathbf{k}_0$ , and  $\beta$  is the angle of rotation about the axis  $\mathbf{i}_1$  of the final frame of reference  $S_1$ . Note that the rotation matrix  $\mathbf{R}$  maps the coordinates of a vector between differently oriented reference frames. As an example, if a vector is represented by the coordinate array  $\mathbf{v} = [v_1 \ v_2 \ v_3]^T$  in the frame of reference  $S_1$ , then its coordinate array  $\mathbf{V} = [V_1 \ V_2 \ V_3]^T$  in the frame  $S_0$  corresponds to

$$\mathbf{V} = \mathbf{R}\mathbf{v}. \quad (5.3)$$

Summarizing, since the location of every point  $P$  of the moving body with respect to the fixed body can be described by the relation

$$\mathbf{P} = \mathbf{C} + \mathbf{R}\mathbf{p}, \quad (5.4)$$

where  $\mathbf{P}$  is the array of coordinates of the position vector ( $\mathbf{P}-\mathbf{O}$ ) with respect to  $S_0$ ,  $\mathbf{C}$  is the array of coordinates of the position vector ( $\mathbf{C}-\mathbf{O}$ ) with respect to  $S_0$  and  $\mathbf{p}$  is the array of coordinates of the position vector ( $\mathbf{P}-\mathbf{C}$ ) with respect to  $S_1$ , then the motion of the manipulator can be conveniently described by the generalized coordinate vector  $\mathbf{X}$

$$\mathbf{X} = [X \ Y \ Z \ \vartheta \ \delta \ \beta]^T. \quad (5.5)$$

### 5.3 Premises: Elastic Forces and Moments Associated to Manipulator Deflections

Consider the structure made by the manipulators of Fig. 5.1 or Fig. 5.2 once the prismatic  $\underline{\mathbf{P}}$  actuators of the UPS-legs are locked. Because of the compliance of the structural and of the actuated legs, a generalized displacement  $\mathbf{X}$  of the moving platform with respect to the fixed base causes the legs to elastically react so that they produce forces and moments which act both on the platform and on the base.

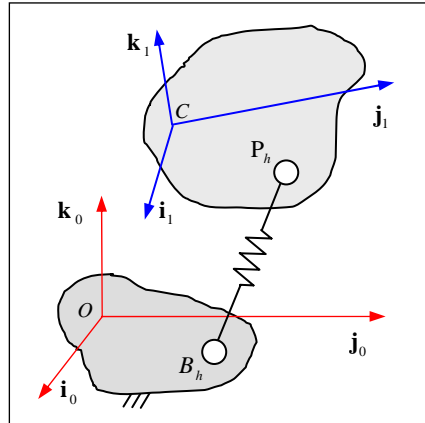


Figure 5.4 Elastic Reaction due to the Compliance of a Single Leg

To evaluate the total solicitation caused by the elastic reactions of all the legs which make the manipulator, first consider the force and the moment generated on the platform by a single leg. In particular, refer to Fig. 5.4 which depicts the  $h$ -th leg considered as a spring.

Upon definitions, for each leg  $h$ , of the leg length  $l_h = \|\mathbf{P}_h - \mathbf{B}_h\|$ , of the leg (spring) stiffness  $k_h$  and of the leg (spring) death-length  ${}^0l_h$ , the elastic force  $\mathbf{f}^{(h)}$ , which is exerted by the  $h$ -th leg on the platform, is given by

$$\mathbf{f}^{(h)} = k_h (l_h - {}^0l_h) \frac{(\mathbf{P}_h - \mathbf{B}_h)}{\|\mathbf{P}_h - \mathbf{B}_h\|} = k_h (1 - {}^0l_h/l_h) (\mathbf{P}_h - \mathbf{B}_h), \quad (5.6)$$

while the elastic moment  $\mathbf{m}^{(h)}$  (about the center  $\mathbf{C}$ ) which is exerted by the  $h$ -th leg on the platform, follows as

$$\mathbf{m}^{(h)} = k_h (1 - {}^0l_h/l_h) (\mathbf{P}_h - \mathbf{C}) \times (\mathbf{P}_h - \mathbf{B}_h) = k_h (1 - {}^0l_h/l_h) (\mathbf{P}_h - \mathbf{C}) \times (\mathbf{C} - \mathbf{B}_h). \quad (5.7)$$

In the context of the 2-dof spherical US\_PMs described in Chapter 3, Eq. (5.6) and Eq. (5.7) can be specialized for the types of legs such manipulators are made by.

In particular, considering the structural legs of type  $CB_i$ , Eq. (5.6) and Eq. (5.7) specialize, respectively, as

$$\mathbf{f}^{(i)} = k_i \left(1 - \frac{l_i^0}{l_i}\right) (\mathbf{C} - \mathbf{B}_i), \quad (5.8)$$

$$\mathbf{m}^{(i)} = 0. \quad (5.9)$$

Moreover, considering the structural legs of type  $P_jB_j$ , Eq. (5.6) and Eq. (5.7) specialize, respectively, as

$$\mathbf{f}^{(j)} = k_j \left(1 - \frac{l_j^0}{l_j}\right) (\mathbf{P}_j - \mathbf{B}_j), \quad (5.10)$$

$$\mathbf{m}^{(j)} = k_j \left(1 - \frac{l_j^0}{l_j}\right) (\mathbf{P}_j - \mathbf{C}) \times (\mathbf{C} - \mathbf{B}_j). \quad (5.11)$$

As for the total contributions, given a manipulator with  $\#I$   $CB_i$ -legs,  $\#J$   $P_jB_j$ -legs and two actuators,  $P_LB_L$  and  $P_MB_M$ , where  $L = I + J + 1$  and  $M = L + 1$ , the total elastic force  $\mathbf{F}$  exerted by the  $M$  legs on the platform is given by

$$\mathbf{F} = \sum_{i=1}^I \mathbf{f}^{(i)} + \sum_{j=I+1}^{I+J} \mathbf{f}^{(j)} + \mathbf{f}^{(L)} + \mathbf{f}^{(M)}, \quad (5.12)$$

while the total elastic moment  $\mathbf{M}$  (about the center  $\mathbf{C}$ ) exerted by the  $M$  legs on the platform follows as

$$\mathbf{M} = \sum_{i=1}^I \mathbf{m}^{(i)} + \sum_{j=I+1}^{I+J} \mathbf{m}^{(j)} + \mathbf{m}^{(L)} + \mathbf{m}^{(M)}. \quad (5.13)$$

With these definitions, it is convenient to define the generalized force vector  $\mathfrak{F}$

$$\mathfrak{F} = \begin{bmatrix} \mathbf{F} \\ \mathbf{M} \end{bmatrix}. \quad (5.14)$$

## 5.4 Manipulator Stiffness: General Expressions

As defined in the introduction to this chapter, the manipulator stiffness can be defined by the gradient of the generalized force vector  $\mathfrak{F}$  with respect to the generalized displacement  $\mathbf{X}$ . That is, the manipulator stiffness is given by the 6x6 matrix  $\mathbf{K}$  such that

$$\mathbf{K} = \nabla_{\mathbf{X}} \mathfrak{F} = \frac{\partial \mathfrak{F}}{\partial \mathbf{X}}. \quad (5.15)$$

Accordingly, the variation of the generalized force  $\partial \mathfrak{F} = [\partial \mathfrak{F}_1 \quad \partial \mathfrak{F}_2 \quad \partial \mathfrak{F}_3 \quad \partial \mathfrak{F}_4 \quad \partial \mathfrak{F}_5 \quad \partial \mathfrak{F}_6]^T$  caused by an infinitesimal variation of the generalized displacement  $\partial \mathbf{X} = [\partial X_1 \quad \partial X_2 \quad \partial X_3 \quad \partial X_4 \quad \partial X_5 \quad \partial X_6]^T$  follows as

$$\begin{bmatrix} \partial \mathfrak{J}_1 \\ \partial \mathfrak{J}_2 \\ \partial \mathfrak{J}_3 \\ \partial \mathfrak{J}_4 \\ \partial \mathfrak{J}_5 \\ \partial \mathfrak{J}_6 \end{bmatrix} = \begin{bmatrix} K_{11} & K_{12} & K_{13} & K_{14} & K_{15} & K_{16} \\ K_{21} & K_{22} & K_{23} & K_{24} & K_{25} & K_{26} \\ K_{31} & K_{32} & K_{33} & K_{34} & K_{35} & K_{36} \\ K_{41} & K_{42} & K_{43} & K_{44} & K_{45} & K_{46} \\ K_{51} & K_{52} & K_{53} & K_{54} & K_{55} & K_{56} \\ K_{61} & K_{62} & K_{63} & K_{64} & K_{65} & K_{66} \end{bmatrix} \begin{bmatrix} \partial X_1 \\ \partial X_2 \\ \partial X_3 \\ \partial X_4 \\ \partial X_5 \\ \partial X_6 \end{bmatrix}. \quad (5.16)$$

Heretofore, the entries  $K_{rs}$  of the stiffness matrix  $\mathbf{K}$  will be called coefficient of influence.

The coefficients of influence depend, in general, on  $\mathbf{X}$ . That is, the manipulator stiffness  $\mathbf{K}$  is configuration dependent. Moreover, note that, for a given manipulator, the expressions of the coefficients  $K_{rs}$  depend also on how the components of the generalized force  $\mathfrak{F}$  and the components of the generalized displacement  $\mathbf{X}$  are chosen. As an example, by defining the components of  $\mathbf{X}$  as given by Eq. (5.5), the expressions of the coefficients  $K_{rs}$  are different if, referring to Eq. (5.14), one chooses the components of the vector  $\mathfrak{F}$  with respect to the system  $S_0$  or with respect to the system  $S_1$ . In practice, the choice of the components  $\mathfrak{J}_g$ , for  $g=1, \dots, 6$ , is free and depends on the problem at hand. If needed, one may also consider choosing a mixed expression which contains some of the components of  $\mathbf{F}$  and  $\mathbf{M}$  with respect to one frame of reference and some of the components of  $\mathbf{F}$  and  $\mathbf{M}$  with respect to another frame of reference. In this latter case, however, one should be aware that the quantity  $(\mathfrak{J}_1^2 + \mathfrak{J}_2^2 + \mathfrak{J}_3^2)$  may differ from  $(\mathbf{F} \cdot \mathbf{F})$ , and that the quantity  $(\mathfrak{J}_4^2 + \mathfrak{J}_5^2 + \mathfrak{J}_6^2)$  may differ from  $(\mathbf{M} \cdot \mathbf{M})$ .

As for the form of  $\mathbf{K}$ , depending on the mutual relationship between the components of  $\mathbf{X}$  and the  $\mathfrak{J}_g$ 's, the stiffness matrix can be symmetric or not. The conditions for  $\mathbf{K}$  to be symmetric are: 1) the directions along which the components of  $\mathbf{F}$  are evaluated correspond to the directions along which the displacement of the manipulator is assessed, 2) the axes about which the components of  $\mathbf{M}$  are evaluated correspond to the axes about which the rotation of the manipulator is assessed.

Thus, evaluation of the coefficients  $K_{rs}$  requires the expression of the force  $\mathbf{F}$  (that is, of all the forces  $\mathbf{f}^{(i)}$ ,  $\mathbf{f}^{(j)}$ ,  $\mathbf{f}^{(L)}$  and  $\mathbf{f}^{(M)}$ ) and of the moment  $\mathbf{M}$  (that is, of all the moments  $\mathbf{m}^{(i)}$ ,  $\mathbf{m}^{(j)}$ ,  $\mathbf{m}^{(L)}$  and  $\mathbf{m}^{(M)}$ ) to be written with respect to some frame of reference.

Referring to the frame  $S_0$ , introducing the coordinate vectors  $\mathbf{B}_i = [A_i \ B_i \ C_i]^T$ ,  $i=1, \dots, I$ , of the points  $B_i$  of the  $CB_i$ -legs, the components of  $\mathbf{f}^{(i)}$  and  $\mathbf{m}^{(i)}$ , for  $i=1, \dots, I$ , with respect  $S_0$  can be written as

$$\mathbf{f}^{(i)} \cdot \begin{bmatrix} \mathbf{i}_0 \\ \mathbf{j}_0 \\ \mathbf{k}_0 \end{bmatrix} = \begin{bmatrix} f_{i_0}^{(i)} \\ f_{j_0}^{(i)} \\ f_{k_0}^{(i)} \end{bmatrix} = k_i \left( 1 - \frac{{}^0 l_i}{l_i} \right) \begin{bmatrix} X - A_i \\ Y - B_i \\ Z - C_i \end{bmatrix}, \quad (5.17)$$

$$\mathbf{m}^{(i)} \cdot \begin{bmatrix} \mathbf{i}_0 \\ \mathbf{j}_0 \\ \mathbf{k}_0 \end{bmatrix} = \begin{bmatrix} m_{i_0}^{(i)} \\ m_{j_0}^{(i)} \\ m_{k_0}^{(i)} \end{bmatrix} = \begin{bmatrix} 0 \\ 0 \\ 0 \end{bmatrix}, \quad (5.18)$$

where the leg lengths  $l_i$  are given by

$$l_i = \sqrt{A_i^2 + B_i^2 + C_i^2 + X^2 + Y^2 + Z^2 - 2(A_i X + B_i Y + C_i Z)}. \quad (5.19)$$

Introducing the coordinate vectors  $\mathbf{B}_j = [0 \ 0 \ C_j]^T$  of the points  $B_j$  of the  $P_j B_j$ -legs (with respect to  $S_0$ ) and the coordinate vectors  $\mathbf{p}_j = [p_j \ 0 \ 0]^T$  of the points  $P_j$  of the  $P_j B_j$ -legs (with respect to  $S_1$ ), the components of  $\mathbf{f}^{(j)}$  and  $\mathbf{m}^{(j)}$ , for  $j = (I+1), \dots, (I+J)$ , with respect  $S_0$  can be written as

$$\mathbf{f}^{(j)} \cdot \begin{bmatrix} \mathbf{i}_0 \\ \mathbf{j}_0 \\ \mathbf{k}_0 \end{bmatrix} = \begin{bmatrix} f_{i_0}^{(j)} \\ f_{j_0}^{(j)} \\ f_{k_0}^{(j)} \end{bmatrix} = k_j \left( 1 - \frac{{}^0 l_j}{l_j} \right) \begin{bmatrix} X + c_\delta c_g p_j \\ Y + c_\delta s_g p_j \\ Z - C_j - s_\delta p_j \end{bmatrix}, \quad (5.20)$$

$$\mathbf{m}^{(j)} \cdot \begin{bmatrix} \mathbf{i}_0 \\ \mathbf{j}_0 \\ \mathbf{k}_0 \end{bmatrix} = \begin{bmatrix} m_{i_0}^{(j)} \\ m_{j_0}^{(j)} \\ m_{k_0}^{(j)} \end{bmatrix} = k_j p_j \left( 1 - \frac{{}^0 l_j}{l_j} \right) \begin{bmatrix} (Z - C_j) c_\delta s_g + s_\delta Y \\ -s_\delta X - (Z - C_j) c_\delta c_g \\ c_\delta c_g Y - c_\delta s_g X \end{bmatrix}, \quad (5.21)$$

where the leg lengths  $l_j$  are given by

$$l_j = \sqrt{p_j^2 + X^2 + Y^2 + (Z - C_j)^2 + 2p_j (c_\delta c_g X + c_\delta s_g Y - s_\delta (Z - C_j))}. \quad (5.22)$$

Introducing the coordinate vector  $\mathbf{B}_L = [A_L \ B_L \ C_L]^T$  of the point  $B_L$  of the  $P_L B_L$ -leg (with respect to  $S_0$ ) and the coordinate vector  $\mathbf{p}_L = [p_L \ 0 \ 0]^T$  of the point  $P_L$  of the  $P_L B_L$ -leg (with respect to  $S_1$ ), the components of  $\mathbf{f}^{(L)}$  and  $\mathbf{m}^{(L)}$  with respect  $S_0$  follow as

$$\mathbf{f}^{(L)} \cdot \begin{bmatrix} \mathbf{i}_0 \\ \mathbf{j}_0 \\ \mathbf{k}_0 \end{bmatrix} = \begin{bmatrix} f_{i_0}^{(L)} \\ f_{j_0}^{(L)} \\ f_{k_0}^{(L)} \end{bmatrix} = k_L \left( 1 - \frac{{}^0 l_L}{l_L} \right) \begin{bmatrix} X - A_L + c_\delta c_g p_L \\ Y - B_L + c_\delta s_g p_L \\ Z - C_L - s_\delta p_L \end{bmatrix}, \quad (5.23)$$

$$\mathbf{m}^{(L)} \cdot \begin{bmatrix} \mathbf{i}_0 \\ \mathbf{j}_0 \\ \mathbf{k}_0 \end{bmatrix} = \begin{bmatrix} m_{i_0}^{(L)} \\ m_{j_0}^{(L)} \\ m_{k_0}^{(L)} \end{bmatrix} = k_L p_L \left( 1 - \frac{{}^0 l_L}{l_L} \right) \begin{bmatrix} (Z - C_L) c_\delta s_g + (Y - B_L) s_\delta \\ -(X - A_L) s_\delta - (Z - C_L) c_\delta c_g \\ (Y - B_L) c_\delta c_g - (X - A_L) c_\delta s_g \end{bmatrix}, \quad (5.24)$$

where the leg length  $l_L$  is given by

$$l_L = \sqrt{p_L^2 + (X - A_L)^2 + (Y - B_L)^2 + (Z - C_L)^2 + 2p_L ((X - A_L) c_\delta c_g + (Y - B_L) c_\delta s_g - (Z - C_L) s_\delta)}. \quad (5.25)$$

Introducing the coordinate vector  $\mathbf{B}_M = [0 \ 0 \ C_M]^T$  of the point  $B_M$  of the  $P_M B_M$ -leg (with respect to  $S_0$ ) and the coordinate vector  $\mathbf{p}_M = [0 \ q_M \ 0]^T$  of the point  $P_M$  of the  $P_M B_M$ -leg (with respect to  $S_1$ ), the components of  $\mathbf{f}^{(M)}$  and  $\mathbf{m}^{(M)}$  with respect  $S_0$  follow as

$$\mathbf{f}^{(M)} \cdot \begin{bmatrix} \mathbf{i}_0 \\ \mathbf{j}_0 \\ \mathbf{k}_0 \end{bmatrix} = \begin{bmatrix} f_{i_0}^{(M)} \\ f_{j_0}^{(M)} \\ f_{k_0}^{(M)} \end{bmatrix} = k_M \left( 1 - \frac{{}^0l_M}{l_M} \right) \begin{bmatrix} X + (s_\delta c_g s_\beta - s_g c_\beta) q_M \\ Y + (s_\delta s_g s_\beta + c_g c_\beta) q_M \\ Z - C_M + c_\delta s_\beta q_M \end{bmatrix}, \quad (5.26)$$

$$\mathbf{m}^{(M)} \cdot \begin{bmatrix} \mathbf{i}_0 \\ \mathbf{j}_0 \\ \mathbf{k}_0 \end{bmatrix} = \begin{bmatrix} m_{i_0}^{(M)} \\ m_{j_0}^{(M)} \\ m_{k_0}^{(M)} \end{bmatrix} = k_M q_M \left( 1 - \frac{{}^0l_M}{l_M} \right) \begin{bmatrix} (Z - C_M)(s_\delta s_g s_\beta + c_g c_\beta) - Y c_\delta s_\beta \\ X c_\delta s_\beta - (Z - C_M)(s_\delta c_g s_\beta - s_g c_\beta) \\ Y (s_\delta c_g s_\beta - s_g c_\beta) - X (s_\delta s_g s_\beta + c_g c_\beta) \end{bmatrix}, \quad (5.27)$$

where the leg length  $l_M$  is given by

$$l_M = \sqrt{q_M^2 + X^2 + Y^2 + (Z - C_M)^2 + 2q_M (X (s_\delta c_g s_\beta - s_g c_\beta) + Y (s_\delta s_g s_\beta + c_g c_\beta) + (Z - C_M) c_\delta s_\beta)}. \quad (5.28)$$

In addition, for convenience, introduce the moments about the axis  $\mathbf{j}_* = \frac{\mathbf{k}_0 \times \mathbf{i}_1}{\|\mathbf{k}_0 \times \mathbf{i}_1\|}$ , i.e.

$$m_{\mathbf{j}_*}^{(i)} = \mathbf{m}^{(i)} \cdot \mathbf{j}_* = 0, \quad (5.29)$$

$$m_{\mathbf{j}_*}^{(j)} = \mathbf{m}^{(j)} \cdot \mathbf{j}_* = k_j p_j \left( 1 - \frac{{}^0l_j}{l_j} \right) (-s_\delta c_g X - s_\delta s_g Y - c_\delta (Z - C_j)), \quad (5.30)$$

$$m_{\mathbf{j}_*}^{(L)} = \mathbf{m}^{(L)} \cdot \mathbf{j}_* = k_L p_L \left( 1 - \frac{{}^0l_L}{l_L} \right) (-(X - A_L) s_\delta c_g - (Y - B_L) s_\delta s_g - (Z - C_L) c_\delta), \quad (5.31)$$

$$m_{\mathbf{j}_*}^{(M)} = \mathbf{m}^{(M)} \cdot \mathbf{j}_* = k_M q_M \left( 1 - \frac{{}^0l_M}{l_M} \right) (X c_\delta c_g s_\beta + Y c_\delta s_g s_\beta - (Z - C_M) s_\delta s_\beta), \quad (5.32)$$

and the moments about  $\mathbf{i}_1$ , i.e.

$$m_{\mathbf{i}_1}^{(i)} = \mathbf{m}^{(i)} \cdot \mathbf{i}_1 = 0, \quad (5.33)$$

$$m_{\mathbf{i}_1}^{(j)} = \mathbf{m}^{(j)} \cdot \mathbf{i}_1 = 0, \quad (5.34)$$

$$m_{\mathbf{i}_1}^{(L)} = \mathbf{m}^{(L)} \cdot \mathbf{i}_1 = 0, \quad (5.35)$$

$$m_{\mathbf{i}_1}^{(M)} = \mathbf{m}^{(M)} \cdot \mathbf{i}_1 = k_M q_M \left( 1 - \frac{{}^0l_M}{l_M} \right) (X (s_g s_\beta + s_\delta c_g c_\beta) + Y (-c_g s_\beta + s_\delta s_g c_\beta) + (Z - C_M) c_\delta c_\beta).$$

Then, define the components  $\mathfrak{F}_g$ , for  $g = 1, \dots, 6$ , of the generalized force vector  $\mathfrak{F}$  as in the following

$$\mathfrak{F}_1 = f_{i_0} = \sum_{i=1}^I f_{i_0}^{(i)} + \sum_{i=I+1}^J f_{i_0}^{(j)} + f_{i_0}^{(L)} + f_{i_0}^{(M)}, \quad (5.36.a)$$

$$\mathfrak{F}_2 = f_{j_0} = \sum_{i=1}^I f_{j_0}^{(i)} + \sum_{i=I+1}^J f_{j_0}^{(j)} + f_{j_0}^{(L)} + f_{j_0}^{(M)}, \quad (5.36.b)$$

$$\mathfrak{F}_3 = f_{k_0} = \sum_{i=1}^I f_{k_0}^{(i)} + \sum_{i=I+1}^J f_{k_0}^{(j)} + f_{k_0}^{(L)} + f_{k_0}^{(M)}, \quad (5.36.c)$$

$$\mathfrak{F}_4 = m_{k_0} = \sum_{i=1}^I m_{k_0}^{(i)} + \sum_{i=I+1}^J m_{k_0}^{(j)} + m_{k_0}^{(L)} + m_{k_0}^{(M)}, \quad (5.36.d)$$

$$\mathfrak{F}_5 = m_{j_*} = \sum_{i=1}^I m_{j_*}^{(i)} + \sum_{i=I+1}^J m_{j_*}^{(j)} + m_{j_*}^{(L)} + m_{j_*}^{(M)}, \quad (5.36.e)$$

$$\mathfrak{F}_6 = m_{i_1} = \sum_{i=1}^I m_{i_1}^{(i)} + \sum_{i=I+1}^J m_{i_1}^{(j)} + m_{i_1}^{(L)} + m_{i_1}^{(M)}. \quad (5.36.f)$$

Note that in the choice of the components of the generalized force  $\mathfrak{F}$ , the moments  $m_{j_*}$  and  $m_{i_1}$  have been preferred to the moments  $m_{j_0}$  and  $m_{i_0}$ , respectively, because the former are physical quantities that are more suitable and practical for understanding the effective solicitation that acts on the manipulator.

Besides, it has to be highlighted that, since the unit vectors  $\mathbf{k}_0$ ,  $\mathbf{j}_*$  and  $\mathbf{i}_1$  are not, in general, mutually orthogonal, the total moment  $\mathbf{M}$  which acts on the platform may differ from the quantity  $m_{k_0} \mathbf{k}_0 + m_{j_*} \mathbf{j}_* + m_{i_1} \mathbf{i}_1$ .

It is now possible to determine the stiffness matrix  $\mathbf{K}$ . Indeed, by considering the generalized coordinate vector  $\mathbf{X}$  we defined in Eq. (5.5), and the generalized force  $\mathfrak{F}$  we defined in Eqs. (5.36), the coefficients of influence  $K_{rs}$ , for  $r = 1, \dots, 6$  and  $s = 1, \dots, 6$ , are obtained from

$$K_{rs} = \frac{\partial \mathfrak{F}_r}{\partial X_s}. \quad (5.37)$$

For convenience, for  $h = 1, \dots, M$ , introduce the following positions

$$f_X^{(h)} = f_{i_0}^{(h)} = \mathfrak{F}_1, \quad (5.38.a)$$

$$f_Y^{(h)} = f_{j_0}^{(h)} = \mathfrak{F}_2, \quad (5.38.b)$$

$$f_Z^{(h)} = f_{k_0}^{(h)} = \mathfrak{F}_3, \quad (5.38.c)$$

$$m_g^{(h)} = m_{k_0}^{(h)} = \mathfrak{F}_4, \quad (5.38.d)$$

$$m_\delta^{(h)} = m_{j_*}^{(h)} = \mathfrak{F}_5, \quad (5.38.e)$$

$$m_\theta^{(h)} = m_{i_1}^{(h)} = \mathfrak{F}_6. \quad (5.38.f)$$

Then, from Eqs. (5.36)-(5.38), the coefficients  $K_{rs}$  can be evaluated by

$$K_{rs} = \sum_{i=1}^I K_{rs}^{(i)} + \sum_{i=I+1}^J K_{rs}^{(j)} + K_{rs}^{(L)} + K_{rs}^{(M)}, \quad (5.39)$$

where, for  $r, s = X, Y, Z, \vartheta, \delta, \beta$  (i.e. for  $r, s = 1, \dots, 6$ ), the  $K_{rs}^{(i)}$ ,  $K_{rs}^{(j)}$ ,  $K_{rs}^{(L)}$ ,  $K_{rs}^{(M)}$  are given below

$$K_{XX}^{(i)} = k_i \left[ \left( 1 - \frac{{}^0l_i}{l_i} \right) + \left( \frac{{}^0l_i (X - A_i)^2}{l_i^3} \right) \right], \quad (5.40.a)$$

$$K_{XY}^{(i)} = K_{YX}^{(i)} = k_i \left( \frac{{}^0l_i (Y - B_i)(X - A_i)}{l_i^3} \right), \quad (5.40.b)$$

$$K_{XZ}^{(i)} = K_{ZX}^{(i)} = k_i \left( \frac{{}^0l_i (X - A_i)(Z - C_i)}{l_i^3} \right), \quad (5.40.c)$$

$$K_{X\vartheta}^{(i)} = 0, \quad (5.40.d)$$

$$K_{X\delta}^{(i)} = 0, \quad (5.40.e)$$

$$K_{X\beta}^{(i)} = 0, \quad (5.40.f)$$

$$K_{YY}^{(i)} = k_i \left[ \left( 1 - \frac{{}^0l_i}{l_i} \right) + \left( \frac{{}^0l_i (Y - B_i)^2}{l_i^3} \right) \right], \quad (5.40.g)$$

$$K_{YZ}^{(i)} = K_{ZY}^{(i)} = k_i \left( \frac{{}^0l_i (Y - B_i)(Z - C_i)}{l_i^3} \right), \quad (5.40.h)$$

$$K_{Y\vartheta}^{(i)} = K_{\vartheta Y}^{(i)} = 0, \quad (5.40.i)$$

$$K_{Y\delta}^{(i)} = K_{\delta Y}^{(i)} = 0, \quad (5.40.l)$$

$$K_{Y\beta}^{(i)} = K_{\beta Y}^{(i)} = 0, \quad (5.40.m)$$

$$K_{ZZ}^{(i)} = k_i \left[ \left( 1 - \frac{{}^0l_i}{l_i} \right) + \left( \frac{{}^0l_i (Z - C_i)^2}{l_i^3} \right) \right], \quad (5.40.n)$$

$$K_{Z\vartheta}^{(i)} = K_{\vartheta Z}^{(i)} = 0, \quad (5.40.o)$$

$$K_{Z\delta}^{(i)} = K_{\delta Z}^{(i)} = 0, \quad (5.40.p)$$

$$K_{Z\beta}^{(i)} = K_{\beta Z}^{(i)} = 0, \quad (5.40.q)$$

$$K_{gg}^{(i)} = 0, \quad (5.40.r)$$

$$K_{g\delta}^{(i)} = K_{\delta g}^{(i)} = 0, \quad (5.40.s)$$

$$K_{g\beta}^{(i)} = K_{\beta g}^{(i)} = 0, \quad (5.40.t)$$

$$K_{\delta\delta}^{(i)} = 0, \quad (5.40.u)$$

$$K_{\delta\beta}^{(i)} = K_{\beta\delta}^{(i)} = 0, \quad (5.40.v)$$

$$K_{\beta\beta}^{(i)} = 0, \quad (5.40.z)$$

where the leg lengths  $l_i$ , for  $i = 1, \dots, I$ , depend on  $X$  and are defined in Eq. (5.19);

$$K_{XX}^{(j)} = k_j \left[ \left( 1 - \frac{{}^0l_j}{l_j} \right) + \left( \frac{{}^0l_j (X + c_\delta c_g p_j)^2}{l_j^3} \right) \right], \quad (5.41.a)$$

$$K_{XY}^{(j)} = K_{YX}^{(j)} = k_j \left( \frac{{}^0l_j (Y + p_j c_\delta s_g) (X + c_\delta c_g p_j)}{l_j^3} \right), \quad (5.41.b)$$

$$K_{XZ}^{(j)} = K_{ZX}^{(j)} = k_j \left( \frac{{}^0l_j ((Z - C_j) - p_j s_\delta) (X + c_\delta c_g p_j)}{l_j^3} \right), \quad (5.41.c)$$

$$K_{Xg}^{(j)} = K_{gX}^{(j)} = k_j p_j \left[ \left( 1 - \frac{{}^0l_j}{l_j} \right) (-c_\delta s_g) + \left( \frac{{}^0l_j (-c_\delta s_g X + c_\delta c_g Y) (X + c_\delta c_g p_j)}{l_j^3} \right) \right], \quad (5.41.d)$$

$$K_{X\delta}^{(j)} = K_{\delta X}^{(j)} = k_j p_j \left[ \left( 1 - \frac{{}^0l_j}{l_j} \right) (-s_\delta c_g) + \left( \frac{{}^0l_j (-s_\delta c_g X - s_\delta s_g Y - c_\delta (Z - C_j)) (X + c_\delta c_g p_j)}{l_j^3} \right) \right], \quad (5.41.e)$$

$$K_{X\beta}^{(j)} = K_{\beta X}^{(j)} = 0, \quad (5.41.f)$$

$$K_{YY}^{(j)} = k_j \left[ \left( 1 - \frac{{}^0l_j}{l_j} \right) + \left( \frac{{}^0l_j (Y + c_\delta s_g p_j)^2}{l_j^3} \right) \right], \quad (5.41.g)$$

$$K_{YZ}^{(j)} = K_{ZY}^{(j)} = k_j \left( \frac{{}^0l_j (Y + c_\delta s_g p_j) ((Z - C_j) - s_\delta p_j)}{l_j^3} \right), \quad (5.41.h)$$

$$K_{Yg}^{(j)} = K_{gY}^{(j)} = k_j p_j \left[ \left( 1 - \frac{{}^0l_j}{l_j} \right) (c_\delta c_g) + \left( \frac{{}^0l_j (-c_\delta s_g X + c_\delta c_g Y) (Y + c_\delta s_g p_j)}{l_j^3} \right) \right], \quad (5.41.i)$$

$$K_{Y\delta}^{(j)} = K_{\delta Y}^{(j)} = k_j p_j \left[ \left( 1 - \frac{{}^0l_j}{l_j} \right) (-s_\delta s_g) + \left( \frac{{}^0l_j (-s_\delta c_g X - s_\delta s_g Y - c_\delta (Z - C_j)) (Y + c_\delta s_g p_j)}{l_j^3} \right) \right], \quad (5.41.l)$$

$$K_{Y\beta}^{(j)} = K_{\beta Y}^{(j)} = 0, \quad (5.41.m)$$

$$K_{ZZ}^{(j)} = k_j \left[ \left( 1 - \frac{{}^0l_j}{l_j} \right) + \left( \frac{{}^0l_j ((Z - C_j) - s_\delta p_j)^2}{l_j^3} \right) \right], \quad (5.41.n)$$

$$K_{Z\delta}^{(j)} = K_{\delta Z}^{(j)} = k_j p_j \left( \frac{{}^0l_j (-c_\delta s_g X + c_\delta c_g Y) ((Z - C_j) - s_\delta p_j)}{l_j^3} \right), \quad (5.41.o)$$

$$K_{Z\delta}^{(j)} = K_{\delta Z}^{(j)} = k_j p_j \left[ \left( 1 - \frac{{}^0l_j}{l_j} \right) (-c_\delta) + \left( \frac{{}^0l_j (-s_\delta c_g X - s_\delta s_g Y - c_\delta (Z - C_j)) ((Z - C_j) - s_\delta p_j)}{l_j^3} \right) \right], \quad (5.41.p)$$

$$K_{Z\beta}^{(j)} = K_{\beta Z}^{(j)} = 0, \quad (5.41.q)$$

$$K_{g\delta}^{(j)} = k_j p_j \left[ \left( 1 - \frac{{}^0l_j}{l_j} \right) (-c_\delta s_g Y - c_\delta c_g X) + \left( \frac{{}^0l_j p_j (-c_\delta s_g X + c_\delta c_g Y)^2}{l_j^3} \right) \right], \quad (5.41.r)$$

$$K_{g\delta}^{(j)} = K_{\delta g}^{(j)} = k_j p_j \left[ \left( 1 - \frac{{}^0l_j}{l_j} \right) (-s_\delta c_g Y + s_\delta s_g X) + \left( \frac{{}^0l_j p_j (-s_\delta c_g X - s_\delta s_g Y - c_\delta (Z - C_j)) (c_\delta c_g Y - c_\delta s_g X)}{l_j^3} \right) \right], \quad (5.41.s)$$

$$K_{g\beta}^{(j)} = K_{\beta g}^{(j)} = 0, \quad (5.41.t)$$

$$K_{\delta\delta}^{(j)} = k_j p_j \left[ \left( 1 - \frac{{}^0l_j}{l_j} \right) (-c_\delta c_g X - c_\delta s_g Y + s_\delta (Z - C_j)) + \left( \frac{{}^0l_j p_j (-s_\delta c_g X - s_\delta s_g Y - c_\delta (Z - C_j))^2}{l_j^3} \right) \right], \quad (5.41.u)$$

$$K_{\delta\beta}^{(j)} = K_{\beta\delta}^{(j)} = 0, \quad (5.41.v)$$

$$K_{\beta\beta}^{(j)} = 0, \quad (5.41.z)$$

where the leg lengths  $l_j$ , for  $j = (I+1), \dots, (I+J)$ , depend on  $X$  and are defined in Eq. (5.22);

$$K_{XX}^{(L)} = k_L \left[ \left( 1 - \frac{{}^0l_L}{l_L} \right) + \left( \frac{{}^0l_L (X - A_L + p_L c_\delta c_g)^2}{l_L^3} \right) \right], \quad (5.42.a)$$

$$K_{XY}^{(L)} = K_{YX}^{(L)} = k_L \left( \frac{{}^0l_L (Y - B_L + p_L c_\delta s_g) (X - A_L + c_\delta c_g p_L)}{l_L^3} \right), \quad (5.42.b)$$

$$K_{XZ}^{(L)} = K_{ZX}^{(L)} = k_L \left( \frac{{}^0l_L (Z - C_L - p_L s_\delta) (X - A_L + c_\delta c_\theta p_L)}{l_L^3} \right), \quad (5.42.c)$$

$$K_{X\theta}^{(L)} = K_{\theta X}^{(L)} = k_L p_L \left[ \left( 1 - \frac{{}^0l_L}{l_L} \right) (-c_\delta s_\theta) + \left( \frac{{}^0l_L (-(X - A_L) c_\delta s_\theta + (Y - B_L) c_\delta c_\theta) (X - A_L + c_\delta c_\theta p_L)}{l_L^3} \right) \right], \quad (5.42.d)$$

$$K_{X\delta}^{(L)} = K_{\delta X}^{(L)} = k_L p_L \left[ \left( \frac{{}^0l_L}{l_L} - 1 \right) (s_\delta c_\theta) + \left( \frac{{}^0l_L ((X - A_L) s_\delta c_\theta + (Y - B_L) s_\delta s_\theta + (Z - C_L) c_\delta) (A_L - X - c_\delta c_\theta p_L)}{l_L^3} \right) \right], \quad (5.42.e)$$

$$K_{X\beta}^{(L)} = K_{\beta X}^{(L)} = 0, \quad (5.42.f)$$

$$K_{YY}^{(L)} = k_L \left[ \left( 1 - \frac{{}^0l_L}{l_L} \right) + \left( \frac{{}^0l_L (Y - B_L + p_L c_\delta s_\theta)^2}{l_L^3} \right) \right], \quad (5.42.g)$$

$$K_{YZ}^{(L)} = K_{ZY}^{(L)} = k_L \left( \frac{{}^0l_L (Z - C_L - p_L s_\delta) (Y - B_L + c_\delta s_\theta p_L)}{l_L^3} \right), \quad (5.42.h)$$

$$K_{Y\theta}^{(L)} = K_{\theta Y}^{(L)} = k_L p_L \left[ \left( 1 - \frac{{}^0l_L}{l_L} \right) (c_\delta c_\theta) + \left( \frac{{}^0l_L (-(X - A_L) c_\delta s_\theta + (Y - B_L) c_\delta c_\theta) (Y - B_L + c_\delta s_\theta p_L)}{l_L^3} \right) \right], \quad (5.42.i)$$

$$K_{Y\delta}^{(L)} = K_{\delta Y}^{(L)} = k_L p_L \left[ \left( \frac{{}^0l_L}{l_L} - 1 \right) (s_\delta s_\theta) + \left( \frac{{}^0l_L ((X - A_L) s_\delta c_\theta + (Y - B_L) s_\delta s_\theta + (Z - C_L) c_\delta) (B_L - Y - c_\delta s_\theta p_L)}{l_L^3} \right) \right], \quad (5.42.l)$$

$$K_{Y\beta}^{(L)} = K_{\beta Y}^{(L)} = 0, \quad (5.42.m)$$

$$K_{ZZ}^{(L)} = k_L \left[ \left( 1 - \frac{{}^0l_L}{l_L} \right) + \left( \frac{{}^0l_L (Z - C_L - p_L s_\delta)^2}{l_L^3} \right) \right], \quad (5.42.n)$$

$$K_{Z\theta}^{(L)} = K_{\theta Z}^{(L)} = k_L p_L \left( \frac{{}^0l_L (-(X - A_L) c_\delta s_\theta + (Y - B_L) c_\delta c_\theta) (Z - C_L - s_\delta p_L)}{l_L^3} \right), \quad (5.42.o)$$

$$K_{Z\delta}^{(L)} = K_{\delta Z}^{(L)} = k_L p_L \left[ \left( \frac{{}^0l_L}{l_L} - 1 \right) c_\delta + \left( \frac{{}^0l_L ((X - A_L) s_\delta c_\theta + (Y - B_L) s_\delta s_\theta + (Z - C_L) c_\delta) (C_L - Z + s_\delta p_L)}{l_L^3} \right) \right], \quad (5.42.p)$$

$$K_{Z\beta}^{(L)} = K_{\beta Z}^{(L)} = 0, \quad (5.42.q)$$

$$K_{\theta\theta}^{(L)} = k_L p_L \left[ \left( 1 - \frac{{}^0l_L}{l_L} \right) (-(Y - B_L) c_\delta s_\theta - (X - A_L) c_\delta c_\theta) + \left( \frac{{}^0l_L p_L (-(X - A_L) c_\delta s_\theta + (Y - B_L) c_\delta c_\theta)^2}{l_L^3} \right) \right], \quad (5.42.r)$$

$$K_{g\delta}^{(L)} = K_{\delta g}^{(L)} = k_L p_L \left[ \left( 1 - \frac{{}^0l_L}{l_L} \right) \left( -(Y - B_L) s_\delta c_g + (X - A_L) s_\delta s_g \right) + \frac{{}^0l_L p_L \left( (X - A_L) s_\delta c_g + (Y - B_L) s_\delta s_g + (Z - C_L) c_\delta \right) \left( (X - A_L) s_g - (Y - B_L) c_g \right) c_\delta}{l_L^3} \right], \quad (5.42.s)$$

$$K_{g\beta}^{(L)} = K_{\beta g}^{(L)} = 0, \quad (5.42.t)$$

$$K_{\delta\delta}^{(L)} = k_L p_L \left[ \left( 1 - \frac{{}^0l_L}{l_L} \right) \left( -(X - A_L) c_\delta c_g - (Y - B_L) c_\delta s_g + (Z - C_L) s_\delta \right) + \frac{{}^0l_L p_L \left( -(X - A_L) s_\delta c_g - (Y - B_L) s_\delta s_g - (Z - C_L) c_\delta \right)^2}{l_L^3} \right], \quad (5.42.u)$$

$$K_{\delta\beta}^{(L)} = K_{\beta\delta}^{(L)} = 0, \quad (5.42.v)$$

$$K_{\beta\beta}^{(L)} = 0, \quad (5.42.z)$$

where the leg length  $l_L$  depends on  $X$  and is defined in Eq. (5.25);

$$K_{XX}^{(M)} = k_M \left[ \left( 1 - \frac{{}^0l_M}{l_M} \right) + \frac{{}^0l_M \left( X + (s_\delta c_g s_\beta - s_g c_\beta) q_M \right)^2}{l_M^3} \right], \quad (5.43.a)$$

$$K_{XY}^{(M)} = K_{YX}^{(M)} = k_M \left( \frac{{}^0l_M \left( X + (s_\delta c_g s_\beta - s_g c_\beta) q_M \right) \left( Y + (s_\delta s_g s_\beta + c_g c_\beta) q_M \right)}{l_M^3} \right), \quad (5.43.b)$$

$$K_{XZ}^{(M)} = K_{ZX}^{(M)} = k_M \left[ \frac{{}^0l_M \left( Z - C_M + q_M c_\delta s_\beta \right) \left( X + (s_\delta c_g s_\beta - s_g c_\beta) q_M \right)}{l_M^3} \right], \quad (5.43.c)$$

$$K_{Xg}^{(M)} = K_{gX}^{(M)} = k_M q_M \left[ \left( 1 - \frac{{}^0l_M}{l_M} \right) \left( -s_\delta s_g s_\beta - c_g c_\beta \right) + \frac{{}^0l_M \left( X \left( -s_\delta s_g s_\beta - c_g c_\beta \right) + Y \left( s_\delta c_g s_\beta - s_g c_\beta \right) \right) \left( X + (s_\delta c_g s_\beta - s_g c_\beta) q_M \right)}{l_M^3} \right], \quad (5.43.d)$$

$$K_{X\delta}^{(M)} = K_{\delta X}^{(M)} = k_M q_M \left[ \left( 1 - \frac{{}^0l_M}{l_M} \right) \left( c_\delta c_g s_\beta \right) + \frac{{}^0l_M \left( X c_\delta c_g s_\beta + Y c_\delta s_g s_\beta - (Z - C_M) s_\delta s_\beta \right) \left( X + (s_\delta c_g s_\beta - s_g c_\beta) q_M \right)}{l_M^3} \right], \quad (5.43.e)$$

$$K_{X\beta}^{(M)} = K_{\beta X}^{(M)} = k_M q_M \left[ \left( 1 - \frac{{}^0l_M}{l_M} \right) (s_\delta c_\delta c_\beta + s_\delta s_\beta) + \frac{{}^0l_M \left( X (s_\delta c_\delta c_\beta + s_\delta s_\beta) + Y (s_\delta s_\delta c_\beta - c_\delta s_\beta) + (Z - C_M) c_\delta c_\beta \right) \left( X + (s_\delta c_\delta s_\beta - s_\delta c_\beta) q_M \right)}{l_M^3} \right], \quad (5.43.f)$$

$$K_{YY}^{(M)} = k_M \left[ \left( 1 - \frac{{}^0l_M}{l_M} \right) + \frac{{}^0l_M \left( Y + q_M (s_\delta s_\delta s_\beta + c_\delta c_\beta) \right)^2}{l_M^3} \right], \quad (5.43.g)$$

$$K_{YZ}^{(M)} = K_{ZY}^{(M)} = k_M \left[ \frac{{}^0l_M (Z - C_M + c_\delta s_\beta q_M) \left( Y + (s_\delta s_\delta s_\beta + c_\delta c_\beta) q_M \right)}{l_M^3} \right], \quad (5.43.h)$$

$$K_{Y\delta}^{(M)} = K_{\delta Y}^{(M)} = k_M q_M \left[ \left( 1 - \frac{{}^0l_M}{l_M} \right) (s_\delta c_\delta s_\beta - s_\delta c_\beta) + \frac{{}^0l_M \left( X (-s_\delta s_\delta s_\beta - c_\delta c_\beta) + Y (s_\delta c_\delta s_\beta - s_\delta c_\beta) \right) \left( Y + (s_\delta s_\delta s_\beta + c_\delta c_\beta) q_M \right)}{l_M^3} \right], \quad (5.43.i)$$

$$K_{Y\delta}^{(M)} = K_{\delta Y}^{(M)} = k_M q_M \left[ \left( 1 - \frac{{}^0l_M}{l_M} \right) (c_\delta s_\delta s_\beta) + \frac{{}^0l_M \left( X (c_\delta c_\delta s_\beta) + Y (c_\delta s_\delta s_\beta) - (Z - C_M) s_\delta s_\beta \right) \left( Y + (s_\delta s_\delta s_\beta + c_\delta c_\beta) q_M \right)}{l_M^3} \right], \quad (5.43.l)$$

$$K_{Y\beta}^{(M)} = K_{\beta Y}^{(M)} = k_M q_M \left[ \left( 1 - \frac{{}^0l_M}{l_M} \right) (s_\delta s_\delta c_\beta - c_\delta s_\beta) + \frac{{}^0l_M \left( X (s_\delta c_\delta c_\beta + s_\delta s_\beta) + Y (s_\delta s_\delta c_\beta - c_\delta s_\beta) + (Z - C_M) c_\delta c_\beta \right) \left( Y + (s_\delta s_\delta s_\beta + c_\delta c_\beta) q_M \right)}{l_M^3} \right], \quad (5.43.m)$$

$$K_{ZZ}^{(M)} = k_M \left[ \left( 1 - \frac{{}^0l_M}{l_M} \right) + \frac{{}^0l_M (Z - C_M + q_M c_\delta s_\beta)^2}{l_M^3} \right], \quad (5.43.n)$$

$$K_{Z\delta}^{(M)} = K_{\delta Z}^{(M)} = k_M q_M \left[ \frac{{}^0l_M \left( X (-s_\delta s_\delta s_\beta - c_\delta c_\beta) + Y (s_\delta c_\delta s_\beta - s_\delta c_\beta) \right) \left( Z - C_M + c_\delta s_\beta q_M \right)}{l_M^3} \right], \quad (5.43.o)$$

$$K_{Z\delta}^{(M)} = K_{\delta Z}^{(M)} = k_M q_M \left[ \left( 1 - \frac{{}^0l_M}{l_M} \right) (-s_\delta s_\beta) + \frac{{}^0l_M \left( X c_\delta c_\delta s_\beta + Y c_\delta s_\delta s_\beta - (Z - C_M) s_\delta s_\beta \right) \left( Z - C_M + c_\delta s_\beta q_M \right)}{l_M^3} \right], \quad (5.43.p)$$

$$K_{Z\beta}^{(M)} = K_{\beta Z}^{(M)} = k_M q_M \left[ \left( 1 - \frac{{}^0l_M}{l_M} \right) (c_\delta c_\beta) + \left( \frac{{}^0l_M (X (s_\delta c_\beta c_\beta + s_\beta s_\beta) + Y (s_\delta s_\beta c_\beta - c_\beta s_\beta) + (Z - C_M) c_\delta c_\beta) (Z - C_M + c_\delta s_\beta q_M)}{l_M^3} \right) \right], \quad (5.43.q)$$

$$K_{g\beta}^{(M)} = k_M q_M \left[ \left( 1 - \frac{{}^0l_M}{l_M} \right) (Y (-s_\delta s_\beta s_\beta - c_\beta c_\beta) - X (s_\delta c_\beta s_\beta - s_\beta c_\beta)) + \left( \frac{{}^0l_M q_M (X (-s_\delta s_\beta s_\beta - c_\beta c_\beta) + Y (s_\delta c_\beta s_\beta - s_\beta c_\beta))^2}{l_M^3} \right) \right], \quad (5.43.r)$$

$$K_{\delta\beta}^{(M)} = K_{\beta\delta}^{(M)} = k_M q_M \left[ \left( 1 - \frac{{}^0l_M}{l_M} \right) (Y c_\delta c_\beta s_\beta - X c_\delta s_\beta s_\beta) + \left( \frac{{}^0l_M q_M (X c_\delta c_\beta s_\beta + Y c_\delta s_\beta s_\beta + (Z - C_M) s_\delta s_\beta) (Y (s_\delta c_\beta s_\beta - s_\beta c_\beta) - X (s_\delta s_\beta s_\beta + c_\beta c_\beta))}{l_M^3} \right) \right], \quad (5.43.s)$$

$$K_{\beta\delta}^{(M)} = K_{\delta\beta}^{(M)} = k_M q_M \left[ \left( 1 - \frac{{}^0l_M}{l_M} \right) (Y (s_\delta c_\beta c_\beta + s_\beta s_\beta) - X (s_\delta s_\beta c_\beta - c_\beta s_\beta)) + \left( \frac{{}^0l_M q_M (X (s_\delta c_\beta c_\beta + s_\beta s_\beta) + Y (s_\delta s_\beta c_\beta - c_\beta s_\beta) + (Z - C_M) c_\delta c_\beta) (Y (s_\delta c_\beta s_\beta - s_\beta c_\beta) - X (s_\delta s_\beta s_\beta + c_\beta c_\beta))}{l_M^3} \right) \right], \quad (5.43.t)$$

$$K_{\delta\delta}^{(M)} = k_M q_M \left[ \left( 1 - \frac{{}^0l_M}{l_M} \right) (-X s_\delta c_\beta s_\beta - Y s_\delta s_\beta s_\beta - (Z - C_M) c_\delta s_\beta) + \left( \frac{{}^0l_M q_M (X c_\delta c_\beta s_\beta + Y c_\delta s_\beta s_\beta - (Z - C_M) s_\delta s_\beta)^2}{l_M^3} \right) \right], \quad (5.43.u)$$

$$K_{\beta\beta}^{(M)} = K_{\beta\beta}^{(M)} = k_M q_M \left[ \left( 1 - \frac{{}^0l_M}{l_M} \right) (X c_\delta c_\beta c_\beta + Y c_\delta s_\beta c_\beta - (Z - C_M) s_\delta c_\beta) + \left( \frac{{}^0l_M q_M (X (s_\delta c_\beta c_\beta + s_\beta s_\beta) + Y (s_\delta s_\beta c_\beta - c_\beta s_\beta) + (Z - C_M) c_\delta c_\beta) (X c_\delta c_\beta s_\beta + Y c_\delta s_\beta s_\beta + (Z - C_M) s_\delta s_\beta)}{l_M^3} \right) \right], \quad (5.43.v)$$

$$\mathbf{K}_{\beta\beta}^{(M)} = k_M q_M \left[ \begin{aligned} & \left( 1 - \frac{{}^0l_M}{l_M} \right) \left( X (s_{\delta}c_{\beta} - s_{\delta}c_{\beta}s_{\beta}) + Y (-c_{\beta}c_{\beta} - s_{\delta}s_{\beta}s_{\beta}) - (Z - C_M) c_{\delta}s_{\beta} \right) + \\ & + \left( \frac{{}^0l_M q_M \left( X (s_{\delta}c_{\beta}c_{\beta} + s_{\beta}s_{\beta}) + Y (s_{\delta}s_{\beta}c_{\beta} - c_{\beta}s_{\beta}) + (Z - C_M) c_{\delta}c_{\beta} \right)^2}{l_M^3} \right) \end{aligned} \right], \quad (5.43.z)$$

where the leg length  $l_M$  depends on  $\mathbf{X}$  and is defined in Eq. (5.28).

Note that, due to the choice of the components of the generalized displacement  $\mathbf{X}$  and of the components of the generalized force  $\mathfrak{F}$ , the matrix  $\mathbf{K}$  is symmetric, i.e.  $K_{rs} = K_{sr}$ .

### 5.5 Manipulator Stiffness: Practical Expressions

The expressions derived in Section 5.4 regard the general form of the stiffness matrix  $\mathbf{K}$  and hold for every configuration  $\mathbf{X}$  away from the reference equilibrium position, i.e. the desired configuration of the manipulator. In this reference configuration, note that the lengths of the legs  $\bar{l}_h$  do not necessarily correspond to the death-lengths  ${}^0l_h$ , for  $h=1, \dots, M$ . This indeed happens when the mechanism is preloaded in the reference configuration. Preloads can be provided either with an external force or with the use of structurally redundant architectures, i.e. for  $(I+J) > 4$  (refer to Fig. 5.2).

Note that, since the legs  $L$  and  $M$  are actuated, the death-lengths  ${}^0l_L$  and  ${}^0l_M$  are not fixed geometric constants like the death-lengths  ${}^0l_i$  and the  ${}^0l_j$ , but vary according to the motion undergone by the manipulator. As a consequence, for every controlled value of  ${}^0l_L$  and  ${}^0l_M$ ,  $\infty^2$  reference configurations exist. Once the controller has set the values of  ${}^0l_L$  and  ${}^0l_M$ , only one reference configuration exists. This yields that, for every location  $\mathbf{X}$  of the platform,  $\infty^2$  stiffness matrices exist. Once the controller has set the values of  ${}^0l_L$  and  ${}^0l_M$ , for every location  $\mathbf{X}$  of the platform, only one stiffness matrix  $\mathbf{K}$  exists.

In practice, a manipulator should be built such that only small elastic deflections about the reference configurations are undergone. Thus, the coefficients of influence  $K_{rs}$  may only need to be evaluated with respect to such configurations so as to simplify consistently their general expression.

With regards to the ATWOKI joint depicted either in Fig. 5.1 or in Fig. 5.2, the reference configurations are the  $\infty^2$  positions characterized by the generalized coordinate vector  $\bar{\mathbf{X}} = [0 \ 0 \ h \ \bar{\vartheta} \ 0 \ \bar{\beta}]^T$ , for every angle  $\bar{\vartheta}$  and  $\bar{\beta}$  controlled by the actuated legs  $P_L B_L$  and  $P_M B_M$ . As before mentioned, the lengths of the legs, which correspond to the configurations  $\bar{\mathbf{X}}$ , are referred to as the reference lengths  $\bar{l}_h$ , for  $h=1, \dots, I, \dots, J, L, M$ . Then, the practical expressions  $\bar{K}_{rs}$  of the coefficients expressed in Eqs. (5.40)-(5.43), as evaluated in the reference configurations  $\bar{\mathbf{X}}$ , are:

$$\bar{K}_{XX}^{(i)} = k_i \left[ 1 - \frac{{}^0l_i}{\bar{l}_i} + \frac{{}^0l_i A_i^2}{\bar{l}_i^3} \right], \quad (5.44.a)$$

$$\bar{K}_{XY}^{(i)} = \bar{K}_{YX}^{(i)} = k_i \left( \frac{{}^0l_i A_i B_i}{l_i^3} \right), \quad (5.44.b)$$

$$\bar{K}_{XZ}^{(i)} = \bar{K}_{ZX}^{(i)} = k_i \left( \frac{{}^0l_i A_i (C_i - h)}{l_i^3} \right), \quad (5.44.c)$$

$$\bar{K}_{Xg}^{(i)} = \bar{K}_{gX}^{(i)} = 0, \quad (5.44.d)$$

$$\bar{K}_{X\delta}^{(i)} = \bar{K}_{\delta X}^{(i)} = 0, \quad (5.44.e)$$

$$\bar{K}_{X\beta}^{(i)} = \bar{K}_{\beta X}^{(i)} = 0, \quad (5.44.f)$$

$$\bar{K}_{YY}^{(i)} = k_i \left[ 1 - \frac{{}^0l_i}{l_i} + \frac{{}^0l_i B_i^2}{l_i^3} \right], \quad (5.44.g)$$

$$\bar{K}_{YZ}^{(i)} = \bar{K}_{ZY}^{(i)} = k_i \left( \frac{{}^0l_i B_i (C_i - h)}{l_i^3} \right), \quad (5.44.h)$$

$$\bar{K}_{Yg}^{(i)} = \bar{K}_{gY}^{(i)} = 0, \quad (5.44.i)$$

$$\bar{K}_{Y\delta}^{(i)} = \bar{K}_{\delta Y}^{(i)} = 0, \quad (5.44.l)$$

$$\bar{K}_{Y\beta}^{(i)} = \bar{K}_{\beta Y}^{(i)} = 0, \quad (5.44.m)$$

$$\bar{K}_{ZZ}^{(i)} = k_i \left[ 1 - \frac{{}^0l_i}{l_i^3} + \frac{{}^0l_i (h - C_i)^2}{l_i^3} \right], \quad (5.44.n)$$

$$\bar{K}_{Zg}^{(i)} = \bar{K}_{gZ}^{(i)} = 0, \quad (5.44.o)$$

$$\bar{K}_{Z\delta}^{(i)} = \bar{K}_{\delta Z}^{(i)} = 0, \quad (5.44.p)$$

$$\bar{K}_{Z\beta}^{(i)} = \bar{K}_{\beta Z}^{(i)} = 0, \quad (5.44.q)$$

$$\bar{K}_{gg}^{(i)} = 0, \quad (5.44.r)$$

$$\bar{K}_{g\delta}^{(i)} = \bar{K}_{\delta g}^{(i)} = 0, \quad (5.44.s)$$

$$\bar{K}_{g\beta}^{(i)} = \bar{K}_{\beta g}^{(i)} = 0, \quad (5.44.t)$$

$$\bar{K}_{\delta\delta}^{(i)} = 0, \quad (5.44.u)$$

$$\bar{K}_{\delta\beta}^{(i)} = \bar{K}_{\beta\delta}^{(i)} = 0, \quad (5.44.v)$$

$$\bar{K}_{\beta\beta}^{(j)} = 0, \quad (5.44.z)$$

where  $\bar{l}_j = \sqrt{A_i^2 + B_i^2 + C_i^2 + h^2 - 2hC_i}$  ;

$$\bar{K}_{XX}^{(j)} = k_j \left[ 1 - \frac{{}^0l_j}{\bar{l}_j} + \frac{{}^0l_j p_j^2}{\bar{l}_j^3} c_{\bar{g}}^2 \right], \quad (5.45.a)$$

$$\bar{K}_{XY}^{(j)} = \bar{K}_{YX}^{(j)} = k_j \left( \frac{{}^0l_j p_j^2}{\bar{l}_j^3} c_{\bar{g}} s_{\bar{g}} \right), \quad (5.45.b)$$

$$\bar{K}_{XZ}^{(j)} = \bar{K}_{ZX}^{(j)} = k_j \left( \frac{{}^0l_j p_j (h - C_j)}{\bar{l}_j^3} c_{\bar{g}} \right), \quad (5.45.c)$$

$$\bar{K}_{Xg}^{(j)} = \bar{K}_{gX}^{(j)} = k_j p_j \left[ - \left( 1 - \frac{{}^0l_j}{\bar{l}_j} \right) s_{\bar{g}} \right], \quad (5.45.d)$$

$$\bar{K}_{X\delta}^{(j)} = \bar{K}_{\delta X}^{(j)} = k_j p_j \left( - \frac{{}^0l_j p_j (h - C_j)}{\bar{l}_j^3} c_{\bar{g}} \right), \quad (5.45.e)$$

$$\bar{K}_{X\beta}^{(j)} = \bar{K}_{\beta X}^{(j)} = 0, \quad (5.45.f)$$

$$\bar{K}_{YY}^{(j)} = k_j \left( 1 - \frac{{}^0l_j}{\bar{l}_j} + \frac{{}^0l_j p_j^2}{\bar{l}_j^3} s_{\bar{g}}^2 \right), \quad (5.45.g)$$

$$\bar{K}_{YZ}^{(j)} = \bar{K}_{ZY}^{(j)} = k_j \left( \frac{{}^0l_j p_j (h - C_j) s_{\bar{g}}}{\bar{l}_j^3} \right), \quad (5.45.h)$$

$$\bar{K}_{Yg}^{(j)} = \bar{K}_{gY}^{(j)} = k_j p_j \left[ \left( 1 - \frac{{}^0l_j}{\bar{l}_j} \right) c_{\bar{g}} \right], \quad (5.45.i)$$

$$\bar{K}_{Y\delta}^{(j)} = \bar{K}_{\delta Y}^{(j)} = k_j p_j \left( - \frac{{}^0l_j p_j (h - C_j) s_{\bar{g}}}{\bar{l}_j^3} \right), \quad (5.45.l)$$

$$\bar{K}_{Y\beta}^{(j)} = \bar{K}_{\beta Y}^{(j)} = 0, \quad (5.45.m)$$

$$\bar{K}_{ZZ}^{(j)} = k_j \left( 1 - \frac{{}^0l_j}{\bar{l}_j} + \frac{{}^0l_j (h - C_j)^2}{\bar{l}_j^3} \right), \quad (5.45.n)$$

$$\bar{K}_{Zg}^{(j)} = \bar{K}_{gZ}^{(j)} = 0, \quad (5.45.o)$$

$$\bar{K}_{z\delta}^{(j)} = \bar{K}_{\delta z}^{(j)} = k_j p_j \left( \frac{{}^0l_j}{\bar{l}_j} - 1 - \frac{{}^0l_j (h - C_j)^2}{\bar{l}_j^3} \right), \quad (5.45.p)$$

$$\bar{K}_{z\beta}^{(j)} = \bar{K}_{\beta z}^{(j)} = 0, \quad (5.45.q)$$

$$\bar{K}_{g\delta}^{(j)} = 0, \quad (5.45.r)$$

$$\bar{K}_{\delta\delta}^{(j)} = \bar{K}_{\delta\delta}^{(j)} = 0, \quad (5.45.s)$$

$$\bar{K}_{g\beta}^{(j)} = \bar{K}_{\beta g}^{(j)} = 0, \quad (5.45.t)$$

$$\bar{K}_{\delta\delta}^{(j)} = k_j p_j \left( \frac{{}^0l_j p_j (h - C_j)^2}{\bar{l}_j^3} \right), \quad (5.45.u)$$

$$\bar{K}_{\delta\beta}^{(j)} = \bar{K}_{\beta\delta}^{(j)} = 0, \quad (5.45.v)$$

$$\bar{K}_{\beta\beta}^{(j)} = 0, \quad (5.45.z)$$

where  $\bar{l}_j = \sqrt{p_j^2 + (h - C_j)^2}$  ;

$$\bar{K}_{xx}^{(L)} = k_L \left[ 1 - \frac{{}^0l_L}{\bar{l}_L} + \frac{{}^0l_L (p_L c_{\bar{g}} - A_L)^2}{\bar{l}_L^3} \right], \quad (5.46.a)$$

$$\bar{K}_{xy}^{(L)} = \bar{K}_{yx}^{(L)} = k_L \left( \frac{{}^0l_L (p_L s_{\bar{g}} - B_L) (p_L c_{\bar{g}} - A_L)}{\bar{l}_L^3} \right), \quad (5.46.b)$$

$$\bar{K}_{xz}^{(L)} = \bar{K}_{zx}^{(L)} = k_L \left( \frac{{}^0l_L (h - C_L) (p_L c_{\bar{g}} - A_L)}{\bar{l}_L^3} \right), \quad (5.46.c)$$

$$\bar{K}_{xg}^{(L)} = \bar{K}_{gx}^{(L)} = k_L p_L \left[ - \left( 1 - \frac{{}^0l_L}{\bar{l}_L} \right) s_{\bar{g}} + \left( \frac{{}^0l_L (A_L s_{\bar{g}} - B_L c_{\bar{g}}) (p_L c_{\bar{g}} - A_L)}{\bar{l}_L^3} \right) \right], \quad (5.46.d)$$

$$\bar{K}_{x\delta}^{(L)} = \bar{K}_{\delta x}^{(L)} = k_L p_L \left( \frac{{}^0l_L (h - C_L) (A_L - p_L c_{\bar{g}})}{\bar{l}_L^3} \right), \quad (5.46.e)$$

$$\bar{K}_{x\beta}^{(L)} = \bar{K}_{\beta x}^{(L)} = 0, \quad (5.46.f)$$

$$\bar{K}_{yy}^{(L)} = k_L \left[ 1 - \frac{{}^0l_L}{\bar{l}_L} + \frac{{}^0l_L (p_L s_{\bar{g}} - B_L)^2}{\bar{l}_L^3} \right], \quad (5.46.g)$$

$$\bar{K}_{YZ}^{(L)} = k_L \left( \frac{{}^0l_L(h-C_L)(p_L s_{\bar{g}} - B_L)}{\bar{l}_L^3} \right), \quad (5.46.h)$$

$$\bar{K}_{Y\bar{g}}^{(L)} = \bar{K}_{\bar{g}Y}^{(L)} = k_L p_L \left[ \left( 1 - \frac{{}^0l_L}{\bar{l}_L} \right) c_{\bar{g}} + \left( \frac{{}^0l_L(A_L s_{\bar{g}} - B_L c_{\bar{g}})(p_L s_{\bar{g}} - B_L)}{\bar{l}_L^3} \right) \right], \quad (5.46.i)$$

$$\bar{K}_{Y\delta}^{(L)} = \bar{K}_{\delta Y}^{(L)} = k_L p_L \left[ \left( \frac{{}^0l_L(h-C_L)(B_L - p_L s_{\bar{g}})}{\bar{l}_L^3} \right) \right], \quad (5.46.l)$$

$$\bar{K}_{Y\beta}^{(L)} = \bar{K}_{\beta Y}^{(L)} = 0, \quad (5.46.m)$$

$$\bar{K}_{ZZ}^{(L)} = k_L \left[ 1 - \frac{{}^0l_L}{\bar{l}_L} + \frac{{}^0l_L(h-C_L)^2}{\bar{l}_L^3} \right], \quad (5.46.n)$$

$$\bar{K}_{Z\bar{g}}^{(L)} = \bar{K}_{\bar{g}Z}^{(L)} = k_L p_L \left( \frac{{}^0l_L(A_L s_{\bar{g}} - B_L c_{\bar{g}})(h-C_L)}{\bar{l}_L^3} \right), \quad (5.46.o)$$

$$\bar{K}_{Z\delta}^{(L)} = \bar{K}_{\delta Z}^{(L)} = k_L p_L \left[ \frac{{}^0l_L}{\bar{l}_L} - 1 - \frac{{}^0l_L(h-C_L)^2}{\bar{l}_L^3} \right], \quad (5.46.p)$$

$$\bar{K}_{Z\beta}^{(L)} = \bar{K}_{\beta Z}^{(L)} = 0, \quad (5.46.q)$$

$$\bar{K}_{\bar{g}\bar{g}}^{(L)} = k_L p_L \left[ \left( 1 - \frac{{}^0l_L}{\bar{l}_L} \right) (B_L s_{\bar{g}} + A_L c_{\bar{g}}) + \left( \frac{{}^0l_L p_L (A_L s_{\bar{g}} - B_L c_{\bar{g}})^2}{\bar{l}_L^3} \right) \right], \quad (5.46.r)$$

$$\bar{K}_{\bar{g}\delta}^{(L)} = \bar{K}_{\delta\bar{g}}^{(L)} = k_L p_L \left( \frac{{}^0l_L p_L (h-C_L)(B_L c_{\bar{g}} - A_L s_{\bar{g}})}{\bar{l}_L^3} \right), \quad (5.46.s)$$

$$\bar{K}_{\bar{g}\beta}^{(L)} = \bar{K}_{\beta\bar{g}}^{(L)} = 0, \quad (5.46.t)$$

$$\bar{K}_{\delta\delta}^{(L)} = k_L p_L \left[ \left( 1 - \frac{{}^0l_L}{\bar{l}_L} \right) (A_L c_{\bar{g}} + B_L s_{\bar{g}}) + \frac{{}^0l_L p_L (h-C_L)^2}{\bar{l}_L^3} \right], \quad (5.46.u)$$

$$\bar{K}_{\delta\beta}^{(L)} = \bar{K}_{\beta\delta}^{(L)} = 0, \quad (5.46.v)$$

$$\bar{K}_{\beta\beta}^{(L)} = 0, \quad (5.46.z)$$

where  $\bar{l}_L = \sqrt{p_L^2 + A_L^2 + B_L^2 + (h-C_L)^2 - 2p_L(A_L c_{\bar{g}} + B_L s_{\bar{g}})}$ ;

$$\bar{K}_{XX}^{(M)} = k_M \left[ 1 - \frac{{}^0l_M}{\bar{l}_M} + \frac{{}^0l_M q_M^2 (s_{\bar{\beta}} c_{\bar{\beta}})^2}{\bar{l}_M^3} \right], \quad (5.47.a)$$

$$\bar{K}_{XY}^{(M)} = \bar{K}_{YX}^{(M)} = k_M \left( -\frac{{}^0l_M q_M^2 s_{\bar{\beta}} c_{\bar{\beta}}^2}{\bar{l}_M^3} \right), \quad (5.47.b)$$

$$\bar{K}_{XZ}^{(M)} = \bar{K}_{ZX}^{(M)} = k_M \left( -\frac{{}^0l_M q_M (h - C_M + q_M s_{\bar{\beta}}) s_{\bar{\beta}} c_{\bar{\beta}}}{\bar{l}_M^3} \right), \quad (5.47.c)$$

$$\bar{K}_{X\theta}^{(M)} = \bar{K}_{\theta X}^{(M)} = k_M q_M \left[ -\left( 1 - \frac{{}^0l_M}{\bar{l}_M} \right) c_{\bar{\beta}} c_{\bar{\beta}} \right], \quad (5.47.d)$$

$$\bar{K}_{X\delta}^{(M)} = \bar{K}_{\delta X}^{(M)} = k_M q_M \left[ \left( 1 - \frac{{}^0l_M}{\bar{l}_M} \right) c_{\bar{\beta}} s_{\bar{\beta}} \right], \quad (5.47.e)$$

$$\bar{K}_{X\beta}^{(M)} = \bar{K}_{\beta X}^{(M)} = k_M q_M \left[ \left( 1 - \frac{{}^0l_M}{\bar{l}_M} \right) s_{\bar{\beta}} s_{\bar{\beta}} - \left( \frac{{}^0l_M q_M (h - C_M) s_{\bar{\beta}} c_{\bar{\beta}}^2}{\bar{l}_M^3} \right) \right], \quad (5.47.f)$$

$$\bar{K}_{YY}^{(M)} = k_M \left[ 1 - \frac{{}^0l_M}{\bar{l}_M} + \frac{{}^0l_M q_M^2 (c_{\bar{\beta}} c_{\bar{\beta}})^2}{\bar{l}_M^3} \right], \quad (5.47.g)$$

$$\bar{K}_{YZ}^{(M)} = \bar{K}_{ZY}^{(M)} = k_M \left( \frac{{}^0l_M q_M (h - C_M + q_M s_{\bar{\beta}}) c_{\bar{\beta}} c_{\bar{\beta}}}{\bar{l}_M^3} \right), \quad (5.47.h)$$

$$\bar{K}_{Y\theta}^{(M)} = \bar{K}_{\theta Y}^{(M)} = k_M q_M \left[ -\left( 1 - \frac{{}^0l_M}{\bar{l}_M} \right) s_{\bar{\beta}} c_{\bar{\beta}} \right], \quad (5.47.i)$$

$$\bar{K}_{Y\delta}^{(M)} = \bar{K}_{\delta Y}^{(M)} = k_M q_M \left[ \left( 1 - \frac{{}^0l_M}{\bar{l}_M} \right) s_{\bar{\beta}} s_{\bar{\beta}} \right], \quad (5.47.l)$$

$$\bar{K}_{Y\beta}^{(M)} = \bar{K}_{\beta Y}^{(M)} = k_M q_M \left[ -\left( 1 - \frac{{}^0l_M}{\bar{l}_M} \right) c_{\bar{\beta}} s_{\bar{\beta}} + \left( \frac{{}^0l_M q_M (h - C_M) c_{\bar{\beta}} c_{\bar{\beta}}^2}{\bar{l}_M^3} \right) \right], \quad (5.47.m)$$

$$\bar{K}_{ZZ}^{(M)} = k_M \left[ 1 - \frac{{}^0l_M}{\bar{l}_M} + \frac{{}^0l_M (h - C_M + q_M s_{\bar{\beta}})^2}{\bar{l}_M^3} \right], \quad (5.47.n)$$

$$\bar{K}_{Z\theta}^{(M)} = \bar{K}_{\theta Z}^{(M)} = 0, \quad (5.47.o)$$

$$\bar{K}_{Z\delta}^{(M)} = \bar{K}_{\delta Z}^{(M)} = 0, \quad (5.47.p)$$

$$\bar{K}_{z\beta}^{(M)} = \bar{K}_{\beta z}^{(M)} = k_M q_M \left[ \left( 1 - \frac{{}^0l_M}{\bar{l}_M} \right) c_{\bar{\beta}} + \left( \frac{{}^0l_M (h - C_M + q_M s_{\bar{\beta}})}{\bar{l}_M^3} \right) (h - C_M) c_{\bar{\beta}} \right], \quad (5.47.q)$$

$$\bar{K}_{\beta\beta}^{(M)} = 0, \quad (5.47.r)$$

$$\bar{K}_{\beta\delta}^{(M)} = \bar{K}_{\delta\beta}^{(M)} = 0, \quad (5.47.s)$$

$$\bar{K}_{\beta\beta}^{(M)} = \bar{K}_{\beta\beta}^{(M)} = 0, \quad (5.47.t)$$

$$K_{\delta\delta}^{(M)} = k_M q_M \left[ - \left( 1 - \frac{{}^0l_M}{\bar{l}_M} \right) (h - C_M) s_{\bar{\beta}} \right], \quad (5.47.u)$$

$$\bar{K}_{\delta\beta}^{(M)} = \bar{K}_{\beta\delta}^{(M)} = 0, \quad (5.47.v)$$

$$K_{\beta\beta}^{(M)} = k_M q_M \left[ - \left( 1 - \frac{{}^0l_M}{\bar{l}_M} \right) (h - C_M) s_{\bar{\beta}} + \left( \frac{{}^0l_M q_M (h - C_M)^2 c_{\bar{\beta}}^2}{\bar{l}_M^3} \right) \right], \quad (5.47.z)$$

where  $\bar{l}_M = \sqrt{q_M^2 + (h - C_M)^2 + 2q_M (h - C_M) s_{\bar{\beta}}}$ .

For convenience, the contributions to the total elastic force and moment which act on the platform when it is located in the reference configurations  $\bar{\mathbf{X}}$  are reported in the following

$$\bar{\mathbf{F}}^{(i)} \cdot \begin{bmatrix} \mathbf{i}_0 \\ \mathbf{j}_0 \\ \mathbf{k}_0 \end{bmatrix} = \begin{bmatrix} \bar{F}_X^{(i)} \\ \bar{F}_Y^{(i)} \\ \bar{F}_Z^{(i)} \end{bmatrix} = k_i \left( 1 - \frac{{}^0l_i}{\bar{l}_i} \right) \begin{bmatrix} -A_i \\ -B_i \\ h - C_i \end{bmatrix}, \quad (5.48)$$

$$\bar{\mathbf{m}}^{(i)} = \begin{bmatrix} m_{i_o}^{(i)} \\ m_{j_o}^{(i)} \\ m_{k_o}^{(i)} \end{bmatrix} = \begin{bmatrix} 0 \\ 0 \\ 0 \end{bmatrix}, \quad (5.49)$$

$$\bar{m}_\beta^{(i)} = \bar{\mathbf{m}}^{(i)} \cdot \mathbf{k}_0 = 0, \quad (5.50.a)$$

$$\bar{m}_\delta^{(i)} = \bar{\mathbf{m}}^{(i)} \cdot \mathbf{j}_0 = 0, \quad (5.50.b)$$

$$\bar{m}_\beta^{(i)} = \bar{\mathbf{m}}^{(i)} \cdot \mathbf{i}_1 = 0, \quad (5.50.c)$$

$$\bar{\mathbf{F}}^{(j)} \cdot \begin{bmatrix} \mathbf{i}_0 \\ \mathbf{j}_0 \\ \mathbf{k}_0 \end{bmatrix} = \begin{bmatrix} \bar{F}_X^{(j)} \\ \bar{F}_Y^{(j)} \\ \bar{F}_Z^{(j)} \end{bmatrix} = k_j \left( 1 - \frac{{}^0l_j}{\bar{l}_j} \right) \begin{bmatrix} c_{\bar{\beta}} p_j \\ s_{\bar{\beta}} p_j \\ h - C_j \end{bmatrix}, \quad (5.51)$$

$$\bar{\mathbf{m}}^{(j)} \cdot \begin{bmatrix} \mathbf{i}_0 \\ \mathbf{j}_0 \\ \mathbf{k}_0 \end{bmatrix} = \begin{bmatrix} \bar{m}_X^{(j)} \\ \bar{m}_Y^{(j)} \\ \bar{m}_Z^{(j)} \end{bmatrix} = k_j p_j \left( 1 - \frac{{}^0l_j}{l_j} \right) \begin{bmatrix} s_{\bar{g}}(h - C_j) \\ -c_{\bar{g}}(h - C_j) \\ 0 \end{bmatrix}, \quad (5.52)$$

$$\bar{m}_{\bar{g}}^{(j)} = \bar{\mathbf{m}}^{(j)} \cdot \mathbf{k}_0 = 0, \quad (5.53.a)$$

$$\bar{m}_{\delta}^{(j)} = \bar{\mathbf{m}}^{(j)} \cdot \mathbf{j}_* = -k_j p_j (h - C_j) \left( 1 - \frac{{}^0l_j}{l_j} \right), \quad (5.53.b)$$

$$\bar{m}_{\beta}^{(j)} = \bar{\mathbf{m}}^{(j)} \cdot \mathbf{i}_1 = 0, \quad (5.53.c)$$

$$\bar{\mathbf{f}}^{(L)} \cdot \begin{bmatrix} \mathbf{i}_0 \\ \mathbf{j}_0 \\ \mathbf{k}_0 \end{bmatrix} = \begin{bmatrix} \bar{f}_X^{(L)} \\ \bar{f}_Y^{(L)} \\ \bar{f}_Z^{(L)} \end{bmatrix} = k_L \left( 1 - \frac{{}^0l_L}{l_L} \right) \begin{bmatrix} -A_L + c_{\bar{g}} p_L \\ -B_L + s_{\bar{g}} p_L \\ h - C_L \end{bmatrix}, \quad (5.54)$$

$$\bar{\mathbf{m}}^{(L)} \cdot \begin{bmatrix} \mathbf{i}_0 \\ \mathbf{j}_0 \\ \mathbf{k}_0 \end{bmatrix} = \begin{bmatrix} \bar{m}_X^{(L)} \\ \bar{m}_Y^{(L)} \\ \bar{m}_Z^{(L)} \end{bmatrix} = k_L p_L \left( 1 - \frac{{}^0l_L}{l_L} \right) \begin{bmatrix} (h - C_L) s_{\bar{g}} \\ -(h - C_L) c_{\bar{g}} \\ A_L s_{\bar{g}} - B_L c_{\bar{g}} \end{bmatrix}, \quad (5.55)$$

$$\bar{m}_{\bar{g}}^{(L)} = \bar{\mathbf{m}}^{(L)} \cdot \mathbf{k}_0 = k_L p_L \left( 1 - \frac{{}^0l_L}{l_L} \right) (A_L s_{\bar{g}} - B_L c_{\bar{g}}), \quad (5.56.a)$$

$$\bar{m}_{\delta}^{(L)} = \bar{\mathbf{m}}^{(L)} \cdot \mathbf{j}_* = k_L p_L \left( 1 - \frac{{}^0l_L}{l_L} \right) (C_L - h), \quad (5.56.b)$$

$$\bar{m}_{\beta}^{(L)} = \bar{\mathbf{m}}^{(L)} \cdot \mathbf{i}_1 = 0, \quad (5.56.c)$$

$$\bar{\mathbf{f}}^{(M)} \cdot \begin{bmatrix} \mathbf{i}_0 \\ \mathbf{j}_0 \\ \mathbf{k}_0 \end{bmatrix} = \begin{bmatrix} \bar{f}_X^{(M)} \\ \bar{f}_Y^{(M)} \\ \bar{f}_Z^{(M)} \end{bmatrix} = k_M \left( 1 - \frac{{}^0l_M}{l_M} \right) \begin{bmatrix} -(s_{\bar{g}} c_{\bar{\beta}}) q_M \\ (c_{\bar{g}} c_{\bar{\beta}}) q_M \\ h - C_M + s_{\bar{\beta}} q_M \end{bmatrix}, \quad (5.57)$$

$$\bar{\mathbf{m}}^{(M)} \cdot \begin{bmatrix} \mathbf{i}_0 \\ \mathbf{j}_0 \\ \mathbf{k}_0 \end{bmatrix} = \begin{bmatrix} \bar{m}_X^{(M)} \\ \bar{m}_Y^{(M)} \\ \bar{m}_Z^{(M)} \end{bmatrix} = k_M q_M \left( 1 - \frac{{}^0l_M}{l_M} \right) \begin{bmatrix} (h - C_M) c_{\bar{g}} c_{\bar{\beta}} \\ (h - C_M) s_{\bar{g}} c_{\bar{\beta}} \\ 0 \end{bmatrix}, \quad (5.58)$$

$$\bar{m}_{\bar{g}}^{(M)} = \bar{\mathbf{m}}^{(M)} \cdot \mathbf{k}_0 = 0, \quad (5.59.a)$$

$$\bar{m}_{\delta}^{(M)} = \bar{\mathbf{m}}^{(M)} \cdot \mathbf{j}_* = 0, \quad (5.59.b)$$

$$\bar{m}_\beta^{(M)} = \bar{\mathbf{m}}^{(M)} \cdot \mathbf{i}_1 = k_M q_M \left( 1 - \frac{{}^0 I_M}{I_M} \right) (h - C_M) c_{\bar{\beta}}. \quad (5.59.c)$$

Note that, since in the reference configurations  $\bar{\mathbf{X}}$  the axes  $\mathbf{k}_0$ ,  $\mathbf{j}_*$  and  $\mathbf{i}_1$  are mutually orthogonal, then the total moment  $\mathbf{M}$  equals  $m_g \mathbf{k}_0 + m_\delta \mathbf{j}_* + m_\beta \mathbf{i}_1$ . Moreover, the moment  $\bar{m}_g$  corresponds to the torque which acts about the first axis of motion of the manipulator, i.e.  $\mathbf{k}_0$ , the moment  $\bar{m}_\beta$  corresponds to the torque which acts about the second axis of motion of the manipulator, i.e.  $\mathbf{i}_1$ , and the moment  $\bar{m}_\delta$  corresponds to the torque which acts on the plane defined by the vectors  $\mathbf{k}_0$  and  $\mathbf{i}_1$  that contains all the  $P_j B_j$ -legs.

## 5.6 Selective Compliance and Principles of Mechanism Design

As mentioned in Section 2.1, a very important advantage of biological joints stands in their selective compliance. The system architecture of the biologically inspired US\_PMs devised in Section 3.4 allows conceiving selectively compliant mechanisms.

In practice, by designing the mechanism stiffness, it is possible to increase the functionality of the systems they are inserted in. Indeed, apart from the possibility to control the system bandwidth and the associated dynamic performances, passive compliance makes the system capable of reacting against overconstraints which may be imposed by the surroundings.

In particular, selective compliance is a means to simply compensate for the poor control of the actuators of the mechanism so as to increase its interaction capabilities, and allows the system to adapt itself to permanent or reversible changes of the environment. As an example, designing a system with a proper compliance may allow to nullify the effects of backlash and wear so as to improve the tribology of the mechanism.

Stiffness design may also allow a mechanical system to pursue other interesting features the ligaments bundles provide diarthroses with.

The articulation concept devised in Section 3.2 is based on the functionality of the stiffer bundles of the ligaments only, i.e. the driving bundles. Since the main concern of that chapter was to realize a mechanism with a given motion, the feature provided by the more compliant (safety and limiting) bundles were not contemplated. Instead, the role of these softer elements becomes very important when kinetostatics is concerned.

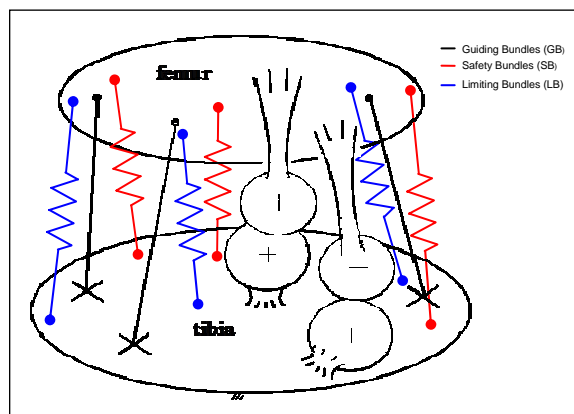


Figure 5.5 Kinetostatic Model of the Knee Joint

As a matter of fact, the safety bundles of the ligaments convey certain solidity to the biological joint in addition to the permanent solidity which is granted by the guiding bundles, while the limiting bundles of the ligaments limit the available range of movement of the biological joint by gradually increasing the resistance to motion. A kinetostatic model which may be used for the practical study of the behavior of a knee joint is depicted in Fig. 5.5. Safety and limiting bundles are represented as springs and are depicted in red and blue, respectively.

Similar to the kinetostatic model shown in Fig. 5.5, a novel articulation concept may be devised in order to add the aforementioned features to the mechanisms conceived in Section 3.4.

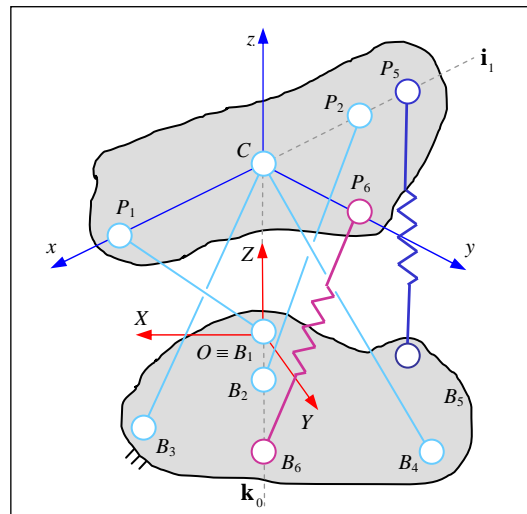


Figure 5.6 “Springy” US\_PM

An example of this articulation concept is depicted in Fig. 5.6. It represents a springy 2-dof spherical mechanism made by the addition of two springy legs, i.e.  $P_5B_5$  and  $P_6B_6$ , to the US\_PM of type (2) presented in Fig. 3.24. In practice, these legs provide the manipulator with elastic moments about the axes of motions. In particular, the spring depicted in magenta (i.e. the springy leg  $P_6B_6$ ) gives an elastic moment about the axis  $\mathbf{i}_1$  and the spring depicted in blue (i.e. the springy leg  $P_5B_5$ ) gives an elastic moment about the axis  $\mathbf{k}_0$ .

The addition of such springs may be useful in order to simplify the control of certain tasks and in order to auto-protect the mechanism. Indeed, such springs provide the system with a “soft-stop” action which can limit the potential damage of uncontrolled movements. Moreover, the springs allow for shock reduction, and filter out noisy and impulsive forces which may be generated either by the actuators or by disturbances from the environment.

In this context, the study of the space of compliant behavior of the mechanism can be carried on by means of the equations presented in Section 5.4 and Section 5.5. Indeed, such equations are sufficient in order to design a manipulator with a desired selective compliance. However, according to results found in the literature, the two following rules need to be mentioned. First, a rank  $k$  stiffness matrix can always be synthesized by more than  $k$  springy legs [104]. Second, the set of stiffness matrices that can be achieved with the parallel connection of springy legs is restricted [105]. Indeed, since each springy leg can only provide a pure force to the platform, the stiffness matrix must be restricted in form.

## Conclusions

Following the introductory overview on the state of the art and on the needs of mechanical systems, other than the rather deep analysis of the main architectures and features of the joints biological creatures are made by, this research work presents novel articulation concepts inspired by nature.

In particular, one of these articulation concepts is used to devise an original two degrees of freedom spherical mechanism called ATWOKI. The name stands for “Almost TWO degrees of freedom Knee Inspired” and is motivated since the mechanism resembles the structure and the practical motion of the knee joint of animals.

From a biological standpoint, the articulation concepts feature ligament like members which provide the system with structural (passive) and proprioceptive (active) functionalities. Indeed, these elements work both as passive elements to drive the system kinematics, to bear forces and to offer selective compliance, and as active elements to monitor the forces and the motions the system is subjected to.

From a mechanical standpoint, the articulation concepts have parallel architectures and are based on the motion capabilities of UPS-type architecturally singular fully parallel manipulators.

Actuation issues, kinematic analyses, stiffness study and other implementation topics are addressed.

As for the actuation, it is shown that the motors can be located so that the control of the manipulator motion can be decoupled about two axes which are fixed, respectively, one with respect to the manipulator base and the other with respect to the manipulator end-effector.

As for the kinematic analyses, algorithms for the direct and inverse position, velocity and acceleration analyses are presented. Implementation guidelines and computational costs are shown which demonstrate how these algorithms are very easy and fast.

As for the stiffness study, tools for the analysis and for the synthesis of mechanism stiffness are presented. In particular, it is shown how the parallel architecture of the novel biologically inspired mechanisms can be used to build selectively compliant systems which may adapt to and compensate for environmental disturbances.

Comparison with a traditional two degrees of freedom spherical joint with serial architecture is provided which shows how the novel articulation concepts allow for the construction of stronger, stiffer, lighter, faster and more accurate manipulators to be used in many different robotics applications, especially when the autonomous systems must interact with the surrounding environment.

References

- [1] Drake S.H., “Using compliance in lieu of sensory feedback for automatic assembly”, in *PhD thesis*, Massachusetts Institute of Technology, 1978.
- [2] Eppinger S.D., “Modeling Robot Dynamic Performance for Endpoint Force Control”, in *PhD thesis*, Massachusetts Institute of Technology, 1998.
- [3] Mason M., “Compliant motion”, in *Robot Motion: Planning and Control*, MIT Press, pp. 305-322, 1982.
- [4] Whitney D.E., “Historical perspective and state of the art in robot force control”, in *International Journal of Robotics Research*, 6(1), 1987.
- [5] Salisbury K., “Active stiffness control of a manipulator in cartesian coordinates”, in *19th IEEE Conference on Decision and Control*, pp. 83-88, 1980.
- [6] Hogan N., “Impedance control: An approach to manipulation: Part i - theory, part ii - implementation, part iii – applications”, in *J. of Dynamic Systems, Measurement and Control*, 107(1),1985.
- [7] Raibert M.H. and Craig J.J., “Hybrid position/force control of manipulators”, in *Journal of Dynamic Systems, Measurement, and Control*, 102, 1981.
- [8] Pratt J., “Virtual model control of a biped walking robot”, in *Master's thesis*, Massachusetts Institute of Technology, 1995.
- [9] Albu-Schäffer A., Fischer M., Schreiber G., Schoeppe F., and Hirzinger G., “Soft Robotics: What Cartesian Stiffness Can We Obtain With Passively Compliant, Uncoupled Joints?”, in *IEEE/RSL Int. Conf. on Intelligent Robots and Systems*, Sendai, Japan, sept. 2004.
- [10] Robinson D.W., “Design and Analysis of Series Elasticity in Closed-loop Actuator Force Control”, in *PhD thesis*, Massachusetts Institute of Technology, 2000.
- [11] Ott C., Albu-Schäffer A., Kugi A., Stramigioli S., and Hirzinger G., “A Passivity Based Cartesian Impedance Controller for Flexible Joint Robots - Part I: Torque Feedback and Gravity Compensation”, in *ICRA2004*, pp. 2666-2672, 2004.
- [12] Albu-Schäffer A., Ott Ch., and Hirzinger G., “A Passivity Based Cartesian Impedance Controller for Flexible Joint Robots - Part II: Full State Feedback, Impedance Design and Experiments”, in *ICRA2004*, pp. 2666-2672, 2004.
- [13] Bar-Cohen Y., *Electroactive Polymer (EAP) Actuators as Artificial Muscles – Reality, Potential and Challenges*, SPIE Press, 2001.
- [14] McNeill and Alexander R., in *Elastic Mechanisms in Animal Movement*. Cambridge University Press, 1988.

- [15] Dye S.F., “An evolutionary perspective of the knee”, *J. Bone Joint Surgery*, 69(A), pp 976-983, 1987.
- [16] Kurosawa H., Walker P.S., Abe S., Garg A. and Hunter T., “Geometry an motion of the knee for implant and orthotic design”, in *J. of Biomechanics*, 18(7), pp. 487-499, 1985.
- [17] Bullough P.G., Goodfellow J., Greenwald A.S., and O’Connor J.J., “Incongruent surfaces in the human hip joint”, in *Nature*, 217, p.1290, 1968.
- [18] Neumann D.A., *Kinesiology of the musculoskeletal system : foundations for physical rehabilitation*, St. Louis, Mosby, 2002.
- [19] Shrive N.G., O’Connor J.J., Goodfellow J.W., “Loading-bearing in the knee joint”, in *Clin. Orthop*, 131, pp. 279-287, 1978.
- [20] Krause W.R., Pope M.H., Johnson R.J., et al., “Mechanical changes in the knee after meniscectomy”, in *J. Bone Joint Surgery*, 58(A), pp. 599-604, 1976.
- [21] Seedhom B.B., “Loadbearing function of the menisci”, *Physiotherapy*, 62, pp. 223-226, 1976.
- [22] Paletta G.A., Manning T. Snell E., et al., “The effect of allograft meniscal replacement on intraarticular contact area and pressures in the human knee”, in *American Journal of Sports medicine*, 25, pp. 692-698, 1997.
- [23] Panjabi and Manohar M., *Biomechanics in the musculoskeletal system*, Augustus A. White III. New York, Churchill Livingstone, 2001.
- [24] Hoppenfeld S., *Physical Examination of the Spine and Extremities*, Norwalk, CT, Prentice-Hall, 1976.
- [25] Guyton A.C., *Textbook of Medical Physiology*, 8<sup>th</sup> edition, Philadelphia, PA, WB Saunders, 1992.
- [26] Ihara H. and Nakayama A., “Dynamic joint control training for knee ligament injuries”, in *Am. J. Sports Med*, 14, pp 309-315, 1986.
- [27] Beard D.J., Dodd C.A., Trundle H.R., et al., “Propioception enhancement for anterior cruciate ligament deficiency. A prospective randomized trial of two physiotherapy regimes”, in *J. Bone Joint Surg. Br.*, 76, pp. 654-659, 1994.
- [28] Fitzgerald G., Axe M., Snyder-Mackler L., “The efficacy of perturbation training in non-operative anterior cruciate ligament rehabilitation programs for physical active individuals”, in *Phys. Ther.*, 200(80), pp128-140.
- [29] Lephart S.M., Riemann B.L., Fu F.H., “Introduction to sensorymotor system”, in Lephart SM, Fu, FH eds. *Proprioception and Neuromuscular control in joint stability*, Champaign, IL, Human kinetics, 2002.

- [30] Ghez C., "The control of movement", in *Principles of Neural Science*, 3<sup>rd</sup> ed., Kandel, ER, Schwartz, JH, Jessell, TM eds., New York, Elsevier Science, 1991.
- [31] Johansson H., Sjolander P., "The neurophysiology of joints", in *Mechanics of Joints: Physiology, Pathophysiology and Treatment*, Wright, V, Radin, EL, eds., New York, NY, Marcell Dekker Inc, 1993.
- [32] Bastian H.C., "The 'muscular sense'; its nature and localization", in *Brain*, 10, pp. 1-136, 1888.
- [33] Denny-Brown D., *Selected Writings of Sir Charles Sherrington*, London, England, Hamish Hamilton Medical Books, 1939.
- [34] Grigg P., "Periferal neural mechanism in proprioception", in *J. Sport Rehabil.*, 3, pp. 2-17, 1994.
- [35] Sherrington C.S., *The integrative action of the nervous system*, New York, C Scribner's Sons, 1906.
- [36] Johansson H. and Sjolander P., "The neurophysiology of joints", in *Mechanics of Joints: Physiology, pathophysiology and treatment*, Wright, V, Radin, EL, eds., New York, NY, Marcel Dekker Inc, 1993.
- [37] Freeman M.A. and Wyke B., "Articular reflexes at the ankle joint: an electromyographic study of normal and abnormal influences of ankle joints mechanoreceptors upon reflex activity in the leg muscles", in *Br. J. Surg.*, 54, pp. 990-1001, 1967.
- [38] Johansson H., Sjolander P. and Sojka P., "A sensory role for the cruciate ligaments", in *Clin. Orthop.*, 268, pp.161-178, 1991.
- [39] Leonard C.T., *The neuroscience of human movement*, St Louis, MO, Mosby Year Book Inc, 1998.
- [40] Sainburg R.L., Ghilardi M.F., Poizner H. and Chez C., "Control of limb dynamics in normal subjects and patients without proprioception", in *J. Neurophysiology*, 73, pp. 820-835, 1995.
- [41] Bard C., Fleury M., Teasdale N., Paillard J. and Nougier V., "Contribution of proprioception for calibrating and updating the motor space", in *Can. J. Physiol. Pharmacol.*, 73, pp. 246-254, 1995.
- [42] Fu F.H., Harner C.D., Johnson D.L., et al., "Biomechanics of the knee ligaments: basic concepts and clinical application", in *Instr. Course Lecture*, 43, pp. 137-148, 1994.
- [43] Wilson D.R., Feikes J.J. and O'Connor J.J., "Ligaments and articular contact guide passive knee flexion", in *Journal of Biomechanics*, 31, pp.1127-1136.
- [44] Parenti-Castelli V., and Di Gregorio R., "A Spatial mechanism with higher pairs for modeling the human knee joint", in *ASME Transaction Journal of Biomechanical Engineering*, 125(2), pp. 232-237, 2003.

- [45] Woo S.L.Y., An K.N., Arnokzy D.V.M., Fithian D. and Myers B., "Anatomy, biology and biomechanis of the tendon, ligament, meniscus", in *Orthopaedic basic science*, SR Simon ed., Rosemont, IL, AAOS, 1994.
- [46] Fung Y.C.B., *Biomechanics: Mechanical Properties of Living tissues*, New york, Springer-Verlag.
- [47] Butler D., Noyes F. and Good E., "Ligamentous restraints to anterior posterior drawer in the human knee. A biomechanical study", in *J. Bone Joint Surg. Am.*, 62, pp. 259-270, 1980.
- [48] Noyes F., Butler D. and Grood E., "Biomechanical analysis of human ligament grafts used in knee-ligament repairs and reconstructions", in *J. Bone Joint Surg. Am.*, 66, pp. 344-352, 1983
- [49] Kuo C., "Field measurements in snow skiing injury research", in *J. Biomech.*, 16, pp. 609-624, 1983.
- [50] Palmar I., "Plastic surgery of the ligaments of the knee", *Act. Chir. Scand*, 91, pp. 37-48, 1944.
- [51] Zimny M.L., Shutte M. and Dabezies E., "Mechanoreceptors in the human anterior cruciate ligament", in *Anat. Rec.*, 214, pp. 204-209, 1986.
- [52] Schultz R., Miller D., Kerr C., et al. "Mechanoreceptors in humancruciate ligaments. A histological study", in *J. Bone Joint Surg. Am .*, 66, pp. 1072-1076, 1984.
- [53] Schutte M., Debezies E., Zimny M., et al., "Neural anatomy of the human anterior cruciate ligament", in *J. Bone Joint Surg. Am.*, 69, pp.243-247, 1987.
- [54] Kennedy J., Alexander I. and Hayes K., "Nerve supply of the human knee and its functional importance", in *Am. J. Sports Med.*, 10, pp. 329-335, 1982.
- [55] Lephart S.M., "Proprioceptive consideration for sport rehabilitation", in *J. Sport. Rehab.*, 3, pp 2-115, 1994.
- [56] Beynnon B., Howe J.G., and Pope M.H., "The measurements of anterior cruciate ligament strain in vivo", in *Int. Orthop.*, 16, pp. 1-12, 1992.
- [57] Lephart S., Pincivero D., Giraldo J., et al., "The role of proprioception in the management and rehabilitation of athletic injuries", in *Am. J. Sports Med.*, 25, pp. 130-137, 1997.
- [58] Hogervorst T. and Brand R.A., "Mechanoreceptor in joint function", in *J. Bone Joint Surg. Am.*, 80, pp. 1365-1378, 1998.
- [59] O'Connor B.L., Visco D.M., Brandt K.D., Meyers S.L. and Kalasinki L.A., "Neurogenic acceleration of osteoarthritis: the effects of previous neurectomy of the articular nerves on the development of osteoarthritis after transaction of the anterior cruciate ligament in dogs", in *J. Bone Joint Surg. Am.*, 74, pp. 367-376, 1992.

- [60] Corrigan J.P., Cashman W.F. and Brandy M.P., "Proprioception in the cruciate deficient knee", in *J. Bone Joint Surg. Br.*, 74, pp. 247-250, 1992.
- [61] Barret D.S., "Proprioception and function after anterior cruciate reconstruction", in *J. Bone Joint Surg. Br.*, 73, pp. 833-837, 1991.
- [62] Blankevoort L.R., Huiskes A. and De Lange, "Helical axes of passive knee joint motions", in *Journal of Biomechanics*, vol. 23, pp. 1219-1229, 1990.
- [63] Dyrby C.O. and Andriacchi T.P., "Internal External Knee Rotation as a Function of Knee Flexion for Activities of Daily Living", in *21<sup>st</sup> Annual Meeting of the American Society of Biomechanics*, 1997.
- [64] Bagadia N., Berta J., Burke J. and Manthei D., "The Redesign of a Ski-Binding System to Reduce the Incidence and/or Grade of Knee Injuries", in *Technical Report*, University of Wisconsin, Madison, 2001.
- [65] Di Gregorio R., Parenti-Castelli V., O'Connor J.J., and Leardini A., "Equivalent spatial parallel mechanisms for the modelling of the ankle passive motion", in *ASME DETC 2004, 28<sup>th</sup> Biennial Mechanisms and Robotics Conference*, Sept 28<sup>th</sup> - October 2nd, 2004, Paper n. DETC2004-57251, Salt Lake City, Utah.
- [66] Ma O. and Angeles J., "Architecture Singularities of Parallel Manipulators", in *Int. Journal of Robotics and Automation*, vol. 7, pp. 23-29, 1992.
- [67] Wohlhart K., "Architectural Shakiness or Architectural Mobility of Platforms", in *Advances in Robot Kinematics*, Kluwer Academic, pp. 365-374, 2000.
- [68] Husty M.L. and Karger A., "Self Motions of the Stewart-Gough-Platforms, an overview", in *Proceedings of the Workshop on Fundamental Issues and Future Research Directions for Parallel Mechanisms and Manipulators*, Quebec, Canada, pp. 131-141, 2002.
- [69] Borel E., "Memoire sur les Displacements a Trajectories Spheriques", in *Memoires Presentes par Divers Savants*, Paris, vol. 33, n.2, pp. 1-128, 1908.
- [70] Bricard R., "Memoire sur les Displacements a Trajectoires Spheriques", in *Journal de l'Ecole Polytechnique*, vol. 11, n. 2, pp.1-96, 1906.
- [71] Husty M.L. and Zsombor-Murray P., "A Special Type of Singular Stewart Gough Platform", in *Advances in Robots Kinematics*, pp.439-449, 1994.
- [72] Karger A. and Husty M., "Singularity and Self-Motions of the Stewart-Gough Platforms", in *Proceedings of the NATO-ASI Workshop on Computational Method in Machine Design*, vol. 2, pp. 270-279, Varna, 1997.

- [73] Roshel O. and Mick S., “Characterization of Architecturally Shaky Platforms”, *Proceedings of ARK’98*, pp. 465-474, 1998.
- [74] Kong X., “Generation of Singular 6-SPS Parallel Manipulators”, in *Proceedings of 1998 ASME Design Technical Conferences*, 98DETC/MECH-5952, 1998.
- [76] Jacobsen S.C., “Rotary-to-Linear and linear-to-rotary motion converters”, *US Patent 3864983*, 1975.
- [77] Mennito G., “Compliant Articulated Robot Leg with Antagonistic LADD Actuation”, in *M. Eng. Thesis*, McGill University, 1995.
- [78] Wohlhart K., “Mobile 6-SPS Parallel Manipulators”, in *Journal of Robotics Systems*, vol. 20, n. 8 , pp. 509-516, 2003.
- [79] Karger A. and Husty M., “Classification of all Self-Motions of the Original Stewart-Gough Platform”, in *Computer-Aided Design*, vol. 30, pp.205-215, 1998.
- [80] Bottema O. and Roth B., *Theoretical Kinematics*, North Holland, Amsterdam, 1979.
- [81] Schönflies A., *Geometrie der Bewegung in Sinthetischer Darstellung*, Lipzieg, 1886.
- [82] Innocenti C., “Polynomial Solution of the Spatial Burmester Problem”, in *ASME Journal of Mechanical Design*, vol. 117, pp. 64-68, 1995.
- [83] Wampler C.W., Morgan A.P. and Sommese A.J., “Numerical Continuation Methods for Solving Polynomial Systems Arising in Kinematics”, in *ASME Journal of Mechanical Design*, vol.112, pp. 59-68, 1990.
- [84] Gaillet A. and Reboulet C., “An Isostatic Six Component Force and Torque Sensor”, in *Proc. 13th Int. Symposium on Industrial Robotics*, 1983.
- [85] Kerr R.D., “Analysis, properties and Design of Stewart Platform Transducer”, in *Journal Transmission Automation and Design*, vol. 111, pp. 25-28, 1989.
- [86] Nguyen C.C., Antrazi S.S., and Zhou Z.L., “Analysis and Implementation of a 6-dof Stewart Platform-Based Force Sensor for Passive Compliant Force Assembly”, in *Proc. IEEE SOUTHEASTCON*, pp. 880-884, 1991.
- [87] Dasgupta B., Reddy S. and Mruthyunjaya T.S., “Synthesis of a Force/Torque Sensor Based on the Stewart Platform Mechanism”, in *Proc. National Convention of Industrial Problems in Machines and Mechanisms (IPROMM’94)*, India, pp. 14-23, 1994.
- [88] Svinin M.M. and Uchiyama M., “Optimal Geometric Structures of Force/Torque Sensors”, in *International Journal of Robotics Research*, vol. 14, pp. 560-573, 1995.

- [89] Dwarakanath T., Crane C., Duffy J. and Tyler C., “In-Parallel Passive Compliant Coupler for Robot Force Control”, in *Proceedings of the ASME Mechanisms Conference*, Baltimore, Md., Sep 2000.
- [90] Griffis M. and Duffy J., “Kinesthetic Control: A Novel Theory for Simultaneously Regulating Force and Displacement”, in *ASME Journal of Mechanical Design*, vol. 113, pp. 508-515, 1991.
- [91] Sugar T. and Kumar V., “Design and Control of a Compliant Parallel Manipulator for a Mobile Platform,” in *Proceedings of the ASME-DETC’98*, DETC/MECH-5863, Atlanta, Georgia, 1998.
- [92] Chirikjian G.S. and Kyatkin A.B., *Engineering Applications of Noncommutative Harmonic Analysis*, CRC Press, 2000.
- [93] Hafez M., Lichter M.D. and Dubowsky S., “Optimized Binary Modular Reconfigurable Robotic Devices”, *2002 IEEE International Conference on Robotics and Automation*, Washington, D.C., May 11-15, 2002.
- [94] Stewart D., “A Platform with Six Degree of Freedom”, in *Proc. of the Institution of Mechanical Engineers*, vol. 180 (Part 1, 15), pp. 371-386, 1965; V. E. Gough and S. G. Whitehall, “Universal Tire Test Machine”, in *Proceedings 9<sup>th</sup> Int. Technical Congress F.I.S.I.T.A*, vol. 117, pp. 117-135, May 1962.
- [95] Innocenti C. and Parenti Castelli V., “Echelon Form Solution of Direct Kinematics for the General Fully-Parallel Spherical Wrist”, in *Mechanism and Machine Theory*, vol. 28, pp. 553-561, 1993.
- [96] Han K., Chung W. and Youm Y., 1996, “New Resolution Scheme of the Forward Kinematics of Parallel Manipulators Using Extra Sensors”, *ASME Journal of Mechanical Design*, Vol. 118, pp. 214-219.
- [97] Innocenti C. and Parenti-Castelli V., 1993, “Analytical Form Solution of the Direct Kinematics of a 4-4 Fully In-Parallel Actuated Six Degree-of-Freedom Mechanism”, *Informatica*, Vol. 17, pp. 13-20.
- [98] Vertechy R., Dunlop G.R. and Parenti Castelli V., “An Accurate Algorithm for the Real-Time Solution of the Direct Kinematics of 6-3 Stewart Platform Manipulators”, in *Advances in Robots Kinematics*, Kluwer Academic Publishers, ISBN 1-4020-0696-9, pp. 369-378, 2002.
- [99] Vertechy R. and Parenti Castelli V., “Real-Time Direct position analysis of Parallel Spherical Wrists by using Extra Sensor Data”, in *ASME 2004 Design Engineering Technical Conference*, Salt Lake City, United States, 28 Settembre – 2 Ottobre, 2004.
- [100] Vertechy R. and Parenti Castelli V., “An Accurate and Fast Algorithm for the Determination of the Rigid Body Pose by Three Point Position Data”, in *Proceedings of CK2005, International Workshop on Computational Kinematics*, 4-6 Maggio, 2005.
- [101] Vertechy R. and Parenti Castelli V., “Real-Time Direct position analysis of Parallel Spherical Wrists by using Extra Sensors”, in *Journal of Mechanical Design*, vol.128, pp. 1-7, 2006.

- [102] Dagalakis N.G., Albus J.S., Wang B.-L. and Lee J.D., “Stiffness Study of a Parallel Link Robot Crane for Shipbuilding Applications”, in *Journal of Offshore Mechanics and Artic Engineering*, vol. 111, August 1989.
- [103] Griffis M. and Duffy J., “Global Stiffness Modelling of a Class of Simple Compliant Couplings”, in *Mechanism and Machine Theory*, vol. 28, 1993.
- [104] Ciblak N. and Lipkin H., “Synthesis of Stiffnesses by Springs”, in *ASME-DETC’98 MECH-5879*, 1998.
- [105] Huang S. and Schimmels M., “The Bounds and Realization of Spatial Stiffnesses Achieved with Simple Springs Connected in Parallel”, in *IEEE Transaction on Robotics and Automation*, vol. 14, pp. 466-475, 1998.